



A System-Wide Model for Solid Waste Separation and Food Waste Discharge to Sewer Systems

A thesis dissertation submitted in partial fulfilment of the requirement for the award of the
Master of Science in Engineering Specialising in Water Quality Engineering

By

Shalongo Angula

ANGSHA003

January 2022

Water Research Group (WRG)
Department of Civil Engineering
University of Cape Town
South Africa

Supervisors: A/Prof. David S. Ikumi and Dr Chris Gaszynski

The copyright of this thesis vests in the author. No quotation from it or information derived from it is to be published without full acknowledgement of the source. The thesis is to be used for private study or non-commercial research purposes only.

Published by the University of Cape Town (UCT) in terms of the non-exclusive license granted to UCT by the author.

Declaration

1. I am presenting this dissertation in partial fulfilment of the requirements for my degree.
2. I know the definition of plagiarism, and hereby declare that the work on which this thesis is based on is my original work (except where acknowledgement indicate otherwise).
3. This thesis has been submitted to the Turnitin module (or equivalent similarity and originality checking software), and I confirm that my supervisor has seen my report and any concerns revealed by such have been resolved with my supervisor.
4. I authorise the University to reproduce for the purpose of research either the whole or any portion of the contents in any manner whatsoever.

Signature: Signed by candidate.....

Date: 15 August 2022.....

ETHICS APPLICATION FORM

Please Note:

Any person planning to undertake research in the Faculty of Engineering and the Built Environment (EBE) at the University of Cape Town is required to complete this form **before** collecting or analysing data. The objective of submitting this application *prior* to embarking on research is to ensure that the highest ethical standards in research, conducted under the auspices of the EBE Faculty, are met. Please ensure that you have read, and understood the **EBE Ethics in Research Handbook** (available from the UCT EBE, Research Ethics website) prior to completing this application form: <http://www.ebe.uct.ac.za/ebe/research/ethics1>

APPLICANT'S DETAILS		
Name of principal researcher, student or external applicant	Shalongo Angula	
Department	Civil Engineering	
Preferred email address of applicant	ANGSHA003@myuct.ac.za	
If Student	Your Degree: e.g., MSc, PhD, etc.	MSc Water Quality Engineering
	Credit Value of Research: e.g., 60/120/180/360 etc.	120
	Name of Supervisor (if supervised):	Dr. David Ikumi
If this is a research contract, indicate the source of funding/sponsorship	N/A	
Project Title	A system-wide model for solid waste separation and food waste discharge to sewer system	

I hereby undertake to carry out my research in such a way that:

- there is no apparent legal objection to the nature or the method of research; and
- the research will not compromise staff or students or the other responsibilities of the University;
- the stated objective will be achieved, and the findings will have a high degree of validity;
- limitations and alternative interpretations will be considered;
- the findings could be subject to peer review and publicly available; and
- I will comply with the conventions of copyright and avoid any practice that would constitute plagiarism.

APPLICATION BY	Full name	Signature	Date
Principal Researcher/ Student/External applicant	Shalongo Angula		19/02/2021
SUPPORTED BY	Full name	Signature	Date
Supervisor (where applicable)	ALPHOSE ZINGOM		24/3/2021
APPROVED BY	Full name	Signature	Date
HOD (or delegated nominee) Final authority for all applicants who have answered NO to all questions in Section 1; and for all Undergraduate research (Including Honours).	DR. DAVID IKUMI		19 Feb 2021
Chair: Faculty EIR Committee For applicants other than undergraduate students who have answered YES to any of the questions in Section 1.			

Acknowledgement

Heavenly Father – Dear God, thank you for granting me this opportunity and for guiding me to the completion of this project. It wouldn't have been possible without your favours.

Professor David Ikumi – Firstly, thank you very much for allowing me to be part of the highly reputable research group. I thank you wholeheartedly for the support, noble guidance and unreserved commitment, which were key to the completion of this project. I sincerely hope that there will be another opportunity to work with you again.

Dr Christopher Gaszynski – Thank you very much for your knowledge and the support, Chris. I appreciate how you simplified concepts, making them easier for me to understand.

Njabulo Thela and Hector Mafungwa – A special thank you for always being ready to offer your resources during my laboratory work.

Christina Mazivila – I am very grateful for the support throughout this project, especially for the hard work and commitment during our laboratory experiments.

Joshua Matesun and Shanil Solanke – It has been an honour to work with you, my WRG colleagues. Best wishes for your studies.

Parents and family – thank you for the love, support, encouragement, and sacrifices you made throughout my entire education journey.

Friends – To my friends in Cape Town, thank you, Emilia, Hilja, Jaziitha, Samuel, Shade and Simenda for the fun times that helped me find a balance between schoolwork and downtime. To my friends in Namibia, thank you all for the love, support and encouragement you extended to me during my stay away.

Department of Civil Engineering (University of Namibia) and GIZ – Thank you for the financial support which made the pursuit of this degree possible. I wish to particularly identify Dr Petrina Johannes and Dr-Ing Joachim Lengricht for making sure that this funding was possible.

Abstract

The emergence of the circular economy, together with the changing paradigms in resource and environmental management, has resulted in a call to (1) convert wastewater treatment plants (WWTPs) to water resource recovery facilities (WRRF) and (2) diversion of organic waste (i.e., food waste) from landfills. Due to excess anaerobic digester (AD) capacities at most WWTPs, it has been proposed to co-digest sewage sludge and food waste in the AD at WWTPs to enhance resources (mainly energy and nutrient) recovery. However, suitable options for sustainable food waste handling (i.e., separation and transport) and the characteristics of food waste have not been established, particularly in South Africa. Without characterising food waste, it is impossible to include it in WWTP simulation models. In this study, food waste and sewage sludges were limited to the household food waste and primary sludge categories, respectively.

A detailed review on alternative sustainable solid waste separation and food waste transport systems was carried out and a review paper was submitted to Environmental Challenges journal for publication. The experimental investigation of the study focused on identifying the biodegradable organic composition of selected substrates, i.e., primary sludge (PS), food waste, and PS and food waste blend. PS was obtained from Belville Wastewater Treatment Works (BWWTW) in Cape Town, while food waste was manually simulated. The augmented biomethane potential (ABMP) experiment was used to obtain the required research data. The ABMP data was used to determine the substrates' biodegradable composition. The biodegradable composition was carried out using two approaches. The first approach is the mass balanced bioprocess stoichiometric calculations, which used the measured start and end concentrations of the ABMP experiment. The second approach is the parameter estimation procedure, which used the mass balanced steady-state AD model of Ikumi *et al.* (2015) together with its built-in parameter estimation function. With the exception of methane COD produced, there were slight to moderate differences between the measured and modelled experiment results. However, the modelled experiments produced significantly higher methane COD than the measured experiment, suggesting a high-level error associated with the gas measurement. As a result, the modelled experiment and the substrates' composition obtained using parameter estimation were chosen to be more accurate and reliable.

The results revealed that anaerobic digestion of food waste and co-digestion of primary sludge and food waste produces 41% and 21% more methane than the anaerobic digestion of primary sludge, respectively. The methane produced is equivalent to the potential energy recoverable. These findings suggest that diverting food waste from landfills to WWTP's AD systems can potentially enhance energy recovery. This highlights the potential need to revise urban wastewater systems to include solid waste separation and food waste diversion to AD systems to enhance resource recovery.

List of Abbreviations used

ABMP	Augmented Biomethane Potential
ABSP	Augmented Bio-sulphide potential
Ac	Acetate
AD	Anaerobic Digestion/Digester
ADM	Anaerobic Digestion Model
AS	Activated Sludge
ASM	Activated Sludge Model
b_{AD}	Biomass death rate
BMP	Biomethane Potential
BOD	Biochemical Oxygen demand
BPO	Biodegradable Particulate Organics
BSO	Biodegradable Soluble Organics
BWWTW	Belville Wastewater Treatment Works
CHP	Combined Heat and Power
COD	Chemical Oxygen Demand
CSTR	Continually Stirred Tank reactor
FAS	Ferrous Ammonium Sulphate
FBSO	Fermentable Biodegradable Soluble Organics
f_C	Carbon (C) to VSS mass ratio
f_{CV}	COD to VSS mass ratio
f_N	Nitrogen (N) to VSS mass ratio
FOG	Fats, Oil and Grease
F_P	Phosphorous (P) to VSS mass ratio
$f_{s'up}$	Fraction of unbiodegradable particulate COD with respect to total influent COD
$f_{s'us}$	Fraction of unbiodegradable soluble COD with respect to total influent COD
FSA	Free and Saine Ammonia
FWD	Food Waste Disposer
GC	Gas Chromatography
GHG	Greenhouse Gasses
HPr	Propionate
ISS	Inorganic Suspended Solids
NDBEPR	Nitrogen Denitrification Biological Excess Phosphorus Removal
OFMSW	Organic Fraction of Municipal Solid Waste

OP	Orthophosphate
PAD	Parent Anaerobic Digester
PE	Parameter estimation
PS	Primary Sludge
PST	Primary Settlement Tank
PWM	Plant-wide Model
PWM_SA	Plant Wide Model South Africa
PWM_SA_AD	Plant Wide Model South Africa for Anaerobic Digestion
PWSSM	Plant-wide Model Steady State Model
R	Sludge age
S_{bp}	Residual biodegradable COD
SCFA	Short Chain Fatty Acid
SST	Secondary Settling Tank
TKN	Total Khaedahl Nitrogen
TP	Total Phosphorus
TSS	Total Suspended Solids
TSS	Total Suspended Solids
UCT	University of Cape Town
UCTADM1	University of Cape Town Anaerobic Digestion Model 1
UPO	Unbiodegradable Particulate Organics
USA	United States of America
USO	Unbiodegradable Soluble Organics
VFA	Volatile Fatty Acids
VSS	Volatile Suspended Solids
WAS	Waste Activated Sludge
WQL	Water Quality Lab
WRC	Water Resource Commission
WRRF	Water and Resource Recovery Facility
WWTP	Wastewater Treatment Plant
Y_{AD}	Biomass yield
PAO	Polyphosphate Accumulating Organisms
PP	Polyphosphate
Z_{AD}	Biomass concentration

Table of contents

Declaration	ii
Acknowledgement	iv
Abstract	v
List of Abbreviations used	vii
Table of contents	ix
List of tables	xiv
List of figures	xvi
1. Introduction	1
1.1 Background to problem	1
1.2 Research problem and questions	2
1.3 Aims and Objectives	3
1.4 Scope and limitations	3
1.5 Study structure	4
2. Literature Review	6
2.1 Introduction	6
2.2 Wastewater treatment optimisation	6
2.2.1 Overview	6
2.2.2 Typical wastewater treatment overview	6
2.2.3 Major challenges in wastewater treatment	7
2.2.4 Wastewater treatment optimisation	8
2.3 Anaerobic digestion	9
2.3.1 Overview	9
2.3.2 Biological AD processes and organisms	9
2.4 Modelling in wastewater treatment	12
2.4.1 Overview	12
2.4.2 Steady-state models	12

2.4.3	Dynamic models	13
2.4.4	Steady-state AD model	14
2.4.5	PWM_SA_AD Model	15
2.5	Energy recovery from wastewater	15
2.5.1	Overview	15
2.5.2	Influence of wastewater composition	16
2.5.3	Wastewater and food waste co-digestion	16
2.6	Alternative sustainable food waste handling systems	20
2.6.1	Overview	20
2.6.2	Sustainable solid waste separation and food waste transport systems	20
2.6.3	Discussion	23
2.7	Biodegradability test	24
2.7.1	Overview	24
2.7.2	Biomethane Potential Test	25
2.7.3	Augmented Biomethane potential	25
2.8	Literature review summary	27
3.	Research Materials and Methodology	28
3.1	Introduction	28
3.2	Parent anaerobic digester	28
3.2.1	Feed preparation	29
3.2.2	Setup and operation	30
3.3	Augmented Biomethane Potential (ABMP) Experiment	32
3.3.1	Overview	32
3.3.2	Feed preparation	32
3.3.3	Experimental Setup	34
3.3.4	Seeding Procedure	38
3.3.5	Sampling of reactors	40

3.3.6	Gas measurement	41
3.4	Experimental testing methods	42
3.4.1	Overview	42
3.4.2	COD tests	42
3.4.3	TKN	43
3.4.4	TP	43
3.4.5	FSA and OP	44
3.4.6	Solids	44
3.4.7	Alkalinity and VFA	45
3.4.8	pH	45
3.4.9	Gas production and composition	45
3.5	Experimental results evaluation	46
3.5.1	Overview	46
3.5.2	Experimental error and uncertainty	46
3.5.3	Mass Balances	47
3.5.4	Percentage change	50
3.6	Influent fractionation	51
3.6.1	Overview	51
3.6.2	Substrate concentration	52
3.6.3	Influent fractionation	53
3.7	Organic composition	54
3.7.1	Overview	54
3.7.2	Unbiodegradable fractions	55
3.7.3	Biodegradable organic composition	56
3.7.4	Elemental composition	56
3.8	Modelling ABMP experiment	58
3.8.1	Overview	59
3.8.2	Model description	59

3.8.3	Parent AD modelling	60
3.8.4	ABMP reactors modelling	62
4.	ABMP Experiment Results and Discussion	68
4.1	Introduction	68
4.2	ABMP Control reactor results	68
4.2.1	Control reactor analytical results	69
4.2.2	Gas measurement for control reactors	72
4.2.3	Mass Balances	74
4.2.4	Composition determination for inoculum in control reactor	76
4.3	ABMP Test Reactor Results	78
4.3.1	Test reactor analytical results	78
4.3.2	Gas measurement in test reactors	83
4.3.3	Mass balances	85
4.3.4	Unbiodegradable organic composition	87
4.3.5	Biodegradable composition	89
5.	ABMP Modelled Experiment	92
5.1	Introduction	92
5.2	Modelled PAD experiment	92
5.3	Modelled ABMP control reactor experiment	93
5.3.1	Modelled control reactor composition identification	94
5.3.2	Modelled control reactor results	95
5.4	Modelled ABMP test reactor experiment	95
5.4.1	Modelled test reactor composition identification	96
5.4.2	Modelled test reactor results	98
6.	Conclusion and Recommendations	101
6.1	Introduction	101

6.2	Summary of conclusion	101
6.3	Recommendations	102
7.	References	104
Appendix A	: ABMP Experiment test data	115
Appendix B	: ABMP modelled experiment summary	119

List of tables

Table 2-1. A Steady-state models	13
Table 2-2. Dynamic models	14
Table 2-3. Annual household food waste generation in South Africa	17
Table 3-1 Operating conditions of the PADs	32
Table 3-2 Typical household food waste composition and weighed representative	34
Table 3-3. Summary of aspirator bottle volumes used	35
Table 3-4 ABMP experiment starting mixtures	39
Table 3-5. Measurements performed on the ABMP reactor	42
Table 3-6: ABMP control reactor parameters and objective values	65
Table 3-7: Source of data for UPO composition determination	66
Table 3-8: ABMP test reactors parameters and objective values	67
Table 4-1. Summary of ABMP control reactor results	70
Table 4-2. ABMP control reactor's observed COD balance	74
Table 4-3. Adjusted control reactors' COD balance (100% methane partial pressure)	75
Table 4-4. Control reactors TKN and TP mass balance	76
Table 4-5. ABMP control reactor stoichiometric composition determination	77
Table 4-6: ABMP test reactors results	80
Table 4-7. Test reactors' methane partial pressure	85
Table 4-8. ABMP test reactor COD balance	86
Table 4-9. TKN and TP mass balances for test reactors	87
Table 4-10. Determination of substrates unbiodegradable fractions	88
Table 4-11. Determination of substrate organic composition by stoichiometry	90
Table 5-1: PAD modelling output summary	93
Table 5-2: Modelled ABMP control reactor variables and weights	94

Table 5-3: ABMP control reactor modelled parameters and composition	94
Table 5-4: ABMP control reactor modelled results	95
Table 5-5: Modelled ABMP test reactor experiment variables and weights	96
Table 5-6: ABMP test reactor modelled parameters and substrate composition	97
Table 5-7: ABMP test reactors modelled experiment results	99
Table 6-1: ABMP data-1*	115
Table 6-2. ABMP data – 2*	117
Table 6-3. ABMP data – 2*	118

List of figures

Figure 1-1. A mind map showing study structure	5
Figure 2-1. UCTADM1 biological processes of AD	11
Figure 2-2. Food waste and wastewater co-digestion at EBMUD WWTP	21
Figure 2-3. Process flow diagram at Oberding food waste processing plant	22
Figure 2-4. Food waste discharge to sewers using FWD	23
Figure 2-5 An ABMP experiment setup	26
Figure 3-1. Chapter 3 layout	28
Figure 3-2. A lab-scale parent anaerobic digester (PAD)	29
Figure 3-3 Methanogenic PAD setup layout	31
Figure 3-4. ABMP experimental setup	36
Figure 3-5 An ongoing ABMP experiment photograph	37
Figure 3-6. ABMP COD influent and effluent streams	48
Figure 3-7: Example of COD fractionation	52
Figure 3-8: ABMP fractionation in control and test reactors	54
Figure 3-9: Organic component fractionation and lumping in ABMP modelling	64
Figure 4-1. ABMP control reactors methane COD masses	73
Figure 4-2. Test A batch reactor's methane COD mass	84
Figure 4-3. Test B batch reactor's methane COD mass	84
Figure 4-4. Test C batch reactor's methane COD mass	84
Figure 6-1: ABMP Control reactor experiment simulation summary	119
Figure 6-2: ABMP test A reactor experiment simulation summary	120
Figure 6-3: ABMP test B reactor experiment simulation summary	121
Figure 6-4: ABMP test C reactor experiment simulation summary	122

1. Introduction

1.1 Background to problem

The introduction of the circular economy concept has caused a shift in resource and environmental management paradigms. As a result, there have been calls for wastewater treatment plants (WWTPs) to be converted to water and resource recovery facilities (WRRF) (Arnell *et al.*, 2016). Besides WWTPs' processes being energy-intensive, they also possess great resources recovery potential (Nghiem *et al.*, 2017). Resources recoverable from WWTPs include clean water for irrigation or drinking, nutrients used for making fertilisers and biogas. However, conventional WWTPs are designed for wastewater treatment to address public health and environmental safety and are thus not suitable for resource recovery. Therefore, optimisation of WWTPs' design and operation is necessary for resource recovery and circular economy in general.

Anaerobic digestion (AD) systems are used worldwide for the treatment and co-treatment of sewage sludge and/or organic solid waste. The main driver for co-treatment of wastewater and organic solid waste in an anaerobic digestion system is resource recovery in the form of biogas and nutrients such as nitrogen and phosphorus (N&P). In an AD system, a biological process mediated by four types of microorganisms (acidogens, acetogens, acetoclastic methanogens and hydrogenotrophic methanogens) is used to break down biodegradable organics and convert them to biogas (Stillwell *et al.*, 2010). Biogas, being a form of renewable energy, has made the AD process popular for treatment of waste sludge due to the potential to recover energy from waste. For example, the East Bay municipality WWTP in the United States of America (USA) became energy neutral after introducing co-treatment of wastewater and solid organic waste (food waste) (Hagey, 2011; Shen *et al.*, 2015). Furthermore, even though biogas is not yet commercialised in South Africa, studies have shown that energy recovery via AD from WWTPs is feasible (Burton *et al.*, 2009; Ferry & Giljova, 2015).

On the other hand, solid wastes, including organic solid waste and wastewater sludge, are traditionally disposed of at landfills. However, landfilling of organic waste is incompatible with the circular economy, significantly contributes to greenhouse gas emissions, potentially

contaminates groundwater and is generally costly (Stillwell *et al.*, 2010; Zan *et al.*, 2020). As a result, new legislations are restricting the disposal of organic waste to landfills, tasking local authorities with seeking new sustainable solutions for organic waste management (De Clercq *et al.*, 2017; Petterson, 2019).

This study aims to investigate the potential for source separation of solid waste, diverting organic solid waste to WWTPs and including organic solid waste in WWTPs' optimisation models.

1.2 Research problem and questions

Discarding household food waste with other municipal solid waste at city landfills leads to high emission of biogas (including methane, a greenhouse gas, which is 22 times more harmful than carbon dioxide) into the atmosphere, besides leachate production that potentially contaminates groundwater. Alternatively, food waste can be discharged into sewers through in-sink macerators or by trucking them to WWTPs. If discharged to sewers, on entering the WWTP, the food waste will be settled out using primary sedimentation tanks (PSTs) and contribute to the formation of primary sludge (PS). The PS is then fed to AD systems. If it is to be trucked, food waste will undergo pre-treatment before discharge directly to the AD system. In the AD, methane gas is generated via the biological breakdown of organics. The methane produced is usually converted to electricity and can contribute to powering the WWTP. The potential methane generated can be calculated using validated mathematical models.

To determine the impact of diverting food waste from landfills to WWTPs, the following is to be quantitatively investigated:

- i. What are the characteristics of sewage sludge and general characteristics of food waste?
- ii. What are the ideal possible solid waste separation and food waste transportation systems?
- iii. Which existing models can be used/extended to simulate food waste and sewage sludge co-digestion?
- iv. How much more energy can be recovered from the co-digestion of food waste and sewage sludge?
- v. Will the diversion of food waste compromise the capacity of a plant to carry out its function efficiently?

- vi. How can the growing sludge volume resulting from the inclusion of food waste be managed?

1.3 Aims and Objectives

The main objective of this research is to assess the potential to revise urban wastewater systems to include solid waste separation and discharge organic waste (i.e., food waste) to sewer systems in order to enhance resource recovery at WWTPs (instead of losing the methane from landfills to the atmosphere associated with GHGs). In order to achieve the main objective, the following specific objectives will be implemented:

- i. Review alternative sustainable systems to divert organic (food) waste to WWTPs or WRRFs
- ii. Utilise augmented batch experiments to determine the characteristics of sewage sludge and food waste.
- iii. Use existing models to simulate anaerobic co-digestion of sewage sludge and food waste.

1.4 Scope and limitations

In this thesis, the term food waste is limited to household food waste. Food wastage or losses occur at all levels of the food supply chain. However, not all food losses end up in landfills. For example, agricultural waste (also referred to as food waste in some studies) is often composted. However, the final destination of household food waste is, in most cases, landfills. Therefore, with a view of solving the landfill crisis, the study was limited to household food waste only.

Due to the limited time to complete this project, it was not possible to carry out the investigation on the impact of food waste on all the unit operations in the entire WWTP. Therefore, the study was limited to the anaerobic digester (AD) unit of operation of the WWTP. Furthermore, the AD influent (before introducing food waste) was assumed to be primary sludge only. In other words, the influence of food waste on other possible AD influent streams (i.e., waste activated sludge-WAS) is beyond this project's scope. Furthermore, this study did not evaluate the processing and management of AD products (i.e., dewatering liquor or stabilised sludge).

The augmented batch-test experiment, used to obtain data, was limited to methanogenic conditions only. In addition, due to extensive work and details required to carry out complete characterisation, the study did not focus on unbiodegradable particulate organic (UPO) composition because UPO composition data for wastewater is readily available in the literature. The study, therefore, focused on biodegradable particulate composition (BPO). In addition, the determination of kinetic parameters was outside the scope of the study because they require frequent measuring at the dynamic period of augmented batch experiments, which was not carried out in this study. The steady-state AD model, which was used in this study, does not allow simultaneous solving of BPO and biodegradable soluble organics (BSO) and, therefore, in this study, BPO includes soluble organics. Furthermore, the steady-state AD model is not calibrated to characterise heavy metals. Thus, the elemental composition in this study excludes heavy metals. As a result, the study was limited to obtaining the biodegradable fraction of the waste sludge organics and the elemental composition of the biodegradable organics in the food waste and the primary sludge.

Lastly, the experimental investigation was run parallel to another project which involved calibration of the primary settling tank (PST) that generated the primary sludge (PS) used in this project. Hence the control batch reactors were shared between these projects.

1.5 Study structure

This thesis report is made up of seven chapters. In Chapter 1, the background and motivation of the study and research questions are discussed. In addition, the objectives and scope of the study are also discussed in Chapter 1. In Chapter 2, the relevant literature on previous studies and other areas of importance in relation to the study are reviewed. The materials and methods, experiments setup and operation, analytical procedures and model descriptions are explained in Chapter 3. Details of the research results and results discussion of the experiments are presented in Chapter 4. Chapter 4 also includes the characterisation of wastewater and food waste. Results for simulation of experiments carried out in Chapter 4 are discussed in Chapter 5. Finally, the report is concluded based on the research findings and recommendations are made for further research in Chapter 6. Figure 1-1 shows a summary of the thesis structure.

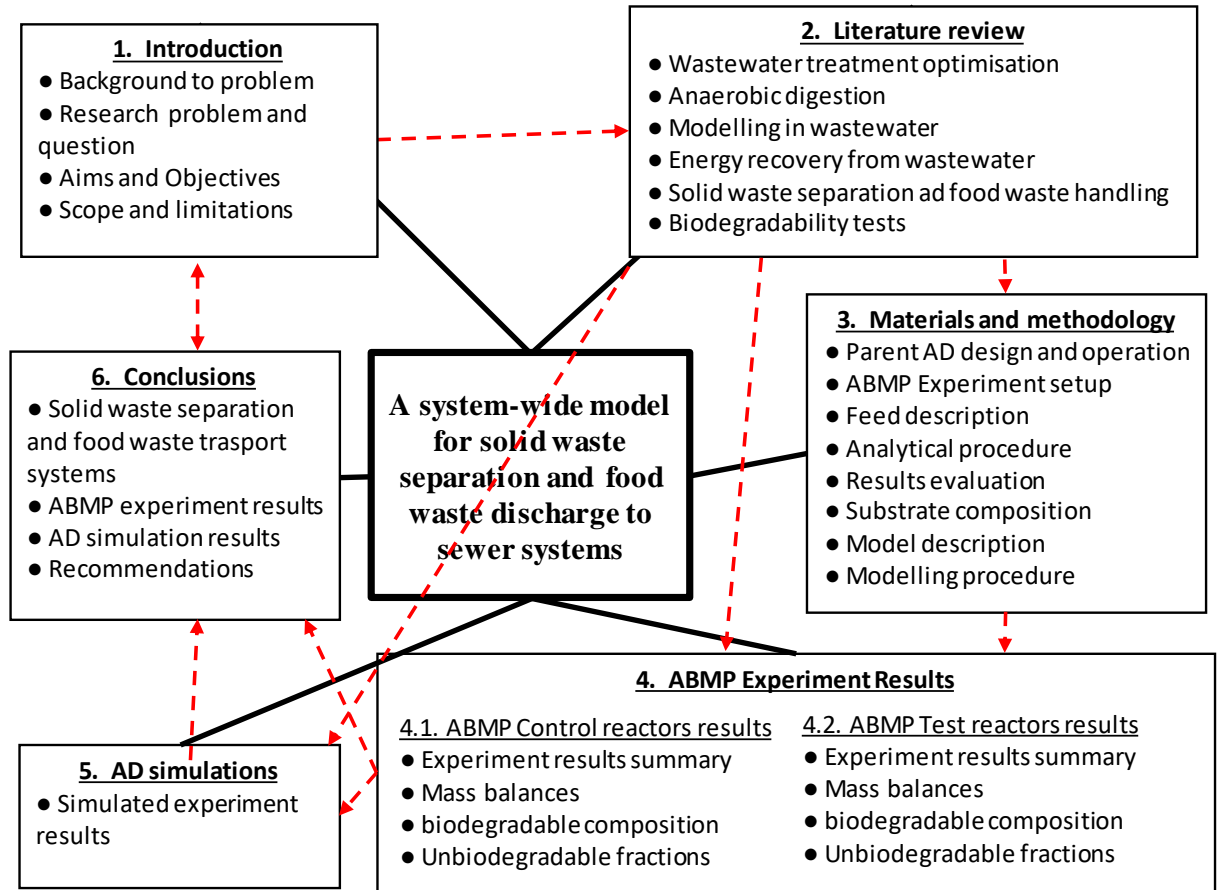


Figure 1-1. A mind map showing study structure

2. Literature Review

2.1 Introduction

This chapter serves to review the literature relevant to the subject of co-digestion of wastewater and food waste at wastewater treatment plants (WWTPs). The literature information was used to identify gaps in the existing knowledge and select suitable experimental methodologies and models for this study. The literature reviewed included wastewater treatment optimisation, anaerobic digestion, modelling, wastewater and food waste co-digestion, alternative sustainable food waste transportation systems and wastewater biodegradability tests method. The section on review of alternative sustainable food waste transport systems (i.e., Section 2.6) was submitted to a journal as a review paper for publication. Finally, a summary of the literature review is presented at the end of the chapter.

2.2 Wastewater treatment optimisation

2.2.1 Overview

The primary reason for wastewater treatment is to ensure protection of public and environmental health. However, the changing paradigms towards more environmentally, socially and economically sustainable infrastructure resulted in a requirement for WWTPs to implement resource recovery and thus be converted to resource recovery facilities (WRRF). As a result, the design and operation of WWTPs have intensified over the years. Mathematical models have been known to contribute towards improved, and optimised operations hence can be useful in decision making for future WRRF. In a successful WRRF model, the input values must be well known to ensure accurate predictions of system outputs.

2.2.2 Typical wastewater treatment overview

The wastewater treatment process at a WWTP is carried out by a chain of physically interconnected units of operation. Each unit of operation has a defined function that facilitates the treatment process (Ikumi, 2011). By common practice, the products of wastewater treatment

are treated effluent and wastewater sludge. The treated effluent is discharged to water streams while sludge is discarded to landfills or composited.

The primary treatment process is sited before the activated sludge (AS) system. It consists of operational units such as screening, grit removers and primary settling tank (PST). The PST removes easily settleable substances from the influent flow wastewater. In the PST, wastewater fractionates into two distinct products: (1) settled wastewater(overflow supernatant) which has reduced strength, and (2) primary sludge (PS), which settles at the bottom of the PST (Wentzel & Ekama, 2003). From the PST, settled wastewater is channelled to the AS system for secondary treatment. The AS system consists of a biological reactor that carries out the actual organic degradation(treatment) and a secondary settlements tank (SST) that clarifies treated mixed liquor to produce effluent and sludge. The PS from PST is channeled to the anaerobic digester (AD; see Section 2.3) for further treatment too. The different WWTPs unit of operation discussed above, works as an integrated system. Which means, changes in upstream processes (i.e., change in influent feed), affects the downstream process (i.e., energy recovery potential in AD or effluent quality).

2.2.3 Major challenges in wastewater treatment

The water sector in general and wastewater treatment operations in particular is an energy-intensive sector. For example, it is estimated that household wastewater treatment alone (excluding industrial wastewater treatment, which is more expensive) accounts for 3% of world's energy needs (Li *et al.*, 2015). South Africa is closely following this trend whereby it is reported that wastewater treatment accounts for over 55% of the energy used in the entire water sector (Swartz *et al.*, 2013). Moreover, these energy demands are likely to keep rising owing to population increases, ageing infrastructures and stricter effluent requirements. Therefore, wastewater treatment processes significantly contribute to the energy-water nexus (Stillwell *et al.*, 2010).

Wastewater treatment also plays a significant role in drinking water security, particularly in water-stressed regions such as South Africa. This is because when poorly treated effluents are discharged into low volume (stressed) water bodies (such as rivers), it causes a high concentration of pollutants to these water bodies. In turn, it becomes difficult to treat water from these streams

and thereby threatening drinking water security (Donnenfeld *et al.*, 2018; Zhen *et al.*, 2018). Moreover, regions that depend on groundwater recharged with wastewater treated effluents (i.e., Atlantis, Western Cape, South Africa) depend on efficient wastewater treatment processes to ensure the sustainability of groundwater utilisation (Tredoux *et al.*, 1999). For example, studies by Donnenfeld *et al.*, (2018 and Zhen *et al.*, (2018) reported that 45% of wastewater effluents discharged into natural water streams are inadequately treated. Undoubtedly, these poor effluents will threaten drinking water supply if not addressed.

Maintaining energy efficiency and sufficiently treated effluents, as discussed above, are some of the expectations from the wastewater treatment sector. However, the parallel demand for energy efficiency (including energy recovery) and meeting effluent standards is not a simple fix. To meet the required final effluent quality standards, the activated sludge (AS) system must be operated at a long sludge age, which is energy intensive. This because, to achieve sufficient effluent qualities require the operation of long sludge ages in the activated sludge (AS) system, which is energy-intensive. At the same time, long sludge age produces waste activated sludge (WAS) with a low biodegradable fraction and thus low energy recovery potential. Maintaining a balance between high-quality effluent and energy efficiency in the AS system is one of the complex challenges in wastewater treatment operations. To overcome these challenges, require optimisation of WWTPs' operation processes as discussed in Section 2.2.4.

2.2.4 Wastewater treatment optimisation

For efficient and sustainable operation, wastewater treatment processes need to be optimised. Wastewater treatment optimisation includes developing models with capacities to simulate complex physical, chemical and biological processes which can aid efficient design and operation of wastewater treatment plants (Xie *et al.*, 2016). As a result, models are today regarded as vital tools for analysing, designing and optimising wastewater treatment processes (Seco *et al.*, 2020). The development of models has evolved from simple unit of operation models to complex plant-wide models (PWM) (Ekama, 2017). The development of mass balanced PWMs aimed at evaluating control strategies in WWTPs under real-time dynamic conditions and exposing significant interactions between various units of operation has been ongoing for the past two decades (Ekama, 2017). The growing popularity of improved models has encouraged the evaluation of potential simultaneous treatment of wastewater with organic waste (i.e., PS

with WAS or food waste) at WWTPs (Iqbal *et al.*, 2020). Modelling and co-treatment of wastewater with organic waste are discussed in detail in Sections 2.4 and 2.5.3, respectively.

2.3 Anaerobic digestion

2.3.1 Overview

Anaerobic digestion (AD) is one of the world's oldest technologies used in wastewater treatment and is still widely used globally. The reasons the AD technology has remained relevant up to date include its capability to reduce volatile solids significantly, produces energy-rich biogas and has capability other organic waste such as WAS, PS and solid organic waste slurries (Sötemann *et al.*, 2005a). Owing to their wide application and complex operation processes, mathematical models have been developed to reduce the design and operation of anaerobic digesters on experience and empirical guidelines.

2.3.2 Biological AD processes and organisms

During AD, biodegradable organics are degraded by fermentation processes to form biogas and release inorganics such as NH_4^+ , PO_4^{3-} and S^{2-} into the bulk solution (Van Lier *et al.*, 2008). The biodegradation of organics occurs in a chain of stages, and at each stage, degradation is facilitated by different organism groups. The stages of organic degradation during AD include hydrolysis, acidogenesis, acetogenesis, acetoclastic methanogenesis and hydrogenotrophic methanogenesis. There exist numerous conceptual schemes that describe biological processes in literature. Based on the University of Cape Town anaerobic digestion model (UCTADM1) scheme of Sötemann *et al.* (2005), the AD process can be described as below:

2.3.2.1 Hydrolysis

Hydrolysis is a process by which complex organic materials (i.e. carbohydrates, lipids and proteins) are broken via extracellular steps to form soluble substrates (i.e. short-chain fatty acids, SCFA) (Sötemann *et al.*, 2005). In UCTADM1, different organic materials are combined, represented by a generic form of $\text{C}_x\text{H}_y\text{O}_z\text{N}_a\text{P}_b$ (Sötemann *et al.*, 2005). The conversion of complex substrates into soluble substrates is necessary because organisms in the subsequent

stages after hydrolysis cannot break down complex organisms and thus require soluble substrates. The hydrolysis stage is facilitated by the acidogens, and the product of hydrolysis is glucose. The hydrolysis rate is generally slow and thus considered as the rate-limiting step in wastewater sludge AD (Sötemann *et al.*, 2005).

2.3.2.2 Acidogenesis

The acidogens organisms group facilitates Acidogenesis. The acidogens ferment glucose, which is produced by hydrolysis to produce biomass, and intermediate products such as propionate (HPr), acetate (Ac), hydrogen and butyrate (Gujer & Zehnder, 1983; Mosey, 1983). Acetate is the preferred acidogenesis product because it provides the acidogens organisms with a high energy yield for growth. In addition, it supplies the acetoclastic methanogens (in the subsequent stage) with their primary substrate required for methane production (Mosey, 1983). Acidogenesis is assumed to be highly influenced by hydrogen partial pressure, a process that allows for a reasonable description of digester failure (Ghoor, 2020; Gaszynski, 2021). For example, in the presence of high hydrogen partial pressure, acidogens produce propionate and butyrate. The formation of propionic acid causes a reversal in the hydrogen production process to the extent that organisms can control the redox potential during heavy surge loads (Gaszynski, 2021).

2.3.2.3 Acetogenesis

The acetogenesis process is facilitated by acetogens organisms which converting short-chain fatty acids, with two or more carbon atoms (higher than C₂), such as propionic and butyric acids, to acetate and hydrogen (Gujer & Zehnder, 1983; Mosey, 1983). This process is essential because methanogenic organisms do not utilise such SCFAs. Low hydrogen partial pressure is required to effectively convert SCFAs to acetate (forward reaction) (Ghoor, 2020). Therefore, effective acetogenesis requires hydrogen utilising organisms (hydrogen methanogens) to operate at their optimum levels.

2.3.2.4 Acetoclastic methanogenesis

The acetoclastic methanogenesis process is facilitated by the acetoclastic methanogen organisms, which converts acetate to methane and carbon dioxide (Sötemann *et al.*, 2005). The acetoclastic

methanogens are responsible for about 70% of methane gas produced by the AD, while hydrogenotrophic methanogens (see Section 2.3.2.5) produce about 30% (Gujer & Zehnder, 1983; Ristow *et al.*, 2005). The acetoclastic methanogens are very sensitive to pH and thus are susceptible to inhibitory compounds. The inhibition can result from a high accumulation of products from precedent processes such as acetate, ammonia, hydrogen and hydrogen sulphide (Ristow *et al.*, 2005). Therefore, propionate and acetate need to be utilised as soon as they are produced to ensure effective digester operation. In turn, this ensures that the digester pH is maintained at around seven, which is the optimum operating pH of the acetoclastic methanogens (Söttemann *et al.*, 2005).

2.3.2.5 Hydrogenotrophic methanogenesis

The hydrogenotrophic process is facilitated by hydrogenotrophic methanogens organisms, which convert hydrogen and carbon dioxide produced by the preceding process into methane and water (Mosey, 1983). The removal of hydrogen in the digester is important for maintaining a low hydrogen partial pressure to ensure favourable conditions for acetogens, as discussed earlier. Like the acetoclastic methanogens, hydrogenotrophic methanogens are also inhibited by low pH.

Figure 2-1 shows a summary of the conceptual process for anaerobic digestion for UCTADM1.

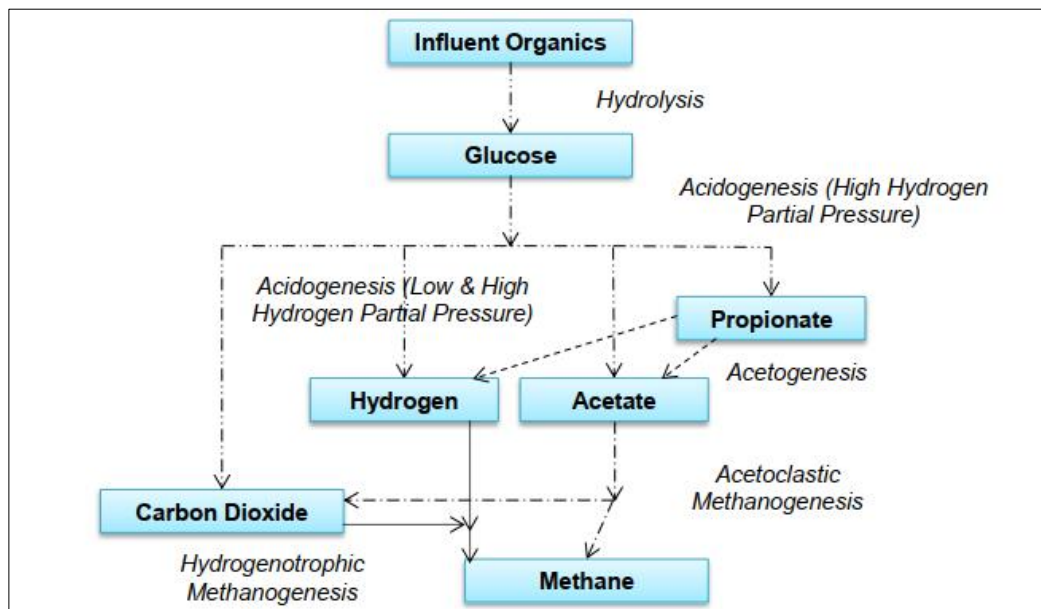


Figure 2-1. UCTADM1 biological processes of AD (Ghoor, 2020)

2.4 Modelling in wastewater treatment

2.4.1 Overview

As discussed at the end of Section 2.2.4, models are valuable tools for analysing, designing, and optimising wastewater treatment processes. Wentzel *et al.* (2008) state that models have helped evaluate existing WWTPs' performances and detect potential requirements for upgrades, design new plants, train plant operators, and carry out sensitivity analysis. There has been significant development in both steady-state and dynamic models over the years.

In the past, models were developed for each unit of operation separately and resulted in two types of standard models, namely activated sludge models (ASMs) and anaerobic digestion models (ADMs). However, compatibility difficulties have been experienced when coupling these models together because these models have different variables. For example, while carbon is not a requirement for ASMs, it is a requirement for ADMs (Ikumi *et al.*, 2014). As a result, building models in isolation has been deemed ineffective for the design and operation of WWTPs (Brink, 2008; Wu, 2015). Therefore, most recent research and modelling efforts are focused on plant-wide modelling (PWM), whereby a WWTP is modelled as a whole in an integrated fashion (Brink, 2008; Seco *et al.*, 2020). This section discusses some developments in the steady-state and dynamic models.

2.4.2 Steady-state models

Steady-state models are relatively simple models that require constant flows and loads as input (Ekama & Wenzel, 2008). Steady-state models are important because they are used to determine the design parameters (i.e., reactor volumes, sludge ages and recycle ratios) which are required inputs for dynamic models. (Ekama, 2009). Additionally, they are easy to use and require less data input as compared to dynamic models. During steady-state modelling, it is assumed that most bioprocesses reach completion, which allows them to be analysed using stoichiometry (Ekama, 2009).

Table 2-1 lists some development in steady-state models as well as their relevant literature.

Table 2-1. A Steady-state models

Model Type	System/Process/Model component	Relevant literature
Activated Sludge (AS) Models	Organic removal	Marais & Ekama (1976), Ekama & Wentzel (2004)
	Nitrogen removal	Ekama & Wentzel (2008)
	Biological excess phosphorus removal (BEPR)	Mebranttu (2007)
	Nitrification-Denitrification biological excess phosphorus removal (NDBEPR) system	Wentzel <i>et al.</i> (1990), Harding (2009)
Anaerobic digestion (AD) models	UCT anaerobic digestion model (UCTADM)	Sötemann <i>et al.</i> (2005)
	WAS +PS and WAS hydrolysis rate	Ikumi <i>et al.</i> (2014)
Secondary settlement tank (SST) model	SST 1DFT	Ekama <i>et al.</i> (1997) Takács & Ekama (2008)
Plant-wide models (PWM)	Plant-wide steady-state model (PWSSM) design and analysis program	Wu (2015)
	Optimisation of WRRF for energy generation	Ekama (2017)
	Mass balance bioprocess stoichiometry	Ekama (2009)
	Three Phase PWSSM	Ikumi <i>et al.</i> (2015) Ikumi (2011)

2.4.3 Dynamic models

Dynamic models are very complex compared to steady-state modes, with varying flows and loads besides time factors (Ekama & Wenzel, 2008). They employ ordinary and partial differential equations to simulate reaction mechanisms for various processes acting on various wastewater elements. Due to this complexity, they are often simulated in software (Ekama, 2009; Ikumi, 2011). PWM_SA tool, a subset of WRRF simulation software platform WEST®, is typical for dynamic wastewater modelling, specifically in South Africa (Ghoor, 2020; Ikumi *et al.*, 2015). Table 2-2 below is a summary of some common dynamic models.

Table 2-2. Dynamic models

Model Type	System/Process/Model component	Relevant literature
Dynamic activated sludge models (ASM)	IWA AS models (i.e., ASM1, ASM2, ASM2d, and ASM3)	Henze <i>et al.</i> (1995, 2000)
	ASM2-3 phase	Ikumi (2011)
Dynamic anaerobic digestion models	IWA AD Models (i.e., ADM1)	Batstone <i>et al.</i> (2002)
	University of Cape Town Dynamic Model (UCTDM)	Söttemann <i>et al.</i> (2005)
	Plant Wide Model SA anaerobic digestion model (PWM_SA_AD)	Brouckaert <i>et al.</i> (2010); Ikumi <i>et al.</i> (2015); Ghoor (2020)
Plant-wide dynamic model	Continuity Based Interfacing Method (CBIM)	Volcke, van Loosdrecht & Vanrolleghem (2006)
	The Supermodel Approach	Jones & Takács (2004)
	The Transformation-Based Approach	Grau, Vanrolleghem & Ayesa (2007)
	Mass Balance Based Plant-Wide Modelling Approach (i.e., PWM_SA)	Brouckaert <i>et al.</i> (2010); Ikumi (2011); Ikumi <i>et al.</i> (2015)

2.4.4 Steady-state AD model

Söttemann *et al.* (2005) developed a steady-state model for sewage sludges by simplifying the UCTADM1 (dynamic) model of Söttemann *et al.* (2005). The UCTADM1 process was discussed in Section 2.3.2. Ikumi *et al.* (2015) extended the AD steady-state model of Söttemann *et al.* (2005) by adding phosphorus component, digestion of WAS and a solid phase—making it a three-phase (liquid, gas, solid) phase model. The steady-state AD model of Ikumi *et al.* (2015) is a mass balanced model that can predict the release of N and P during AD, track elemental compounds, and identify potential mineral precipitation problems. Steady-state models, in general, are suitable for modelling experiments in which many bioprocesses can be assumed to have reached completion¹ (Ekama, 2009). For example, Maake & Ikumi (2021) deliberately operated AD batch reactors at a long sludge age to ensure complete utilisation of biodegradable

¹ An experiment is assumed to have reached completion when the substrate biodegradable organics are used up, which reduces the bioprocesses to stoichiometry only.

organics and used the steady-state AD model of Ikumi *et al.* (2015) to simulate the experiments. However, to date, both steady-state AD models of Sötemann *et al.*, 2005 and Ikumi *et al.*, (2015) are only calibrated for hydrolysis of PS and WAS. Nevertheless, the steady the steady-state model of Ikumi *et al.* (2015) was selected for modelling the batch ABMP batch reactors..

2.4.5 PWM_SA_AD Model

Brouckaert, Ikumi & Ekama (2010) developed the PWM_SA_AD model by extending the UCT AD model (UCTADM1) of Sötemann *et al.* (2005) to include a solid phase of mineral precipitation. The PWM_SA_AD model is developed as a sub-model of the Plant Wide Model South Africa (PWM_SA) model. The PWM_SA model is a three-phase (aqueous-gas-solid) plant-wide model developed by the Universities of Cape Town and KwaZulu Natal and coded into the WRRF simulation software platform WEST® (Brouckaert *et al.*, 2010; Ikumi *et al.*, 2015). As a sub-model of the PWM_SA model, the PWM_SA_AD model contains all features of the PWM_SA model. PWM_SA_AD model is commonly used in the Water Research Group (WRG) at UCT for simulating anaerobic digestion. In addition, the model is regularly updated as per ongoing research within the WRG.

2.5 Energy recovery from wastewater

2.5.1 Overview

Traditional energy sources are becoming exhausted due to escalating energy demand from rising populations and economies. Therefore, the world is challenged to identify alternative sustainable energy sources, and biogas is one of the alternatives with so much potential. In wastewater treatment, biogas is generated during anaerobic digestion of biodegradable organics. However, biogas generated during wastewater treatment is often not utilised due to their non-commercialisation. This section discusses factors affecting biogas recovery and how biogas recovery can be enhanced.

2.5.2 Influence of wastewater composition

Energy is produced from wastewater treatment during the AD process, whereby AD organisms (see Section 2.3.2) biologically break down biodegradable organics to produce methane-rich biogas. Therefore, the influent wastewater composition highly influences the quality and quantity of biogas produced from the AD. Wastewater with high biodegradable organics in the influent is preferred for high biogas yield (Musvoto & Ikumi, 2016). A study by Ekama (2017) also confirms that diverting more organics to the AD systems by increasing the removal efficiency of the PST increases biogas yield. In addition, when the PST removes more organics, it results in little organics in settled wastewater (i.e., the overflow from the PST) which reduces aeration costs in the AS system.

To enhance biogas recovery, it is therefore required to increase the organics discarded to AD systems. Some methods for increasing organic discarded to AD systems include co-digestion of wastewater with other organic wastes and increasing PST removal efficiency (Ekama, 2017; Nghiem *et al.*, 2017). However, additional organic loading to AD systems may also result in negative consequences, leading to unit operations or plant failure. For example, when additional organics are added to influent wastewaters, it increases the organic content of PS. Consequently, it enhances biogas production, but it also causes significant variations in the settled wastewater characteristics (Ekama, 2017). This variation in settled wastewater composition can subsequently lead to a change in AS system design parameters (i.e., increased settled wastewater organic load requires an increased sludge age, reactor volume and SST area). Therefore, it is crucial to thoroughly evaluate the plant's loading capacity, particularly the AD and AS systems, before introducing an additional source of wastes or changing PST removal efficiencies (Iqbal *et al.*, 2020).

2.5.3 Wastewater and food waste co-digestion

2.5.3.1 Food waste composition

In general, food waste refers to food losses arising throughout the entire food supply chain and the food that is discarded by the consumer (Nahman & de Lange, 2013). However, in the scope of this thesis, the term food waste is limited to avoidable and unavoidable food discarded by

households. Household food waste is largely biodegradable organics, and when it is discarded to landfills, it significantly contributes to GHG emissions and leachate production (Hagos *et al.*, 2017; Mehariya *et al.*, 2018). Leachate can potentially contaminate groundwater, while GHG contributes to global warming. Furthermore, when food waste is disposed to landfills, we miss out on potentially recoverable resources such as biogas and nutrients (Zan *et al.*, 2020).

Food waste has not been well documented in South Africa, indicating how food waste is still not regarded as a resource. However, subsequent studies by Nahman *et al.* (2012), Nahman & de Lange (2013) and Oelofse & Nahman (2013) attempted to quantify the magnitude of food waste produced throughout the food supply chain, including household level. Table 2-3 shows the estimated food waste composition and quantity produced by households in South Africa annually.

Table 2-3. Annual household food waste generation in South Africa (Nahman & de Lange, 2013)

Commodity Group	Weight (1000 tonnes) per year
Cereal	2 605
Roots and tubers	955
Oilseeds & pulses	346
Fruits and vegetables	4 491
Meat	753
Fish and seafood	225
Milk	831
Total	10 206

To the best of the author's knowledge, available literature in South Africa on the food waste subject focused on quantification and physical composition. However, to accurately determine the potential biogas recoverable from food waste, the food waste organic composition is required to be known. Furthermore, food waste's organic composition varies significantly from location to location due to varying income levels and diet patterns, resulting in varied biogas yield per mass of food waste. Therefore, it is critical to determine the characteristics of food waste at a local level rather than using projected figures.

2.5.3.2 Food waste management: Challenges and opportunities

Food waste is a substantial fraction of the organic fraction of municipal solid waste (OFMSW). However, due to its very putrescible nature, food waste management is generally a challenging task worldwide. If not adequately handled, food waste significantly contributes to public health, environmental and social challenges (Iacovidou *et al.*, 2012; Zan *et al.*, 2018). For example, in Europe, food waste alone contributes up to 16% of global warming potential. Traditionally, food waste and other organic waste are disposed of in landfills. However, due to paradigm shifts in environment management, landfilling of organic waste, including food waste, is regarded as unsustainable. As a result, landfilling of food waste is banned in some countries like Germany and Italy and levied in Australia (Nghiem *et al.*, 2017). In fact, various countries across the globe have put up strategies and policies that promote smart waste management and food waste reduction (De Clercq *et al.*, 2017).

On the other hand, opportunities exist in diverting food waste from landfills through smart waste management practices. Because food waste is mostly organic, it contains nutrients and resources that can potentially be recovered. Anaerobic digestion (AD) is a leading technology used to treat organic-rich wastes to produce methane-rich biogas, which can be converted to energy such as electricity. Apart from energy, scarce nutrients such as phosphate and nitrogen, which can be used for fertilisers, can also be recovered from anaerobic digestion of organic-rich substrates such as food waste (Sikosana *et al.*, 2016, 2017). The process of AD was discussed earlier in Section 2.3.2. Despite overwhelming evidence of science supporting resource recovery from anaerobic digestion of food waste, various technical and social challenges exist. Thus, AD of food waste is not commonly practiced.

Due to technical challenges of anaerobic mono-digestion of food waste, researchers have proposed anaerobic co-digestion of food waste with other substrates. Co-substrates to food waste can be one or more organic wastes such as wastewater sewage or sludge, ground coffee, manure, dairy waste (Menardo & Balsari, 2012; Nghiem *et al.*, 2017). It is believed that co-digestion of food waste with other organic waste offers better process efficiency by offering complementary benefits such as nutrient availability, lower feed volume, better biogas yield than mono-digestion (Mehariya *et al.*, 2018).

2.5.3.3 Wastewater and food waste co-digestion

The overall progress made in water conservation and slow population growth has left AD at many WWTPs with excess capacity that is unlikely to be used in the future (Nghiem *et al.*, 2017). Thus, the wastewater sectors are actively exploring options to utilise the excess digester capacities. Food waste and wastewater co-digestion for biogas recovery is one of the available promising options to utilise the excess capacities of digesters at WWTPs. Full-scale wastewater and food waste co-digestion projects are already taking place in some parts of the world, including Italy and Germany (Nghiem *et al.*, 2017; Cecchi & Cavinato, 2019), California (Gray *et al.*, 2008) and Sweden (Davidsson *et al.*, 2017).

Food waste and wastewater co-digestion is driven by economic and environmental benefits (Nghiem *et al.*, 2017). The environmental benefits are driven by the diversion of organic waste to landfills, while economic benefits are driven by resource recovery/circular economy. However, it is believed that food co-digestion of food waste and wastewater has more environmental benefits than the true economic gains, resulting in the slow full-scale implementation of food waste and wastewater co-digestion projects (Nghiem *et al.*, 2017).

To enhance the true economic benefits of food waste and wastewater co-digestion requires optimisation of system-wide processes. As discussed in Section 2.5.2, resource recovery from wastewater is greatly dependent by the influent wastewater characteristics. Therefore, by improving the quantity and quality of food waste entering the wastewater and subsequently, the AD can greatly enhance resource recovery. Improving the quantity and quality of food waste require effective solid waste separation and food waste transport to the WWTP system. Therefore, identifying alternative sustainable solid waste separation and food waste transport to WWTPs systems was an essential objective of this project. Different sustainable solid waste separation and food waste transport systems were identified and rigorously reviewed in Angula & Ikumi (2022) and summarised in Section 2.6.

2.6 Alternative sustainable food waste handling systems

2.6.1 Overview

The objective of this section is to rigorously review various alternative sustainable systems for solid waste separation and transportation of food waste to wastewater treatment facilities for co-digestion with wastewater sludge, which was an important objective of this study. This section is an extract from a review paper by Angula & Ikumi (2022), which has been submitted to a journal for publication. This thesis and write up of the journal paper were carried out in parallel by the same lead author. The identified systems were discussed with reference to full-scale case-studies. Finally, the identified systems were analysed and compared in terms of their strengths, weaknesses, opportunities and threats (SWOT analysis).

2.6.2 Sustainable solid waste separation and food waste transport systems

2.6.2.1 Decentralised systems

Decentralised food waste and sewage sludge co-digesting WWTPs receive food waste, with transport modes differing from site to site. Upon their arrival at a WWTP, food waste must undergo physical and mechanical pre-treatment before co-digesting it with sewage sludge. The pre-treatment process includes removing coarse contaminants and inert materials (i.e. plastics, glass and bones) and grinding food waste into smaller particles (Hagey, 2011; Edwards *et al.*, 2017). The products of pre-treatment are a liquid food waste slurry and residual inert solid waste. The food waste slurry is stored in storage tanks before discharging it to the WWTP's anaerobic digester where it will be co-digested with the wastewater sludge. Residual inert solid waste is dewatered on site before getting sent to landfills or incinerating facilities.

The Rovereto plant (Italy) and East Bay Municipality Utility District (EBMUD) WWTP (USA) are examples of decentralised food waste and wastewater co-digesting WWTPs equipped with on-site pre-treatment facilities (Hagey, 2011; Nghiem *et al.*, 2017). Figure 2-2 below shows the process of food waste pre-treatment at a WWTP at EBMUD WWTP. Food waste pre-treatment is believed to be a complex and capital and energy intensive process (Bernstad *et al.*, 2013; Nghiem *et al.*, 2017). As a result, some WWTPs such as Moosburg (Germany) eliminate pre-

treatment process by only accepting liquid food waste such as brewery, dairy wastes and pre-treated food waste from food waste processing plants (Sembera *et al.*, 2019).

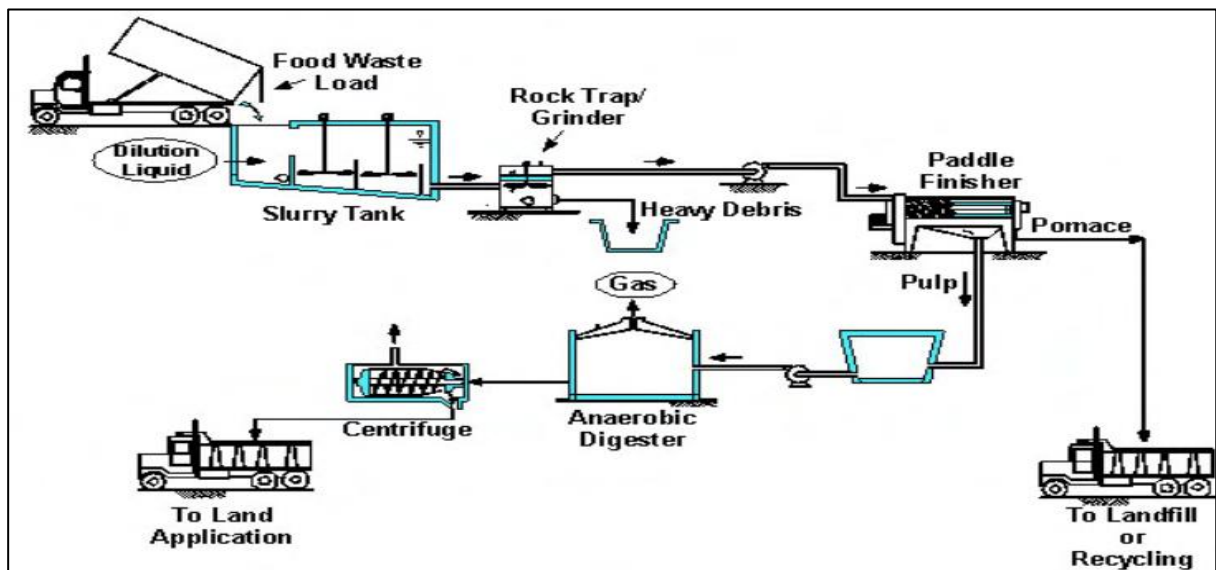


Figure 2-2. Food waste and wastewater co-digestion at EBMUD WWTP (Gray *et al.*, 2008)

2.6.2.2 Centralised systems

In a centralised system, food waste pre-treatment takes place at a central food waste processing plant. Centralised food waste processing facilities' primary business is to pre-treat food waste sourced from various industries and make the pre-treated food waste slurries available to resource/nutrient recovery facilities, including co-digesting WWTPs. Centralised food waste facilities are built to pre-treat rich-organic substrates and thus offer the flexibility and capacity to co-process food waste with other types of organic waste, depending on availability (Nghiem *et al.*, 2017). The operation of a food waste processing plant includes removal of inert materials by mechanical processing, hygienisation, removal of fats, oil and grease (FOG) by centrifuging, followed by storing and transporting the pre-treated slurry to WWTPs (Nghiem *et al.*, 2017; Macintosh *et al.*, 2019).

The Oberding food waste processing plant (Germany) has been described as the leading example of a centralised food waste processing plant with up to date technologies (Nghiem *et al.*, 2017; Cecchi & Cavinato, 2019; Macintosh *et al.*, 2019). Food waste is hauled, via trucks, from different sources as far as 200km from the plant. Following the pre-treatment stage, the pre-treated food waste is made available mainly to the local WWTP (Moosburg) and other resource

recovery plants. The pre-treated slurry is transported in tankers with a capacity to maintain a temperature not lower than 90°C to prevent food waste from solidifying (Nghiem *et al.*, 2017). The operation flow of Oberding is illustrated in Figure 2-3. Case studies of wastewater co-digestion with pre-treated food waste from Oberding plant reported that food waste greatly enhanced methane (biogas) potential but also caused problems such as inconsistent biogas quality, solid sedimentation, reduced sludge dewaterability and increased nitrogen backload (Macintosh *et al.*, 2019; Sembera *et al.*, 2019).

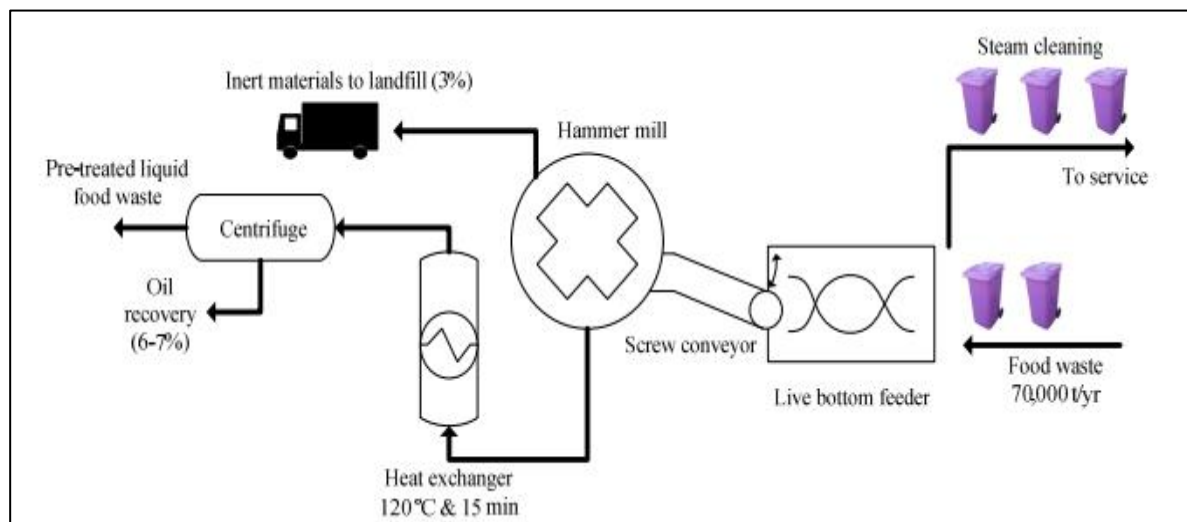


Figure 2-3. Process flow diagram at Oberding food waste processing plant (Nghiem *et al.*, 2017)

2.6.2.3 Food waste disposer systems

Food waste disposers (FWD) or in-sink macerators are devices built on the underside of kitchen sinks that grind food waste into fine particles and flush the effluent into the sewerage system, as depicted in Figure 2-4 (Thomas, 2011). They have been in existence for about a century, initially used for hygiene purposes, but most recently used as an effective means for diverting food waste from landfills (Iacovidou *et al.*, 2012). Although they are common in countries like USA, New Zealand and Australia, to the rest of the world they are still at a novel stage because their impacts to the sewer and WWTP systems have not been well established (Evans, 2012). The use of FWDs is largely being promoted as an alternative sustainable method that reduces transportation costs and odours which are prevalent in manual handling of food systems discussed in Sections 2.6.2.1 and 2.6.2.2.

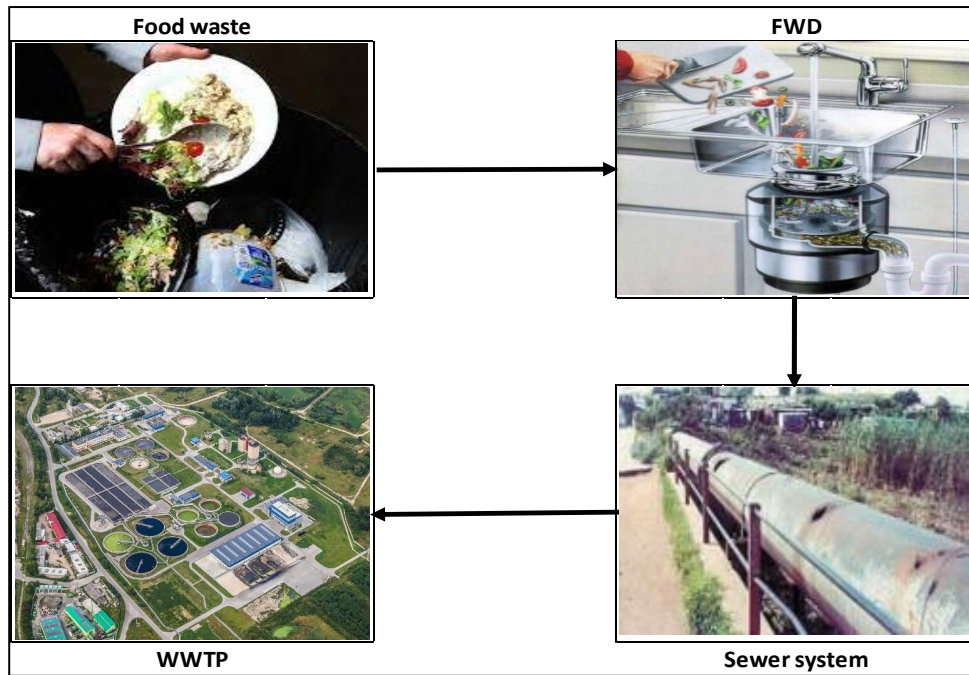


Figure 2-4. Food waste discharge to sewers using FWD

It has been widely reported that the use of FWD greatly enhances biogas recovery at the WWTP (Bernstad Saraiva *et al.*, 2016; Davidsson *et al.*, 2017; Iqbal *et al.*, 2020). However, because of poor knowledge of the impact of FWD on the sewer networks and WWTPs infrastructure, their use is either banned or regulated by several European countries (Thomas, 2011; Iacovidou *et al.*, 2012). Reasons for their objections include (1) energy and water consumption of FWDs, (2) potential corrosion in concrete pipes, (3) clogging due to oil and grease loads, (4) poor effluent qualities, settling in sewerage systems and (5) potential need to retrofit sewer and WWTPs infrastructure (Bolzonella *et al.*, 2003; Guven & Ozturk, 2018; Cecchi & Cavinato, 2019). Nevertheless, the consequences of adopting FWDs will vary from location to location due to variations in food waste characteristics and different levels of sewer infrastructure (Guyen & Ozturk, 2018; Zan *et al.*, 2020).

2.6.3 Discussion

Angula and Ikumi (2022) compared the alternative sustainable systems discussed in Section 2.6.2 using the strength, weakness, opportunity and threats (SWOT) analysis. In summary of their discussion, it was found that the centralised and decentralised systems, which have nearly similar operation processes, also share nearly similar strengths, weaknesses, opportunities and threats.

The centralised system was described to be more efficient than the decentralised system. In addition, food waste handling (collection and transportation) and pre-treatment were identified as the major components of the two systems that made them unattractive and a major challenge to full-scale implementation of food waste and wastewater sludge co-digestion. This is because manual handling of food waste results in significant loss of organic (which results in loss of potential losses and GHG generation) and unhygienic, while pre-treatment is often not economically viable. On the other hand, the FWD system potentially eliminates the need for manual handling and pre-treatment, which are the major setbacks in the decentralised and centralised systems. However, being a novel technology, the impact of using FWD on the sewer and WWTPs has not been well established to date.

The selection of suitable solid waste separation and food waste transport systems will vary from location to location because it is influenced by various factors, including the main driver for solid waste separation. For example, for a system designed to optimise energy recovery, food waste characteristics, food waste handling (i.e., transportation from source to WWTP) and capacity for modelling and simulating WWTPs to optimise energy recovery are critical factors (Mehariya *et al.*, 2018). Nevertheless, this study selected the FWD system for system-wide modelling because its strengths and opportunities outweigh the weaknesses and threats. In addition, the lack of its implementation is mainly because of unestablished facts on its impact on existing sewer systems, which can be addressed in a system-wide study (extending investigations beyond a WWTP boundary, i.e., from the waste sources to the products generated by the WWTP unit operations).

2.7 Biodegradability test

2.7.1 Overview

The two primary tests used to determine the strength of organics (pollutants) present in wastewater are chemical oxygen demand (COD) and biochemical oxygen demand (BOD). Typical methods commonly used to test the biodegradability of wastewater include BOD measurements and respirometry methods (Hulsbeek *et al.*, 2002; Vanrolleghem, 2002). However, these test methods employ complex and costly procedures, and thus most municipalities do not have the capacity to carry out these tests. Moreover, although BOD is closely related to biodegradability, standardised anaerobic biodegradability tests are

recommended to conduct biodegradability tests for wastewaters (Van Lier *et al.*, 2008). Standard anaerobic biodegradability tests are carried out by exposing a test sample to an inoculum. The cumulative amount of methane produced after digestion is complete is equivalent to the quantity of biodegradable organic in the test sample (Van Lier *et al.*, 2008).

2.7.2 Biomethane Potential Test

The biochemical methane potential or biomethane potential (BMP) test is a common standard anaerobic biodegradability test method (Angelidaki *et al.*, 2009; Holliger *et al.*, 2016). The BMP test compares two anaerobic digestion seeding conditions, namely the control and test reactors. The control reactor is fed with AD inoculum only, while the test reactor contains the same inoculum and organic substrate. The control and test reactors are run in parallel. The measured difference in methane potential volume of the test and control reactor is equivalent to the biodegradability of the test sample (Angelidaki *et al.*, 2009; Holliger *et al.*, 2016).

The BMP test is carried out either in a continuously fed reactor or batch reactor. According to Owen *et al.* (1979) cited in Gaszynski (2021), BMP continuously fed reactors reasonably replicate full-scale AD operation, but the test procedure is complex and costly. As a result, BMP batch testing is the commonly used BMP test owing to its simplicity and inexpensiveness. However, the BMP batch test method is not sufficient on its own to carry out wastewater biodegradable organics composition because it does not involve aqueous measurements necessary to track changes in particulates and dissolved constituents taking place during degradation of organics (Gaszynski *et al.*, 2019).

2.7.3 Augmented Biomethane potential

To address the shortcomings of BMP regarding the aqueous measurements, Botha (2015) extended the BMP test to augmented biomethane potential (ABMP). Besides biogas measurement, ABMP also measures additional parameters, including total and soluble COD, FSA, OrthoP, alkalinity, VSS, and pH. Therefore, a complete characterisation of organic substrates or wastewaters can possibly be carried out by employing the ABMP test, which is relatively inexpensive. The ABMP setup is simple and similar to the BMP setup, employing a

control and test rest reactor operated in parallel. Figure 2-5 shows a layout of an ABMP experiment setup.

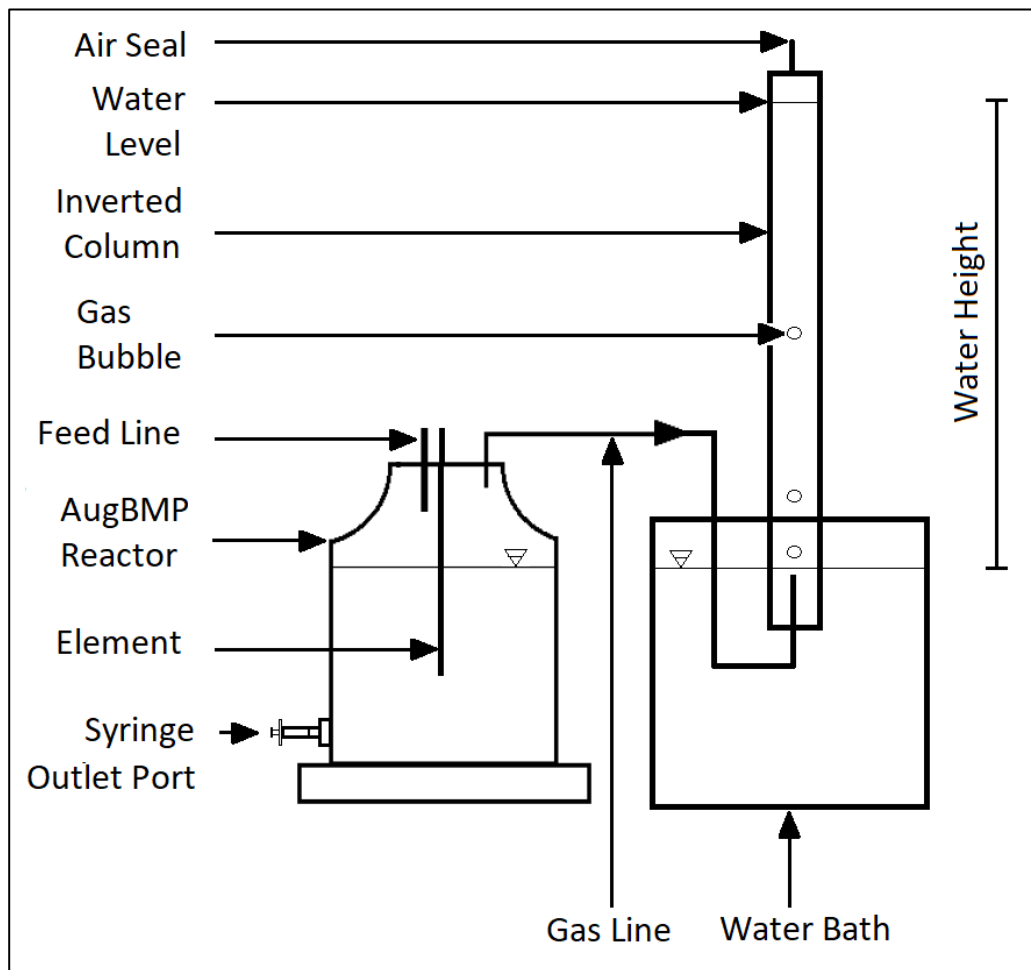


Figure 2-5 An ABMP experiment setup (Gaszynski, 2021)

Both BMP and ABMP use similar gas measurements methods, either volumetric, manometric or gas chromatography. The volumetric gas measurement, which is most common, uses a liquid displacement technique, whereby the gas produced from the reactor is directed through a carrier liquid, and the volume of displaced liquid is equivalent to the volume of biogas produced (Raposo *et al.*, 2011). Gas measurement is the leading cause of inaccuracy in BMP and ABMP, and it primarily results from the choice of carrier liquid (Parajuli, 2011). Gaszynski (2021) have also confirmed BMP errors resulting from gas measurement.

In an attempt to improve the BMP test method, Gaszynski (2021) also augmented the BMP test and developed a novel biodegradability test – the Augmented Biochemical Sulphide Potential

test (ABSP). The ABSP test uses sulphate reducing bacteria instead of methanogenic organisms and is carried out on a sealed reactor without a headspace. In ABSP tests, all measurements are carried out in an aqueous phase, which alleviates the gas measurement error associated with the ABMP test (Gaszynski, 2021).

2.8 Literature review summary

The wastewater treatment sector has embarked on a journey to evolve from the traditional end-of-pipe treatment philosophy to a more sustainable method of circular economy (resource recovery) whereby WWTPs are required to transform into WRRFs. To enhance resource recovery from wastewater requires optimisation of wastewater treatment processes by building mathematical models with capacities to simulate the complex processes which can aid efficient design and operation of WWTPs.

Anaerobic digestion (AD) was identified as one of the units of operation of the WWTP with resource recovery (i.e., mainly biogas and nutrients). Literature provided background into AD modelling with a specific focus on organisms that facilitate the AD process. In addition, a background of the steady-state models, dynamic models and plant-wide models was discussed. Following the review of various models, the steady-state AD model of Ikumi *et al.* (2015) was selected as the most suitable model for use in this project.

The process of energy (biogas) recovery from wastewater was discussed, focusing on how energy recovery is influenced by influent wastewater composition and how energy recovery can be enhanced by co-digesting wastewater and food waste. A rigorous review of solid waste separation and food waste transport system was carried out and identified the use of food waste disposers (FWD) as a potentially more sustainable option, compared to trucking food waste to a WWTP or centralised food waste processing plant.

3. Research Materials and Methodology

3.1 Introduction

In order to determine the existing (i.e., without food waste) and probable (i.e., with food waste) influent wastewater characteristics, laboratory experiments were carried out, followed by some model implementations. This chapter presents a detailed discussion on the research materials, experiment setup and procedure, analytical test procedure, evaluation of experiment results and model description and implementation procedure. The flow of chapter 3 is illustrated in Figure 3-1.

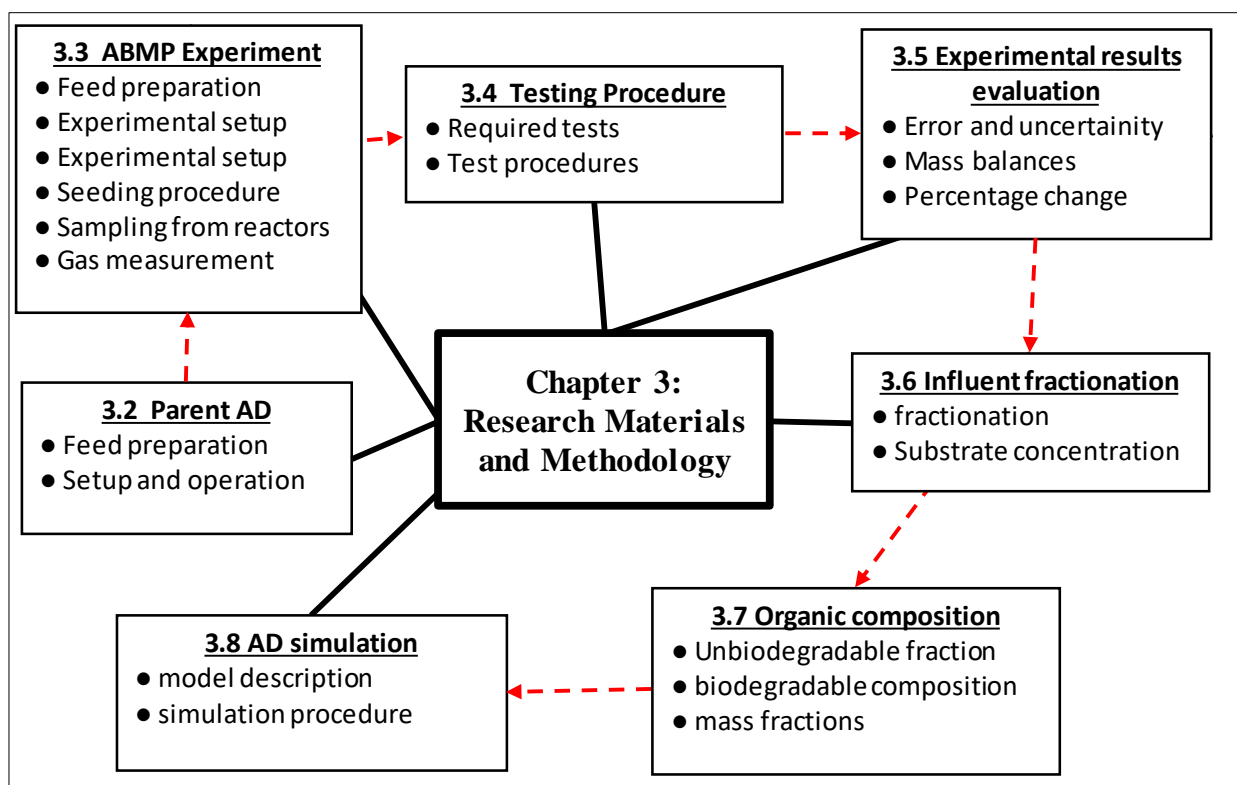


Figure 3-1. Chapter 3 layout

3.2 Parent anaerobic digester

A stable seed or inoculum obtained from an active anaerobic digestion (AD) is required for an augmented biomethane potential (ABMP) experiment. A suitable inoculum can be obtained by feeding an AD with a complex comprising a wide variety of microbes. In this study, two

methanogenic parent anaerobic digesters (PAD) were operated to grow the required seed for the ABMP experiment. Two PADs were set up to ensure there was an adequate seed for ABMP experiments. The PADs were operated at approximately similar sludge age (~50 days) and was fed with primary sludge (PS) obtained from Belville Wastewater Treatment Works (BWWTW) in Cape Town. Figure 3-2 shows a picture of a PAD under operation.

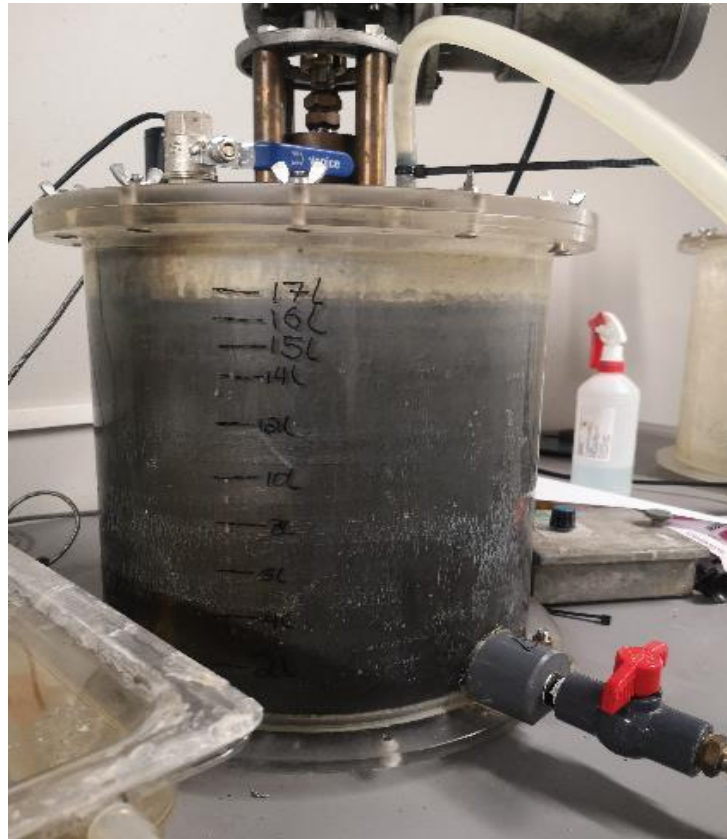


Figure 3-2. A lab-scale parent anaerobic digester (PAD)

3.2.1 Feed preparation

Primary sludge (PS) used for feeding the PADs was sampled from the bottom of the PST pump station at BWWTW. A total of 100ℓ PS sample was collected and transported in 2x 50ℓ drums to the Water Quality Lab (WQL) at UCT. In the laboratory, the PS from one of the drums was ground with a 1000W Russell Hobbs blender (Model number RHB315) to obtain a homogeneous PS mixture. The ground mixture was then transferred into 5x 10ℓ containers. Four of these 10ℓ containers and the remaining 50ℓ drum were stored in a freezer at -20°C. The remaining 10ℓ container was stored in a cold room at -4°C and used for daily feeding the PADs.

Primary sludge (PS) usually undergoes considerable anaerobic fermentation, even at low temperatures of -4°C . This fermentation causes an increase in short chain fatty acids (SCFA) concentration of the stored PS. Therefore, to limit the prospect of characteristic alterations, PS storage required storage under cool temperatures that reduced the rate at which fermentation would occur. This allowed PS to be stored for a maximum period of two months without significant alteration of PS feed characteristics. To prepare frozen samples for daily feeding, a sample container (10ℓ) was removed from the freezer and thawed in the cold room for about 3-5 days. The container was removed from the freezer just before the container stored in the cold room finishes (~5 days). Then, the process was repeated until the feed was finished, upon which more PS was collected from BWWTW.

3.2.2 Setup and operation

The PADs were operated as continuously stirred tanks reactors (CSTRs), which, apart from their volumes, had identical setup and operations. They were made of Perspex material and were fitted with an electric motor, a 200W submersible aquarium fish tank heater and an electric temperature controller. An electric motor fixed at the digester lid was used to provide a continuous stir in the digester to ensure the digester content is kept homogeneously mixed and maintains the same temperature throughout the digester. A fish tank heater was used to heat the digester, while an electric temperature controller was used to regulate the temperature. Additionally, the digesters had an inlet port located at the top of the digester used to feed it and an outlet port near its bottom, which was used to waste the effluent. Figure 3-3 below shows the layout of the PAD.

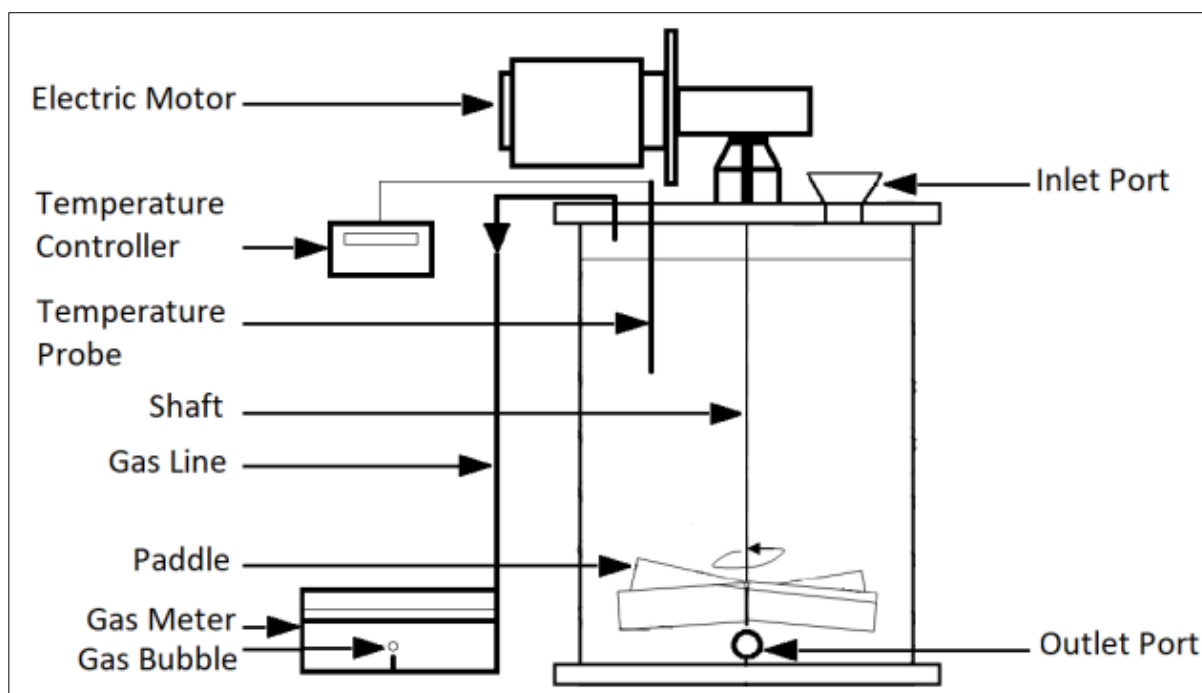


Figure 3-3 Methanogenic PAD setup layout (Gaszynski, 2021)

The anaerobic digestion process produces biogas. The biogas produced left the digester through the gas port (also located at the top of the digester), passes through a gas line and was captured in the wet-tip gas meter. The gas meter contained a tipping mechanism made from plastic and was set on a central pivot of the gauge. This tipping mechanism collects the gas bubbles in the water (contained in the gas gauge). Every time 45mℓ of the gas is collected in the wet-tip gas meter, the tipping mechanism tips and releases the gas. In addition, an electric counter, which recorded the number of tips, was connected to the gas meter. This helped monitor the consistency in biogas production, which was a simple way to ensure that the PAD was working. The PADs were operated under mesophilic conditions at 36°C, and each was fed the same volume and of PS daily (daily batch-wise feeding). Long sludge ages of approximately 50 days were intentionally selected to set steady-state conditions in the PADs. The steady-state conditions were desired in order to reasonably estimate the PAD effluent biomass concentration using steady-state model equations. The biomass concentration was needed to calculate the kinetics, which were ancillary aspects of the project. The two PADs are summarised in Table 3-1.

Table 3-1 Operating conditions of the PADs

AD ID	Start date	Total volume(ℓ)	Operating volume(ℓ)	Headspace volume (ℓ)	Feed volumeℓ/d)	Waste volume(ℓ/d)	Sludge age (d)
1	24/02/2021	20	17	3	0.35	0.35	48.6
2	15/05/2021	30	26	4	0.50	0.50	52.0

Feeding took place once every day and was carried out in the shortest time possible (~1 minute) to prevent oxygen from entering the digester. Furthermore, alkalinity (Na_2CO_3) was added at the start of the experiment to increase digester pH to around seven, where it was maintained.

3.3 Augmented Biomethane Potential (ABMP) Experiment

3.3.1 Overview

The ABMP test is used to measure the potential yield of biogas from anaerobic digestion of organic material besides the wastewater standard characterisation measurements. The standard measurement tested in this study is summarised in Table 3-5. The experimental setup comprised two main seeding conditions: the control batch reactors fed with the inoculum (seed) only and the test batch reactors which was fed with inoculum and organic substrates of interest. Analytical tests were performed on each reactor at the start and end of the experiment. The results were used to determine the composition of the organic substrates, which was the experiment's objective.

3.3.2 Feed preparation

The ABMP reactors were fed as batch reactors. The control reactors were fed with seed (inoculum) only, while the test reactors were fed with the seed and an organic substrate of interest. The substrates of interest in this study were PS, food waste and a blend of PS and food waste. The use of three substrates means three seeding conditions were required for test reactors, resulting in a total of four seeding conditions (one control and three tests). The inoculum used was taken from the PAD on the day the experiment started, while the PS was obtained from Belville Wastewater Treatment Works (BWWTW). The PS was stored in a freezer at -20°C and subsequently thawed in a cold room at 4°C before it was used for feeding.

Real food waste was not readily available. As a result, food waste was manually simulated based on South Africa's typical food waste composition of Nahman & de Lange (2013). The study by Nahman & de Lange (2013) estimated the quantities and composition of food waste from previous waste stream studies that attempted to characterise the overall waste stream in terms of the relative contribution of different waste groups (including food waste). Table 3-2 shows the typical food waste composition, commodity weighed contribution, and the actual products used to prepare food waste for this study. The products chosen to prepare food waste were chosen to best suit the form in which the commodity representative can be found at the household level. i.e., wheat bread instead of wheat grains. Meat products were de-boned and boiled on a kitchen stove for approximately 10 minutes before mixing. Boiling them was done for three reasons, namely:

- i. Heating them will help break down sugars and other enzymes, which changes the hydrolysis rate and subsequently lower the sludge age;
- ii. pathogens and other bacteria groups present in fresh meat are capable of inhibiting the growth of methanogens and
- iii. meat products are rarely wasted in their raw form in households (Cronje *et al.*, 2018).

Furthermore, all solid particles were cut into smaller pieces which enabled them to be weighed out in small quantities and made them easy for grinding.

After weighing the required food waste samples, they were ground to form a liquid food waste slurry. Then, grinding was carried out in a way that simulated a typical food waste disposer (FWD) operation. This was done by macerating food waste with water on a ratio of 1ℓ of tap water per 100g of food waste (i.e., 1ℓ/100g F) for roughly 60 seconds (Zan *et al.*, 2018). In the absence of an actual FWD /macerator in the WQL, a 1000W Russell Hobbs blender (which was also used to macerate PS) was used for macerating food waste. Given that the blender's capacity is only 1.75ℓ and the food mass was 1800g, maceration was done in 18 batches (1ℓ water +100g FW each batch). The 18 batches of the macerated food waste slurries were mixed in a big bucket after that. In the remainder of this report, the water and food waste mixture prepared above is referred to as food waste. Table 3-2 shows the typical food waste composition according to Nahman & de Lange (2013) and the actual preparation of food waste in this study.

Table 3-2 Typical household food waste composition and weighed representative

Relative contribution to household food waste (Nahman & de Lange, 2013)				Actual products used to prepare food waste		
Commodity group		Commodity representatives		Product description	Req. mass(g)	Actual mass (g)
Group	Weight	Product	Weight			
Cereals	26%	Maize	75%	Maize meal porridge	351.00	351.15
		Wheat	25%	Whole grain bread	117.00	117.15
Roots and tubers	9%	Potatoes	81%	Potatoes	131.22	131.29
		Onions	19%	Onions	30.78	30.99
Oil seeds and pulses	4%	Sunflower	65%	Sunflower cooking oil	46.80	46.90
		Soya beans	35%	Savoury soya mince	25.20	25.33
Fruits and vegetables	44%	Tomatoes	45%	Fresh tomatoes	356.40	356.47
		Citrus	55%	Citrus oranges	435.60	435.67
Meat	7%	Chicken	55%	Boiled chicken thighs	69.30	69.28
		Beef	27%	Boiled beef mince	34.02	34.12
		Lamb	6%	Boiled lamb steak	7.56	7.63
		Pork	12%	Boiled pork steak	15.12	15.25
Seafood	2%	Hake	100%	Fried hake fillet	36.00	36.07
Milk	8%	Milk	100%	Full cream milk	144.00	144.12
Total	100%		-		1800.00	1801.42

After food waste mix preparation, the container containing food waste was stored in the freezer at -20°C and subsequently thawed in a cold room at 4°C before it was used for feeding. Lastly, the blend of PS and food waste was prepared on the day of seeding.

3.3.3 Experimental Setup

The ABMP experiment was set up for volumetric gas measurement and was adopted from (Gaszynski *et al.*, 2019). For statistical significance, the experiment was carried out in triplicates, therefore utilising three reactors for each seeding condition (see Section 3.3.4 for more about seeding). Four seeding conditions were carried out, resulting in a total of twelve reactors required for the experiment. The setup comprises batch-fed AD reactors, a water bath, and inverted columns supported by a purpose-made rig. Glass aspirator bottles were used as the reactor in this experiment. Due to not having enough bottles of the same size available for the experiment, a

combination of three different sizes of bottles were used. However, the difference in the control reactor volume sizes was accounted for in the evaluation of the results. The aspirator bottle volumes used are summarised in Figure 3-3.

Table 3-3. Summary of aspirator bottle volumes used

Seeding conditions	Quantity and volume of aspirator bottles		Total
	2.5ℓ	6ℓ	
Control reactors	2	2	4
Test reactors 1	-	3	3
Test reactors 2	-	3	3
Test reactors 3	-	3	3
Total	2	11	13

Control reactors were shared between this project and another project that was run parallel to this project as discussed in Section 1.4, which influenced the choice and number of aspirator bottles used for the control reactors. Furthermore, in this report, the two types of control reactors are differentiated as type I control reactors (6ℓ) and type II control reactors (2.5ℓ).

The top of the reactor was covered with a rubber stopper with three holes drilled on it. A tube was inserted in the first hole, and this hole served as the feed inlet. The second hole was used for biogas escape from the reactor, while the third hole served as a conduit for a heater cable. Additionally, the inlet tube was kept airtight during the entire experiment to maintain anaerobic conditions. Another reactor hole located just above its bottom served as an outlet for taking samples out of the reactor. The outlet port was sealed with a rubber stopper and a syringe. A syringe was used to draw a sample from the reactor. A syringe was preferred over a tap valve because it pushes the fluid back into the reactor after sampling, preventing particles from accumulating in the outlet port.

Provisions were made to ensure that usual mesophilic anaerobic digester operating conditions were preserved. The reactors' mesophilic temperature was maintained at 34°C by using 100W underwater fish-tank heaters. Moreover, the reactors were mixed manually about two times each day by gently shaking the reactor in a horizontal motion for around 20 seconds. Maximum efforts were made to guarantee that the reactor has no liquid leaks, is gas-tight, and that any biogas

generated exits solely through the biogas escape pipe. Additionally, neutral pressure was maintained inside the reactor, as illustrated in Figure 3-4.

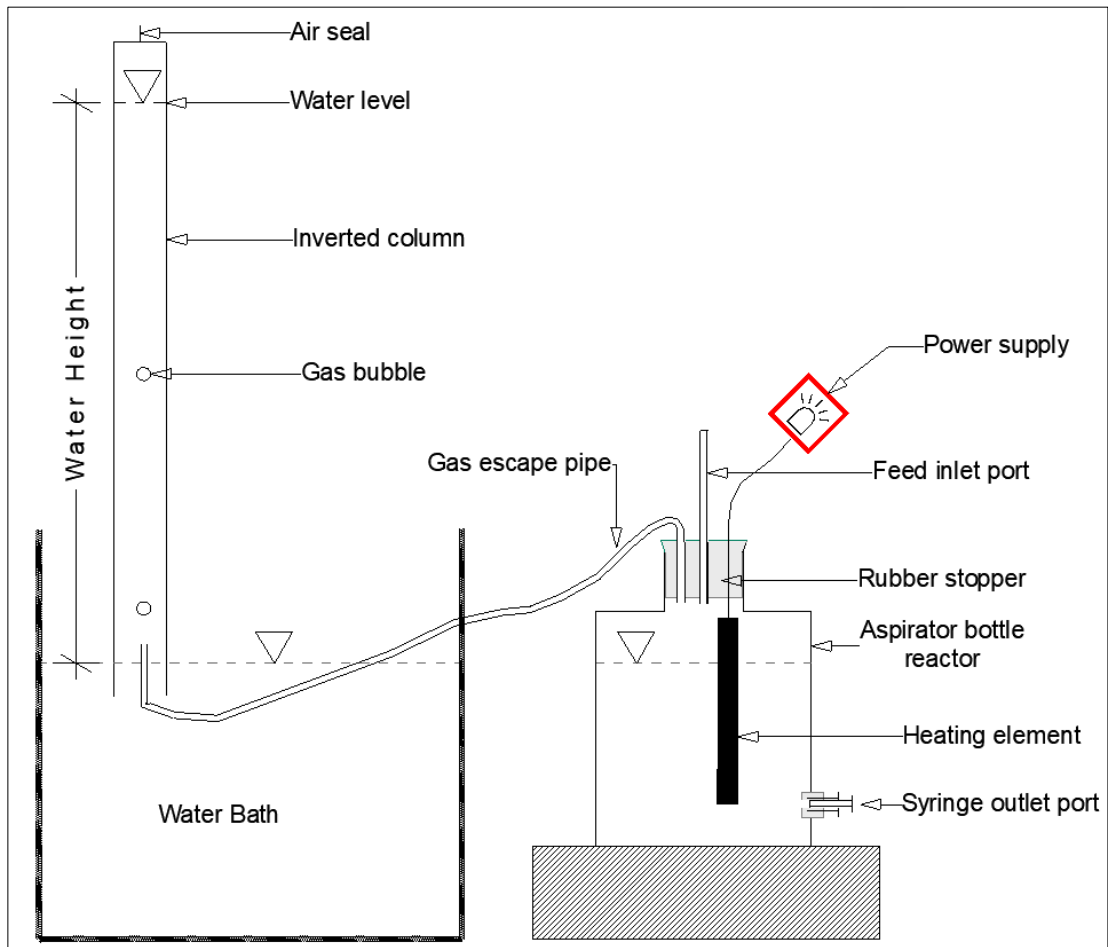


Figure 3-4. ABMP experimental setup

The gas escape hole was connected to the bottom of the inverted column, which was submerged in the water bath. Then, inverted columns were placed on a custom-built rig. The rig used in this experiment was made by Gaszynski (2021) consist of twelve inverted columns. The columns, which were made from Perspex, have a height of 2m, an interior diameter of 60mm and were graduated using a measuring tape pasted on their outer surface. However, three columns on this rig were used by a parallel study (parallel study is discussed in Section 1.4). Since twelve columns were required for this project (a column for every reactor), three additional columns were added to the rig as a temporary solution. As a substitute for columns, 1ℓ graduated volumetric glass cylinders were used. The purpose of using graduated columns is to determine

the produced gas volume during the experiment. Therefore, it was assumed that different column types for gas collection do not affect the experiment results.

The inverted columns were submerged in a water bath filled with tap water and kept at room temperature. The Perspex columns were filled with water from the bath, which was sucked into the inverted column by a vacuum pump connected at the top of the column. The volumetric cylinder columns, which only have an opening on one end, were filled to the 1 l mark with tap water, flipped upside down while covering the opening with the hand, and submerged in the water bath. Once the column was positioned, it was then bolted on the rig to prevent them from moving during the experiment.



Figure 3-5 An ongoing ABMP experiment photograph

3.3.4 Seeding Procedure

Seeding refers to the process of feeding the batch reactors just before starting the ABMP experiments. The experiment used two main general seeding conditions recommended by Angelidaki *et al.* 2009 and Holliger *et al.* (2016). The first seeding condition was the control batch reactor, which consisted only of the inoculum (biomass from PAD). The second seeding condition was the test batch reactor which was fed with the inoculum and substrate. Since two substrates were under investigation in this project, more than one test batch reactor was required. With the substrates being PS and food waste, the following substrate combinations were used in this project: (i) PS only, (ii) Food waste only, and (iii) PS + food waste (1:1 by volume). This resulted in a total of four distinct seeding conditions (including the control batch reactor). The same inoculum mass was added in all mixtures (controls and tests) as recommended by (Holliger *et al.*, 2016). This was done to set a clear baseline for the products released from the control reactors. Therefore, any product released above this baseline in test reactors was due to the substrate.

It is recommended that the inoculum to be used for ABMP should either be used as fresh as possible or degassed if used from storage (Holliger *et al.* 2016). For this project, fresh biomass taken directly from the PADs on the day the experiment began was used as the inoculum. Residual biodegradable organics in the inoculum were accounted for in the control reactors. The biomass from the two PADs was first mixed before diluting it with distilled water (1:1 by volume) before seeding the ABMP. Dilution of the original biomass was necessary to ensure there was enough biomass for all the reactors. This diluted biomass was then used for seeding all the reactors. Therefore, the term biomass in this section refers to this initially diluted biomass. As recommended by Angelidaki *et al.* (2009), it was ensured that the substrate concentration(COD, TSS or VSS) in the reactor is less than the inoculum concentration. This was done by first testing the inoculum and substrates' COD concentrations, and after that, appropriate seeding ratios were determined empirically.

Only inoculum and water were used in the control reactors. The mixture was prepared in a 20ℓ bucket by mixing biomass and distilled water. This resulted in a mixture of 14ℓ, which was distributed to the four individual control reactors as shown in Table 3-4. Type I control reactors were labelled C-1 and C-2, while type II control reactors were labelled C-3 and C-4. Because

both type I and type II control reactors were fed the same mixture, the concentrations in all control reactors are the same but have different masses caused by the difference in reactor volumes.

The three test seeding conditions contained inoculum (biomass), substrate and water. The substrates were prepared as follows; (i) 1ℓ of PS only (substrate 1), (ii) 1ℓ food waste only (substrate 2) and (iii) 0.5ℓ PS + 0.5ℓ food waste (substrate 3). The test samples containing substrate 1, substrate 2 and substrate 3 are referred to as test A(TA), test B(TB) and test C(TC), respectively, in the remainder of the report. Test A reactors were labelled TA-1, TA-2, TA-3, whereas test B reactors were labelled TB-1, TB-2, TB-3 and test C reactors were labelled TC-1, TC-2 and TC-3. Preparation of PS and food waste used is described in Section 3.3.2, while the inoculum was identical to that used in the control sample. For each test sample, a total of 15ℓ sample was prepared by mixing the inoculum, distilled water and substrate before distributing the mixture to three reactors in equal volumes for each test as shown in Table 3-4.

Table 3-4 ABMP experiment starting mixtures

Total mix						
Component volumes	unit	Control	Test A	Test B	Test C	
biomass	ℓ	8.00	8.00	8.00	8.00	
Water	ℓ	6.00	5.80	5.80	5.80	
Primary sludge	ℓ	0.00	1.20	-	0.60	
Food waste	ℓ	0.00	-	1.20	0.60	
Total volume	ℓ	14.00	15.00	15.00	15.00	
Individual reactors						
	unit	Control I	Control II	Test A	Test B	Test C
Mix volume added	ℓ	5.00	2.00	5.00	5.00	5.00

Even though the same mass of inoculum was added to both mixtures (control and tests), the concentration of the inoculum was different. Unequal mixing conditions caused these unequal concentrations. This varying inoculum concentration needed to be accounted for to set the same baseline in all reactors. Therefore, since the tests and control mix volume were 15ℓ and 14ℓ

respectively, it resulted in the concentration of the inoculum in the test reactors to be diluted by 1.071 (i.e., $15 \div 14$). This dilution factor was crucial to consider during substrate fractionation and composition determination, as discussed in section 3.7.3 and 3.6.3.

It was vital to ensure that the mixtures were not contaminated during and after mixing and that the reactors maintained inert conditions. To avoid contamination and substrate degradation by oxygen, mixing and transferring the mixture to reactors were performed as quickly as possible. The mixture was poured into the reactor via the top opening and was closed immediately with the specially prepared rubber stopper. Furthermore, the reactors were continuously flushed with nitrogen gas before and during the pouring of the mixture. After pouring, the reactor headspace was again flushed with nitrogen and sealed with a rubber stopper as quickly as possible. Flushing with nitrogen ensured initially inert gas-phase conditions in the reactors.

3.3.5 Sampling of reactors

Sampling from reactors and testing after that was required to track changes in reactor parameters. In addition, the change in reactor concentrations throughout the experiment is used to determine the substrate composition. Therefore, the major reactor sampling points were the experiments' first (day 0) and last (day end) days. This project's scope did not include determining kinetics parameters such as hydrolysis and substrate uptake rates; therefore, reactor composition was not prioritised between day 0 and day n points. However, various intermediate sample points were collected and tested between days 0 and end to check the consistency and trend of changes taking place in the reactors. The last day was chosen when there was no substantial change in reactor activity, i.e., no significant biogas generation.

A sample was obtained from the reactor through a syringe located on its outlet port, as shown in Figure 3-4. Unlike a tap valve, a syringe allows the residual effluent to be pushed back into the reactor after sampling. Before sampling, the reactor was vigorously mixed by shaking it with hands. During sampling, a nitrogen gas-filled gas bag was connected to the feed outlet. This was done to avoid the negative pressure that would result if the reactor had been sealed during sampling. Nitrogen is an inert gas, and it was found to be suitable to maintain anaerobic conditions in the reactor. A sample between 70-100 mL was drawn from the reactor, and pH was

measured immediately after sampling. Other additional measurements carried out on the sample are discussed in Section 3.4.

3.3.6 Gas measurement

Biogas produced by the ABMP reactors was captured on the inverted water columns. In other words, the biogas produced in by the reactor displaces the water in the column, and the volume of water displaced is equivalent to the volume of biogas produced. For control reactors, 1000 ml graduated cylinders were used as columns which allowed the produced biogas volume to be read from the columns directly. The test reactors used purpose-made 60mm diameter columns with a measuring tape attached, which allowed the gas volume to be calculated from height drop and column diameter.

To capture the methane potential curve, regular measurements of columns' water levels were taken. However, the gas volume inside the inverted columns was impacted by the column water level relative to the bath water level. As a result, column pressure adjustments were made when calculating the biogas's methane molar and COD equivalents. The bathwater level was at atmospheric pressure. However, the column water level was higher than the bath water level, resulting in low gas pressure in the water column. This means, the higher the column water level relative to the bath water level, the larger the volume the biogas occupies. Therefore, the column pressure was calculated using Equation 3.1.

$$P = \rho gh \quad 3.1$$

Where; ρ = density of water

$$g = 9.81 \text{ m/s}^2$$

h = column water level(height) relative to bath water level

3.4 Experimental testing methods

3.4.1 Overview

Table 3-5 summarises the analytical measurements performed on the samples collected from the ABMP reactors. The analytical tests were carried out using wet chemistry analysis.

Table 3-5. Measurements performed on the ABMP reactor

COD	Nitrogen	Phosphorus	Solids	Alkalinity	pH	Gas
Total	TKN	TP	TSS	Carbonate	pH	Gas composition
Soluble	FSA	OP	VSS	Ammonium		Methane COD mass
			ISS	Phosphate		
				VFA		
				Total		

Except gas composition test, all other tests were conducted in the Water Quality Lab (WQL) (Department of Civil Engineering, UCT). Gas composition test was carried out in the Centre for Bioprocess Engineering Research (CeBER) (Department of Chemical Engineering, UCT). These experimental tests were used for substrates characterisation and in modelling carried out under this project. The tests are described in further detail from Section 3.4.2 to 3.4.9.

3.4.2 COD tests

Chemical oxygen demand (COD) is the measure of electron donating capacity or energy of the organics. In this study, it was required to measure the unfiltered (total) and unfiltered(soluble) COD. The COD tests were carried out in accordance with Standard Methods (1985), which uses dichromate and sulphuric acid open flux method, followed by titration with ferrous ammonium sulphate (FAS). In addition, the test principle uses standard potassium dichromate ($K_2Cr_2O_7$) solution (~ 0.25 Normality) as an electron acceptor while the organics contained in the sample and FAS are the electron donors. To ensure that all tests use same sample, the sample used for unfiltered COD test was taken from the sample used for TKN and TP tests (discussed in Sections 3.4.3 and 3.4.4). Similarly, the sample used for filtered COD was taken from the sample used for FSA, OP, VFA and alkalinities tests (discussed in Sections 3.4.5 and 3.4.7). Furthermore, in

some parts of this thesis, the phrases total and unfiltered COD as well as soluble and filtered COD may have been used interchangeably.

COD testing was carried out immediately (as fast as possible) after sampling. The sampling process was described in Section 3.3.5. The filtered samples were prepared by centrifuging a 50ml in a centrifuge for 10 minutes at 6000 rpm. After that, the centrifuged sample was filtered through a glass fibre (S&S GF 52), followed by a 0.45µm membrane (S&S ME 25/21 ST) filter paper using a vacuum filter. Additionally, all samples (filtered and unfiltered) were diluted to appropriate dilutions for required tests.

3.4.3 TKN

Total Kjeldahl Nitrogen (TKN) is the measure of combined organic nitrogen (OrgN), and free (NH₃) and saline ammonia (NH₄⁺) (FSA) (i.e., excluding oxidised nitrogen such as NO₃ and NO₂). TKN was measured using the micro-Kjeldahl distillation method (Standard Methods, 1985, Method 420B). The test procedure involves digesting the test sample with a digestion mix (containing H₂SO₄, HgO and K₂SO₄ solutions) which releases organically bound nitrogen as ammonia (Wentzel *et al.*, 2003). This is then followed by steam distillation with NaOH to vapourise FSA, and the vapour is collected in boric acid. Finally, the sample collected in boric acid was titrated with standard sulphuric acid (H₂SO₄) solution (Normality=0.001N). Only unfiltered TKN measurement was measured in this study. The sample preparation is discussed in section 3.4.2.

3.4.4 TP

Total Phosphorus is a measure of combined ortho-phosphate (OP) species (i.e., PO₄³⁻, HPO₄²⁻, H₂PO₄⁻ and H₃PO₄) and organic phosphorus (OrgP). TP was measured using the persulphate digestion method (Standard Methods, 1985, Method 424 CIII). First, the test sample was digested using H₂SO₄ and H₂S₂O₈ (potassium persulphate) solutions on the boiling water bath at 96°C. Following the digestion, the samples were tested using the Vanadomolybdate ('colour') reagent in a spectrophotometer (Standard Methods, 1985, vanadomolybdophosphoric acid colourimetric method). The colour intensity of the sample was analysed using the Gallery Discrete Analyser (ThermoFisherScientific Gallery).

3.4.5 FSA and OP

The concentration of FSA and OP were measured in the Gallery Discrete Analyser (or simply the gallery). A filtered sample (as prepared in 3.4.2) of about 2mℓ was used to test both FSA and OP. The Gallery used ammonia and phosphate standard reagents² to test for FSA and OP, respectively.

3.4.6 Solids

The Solids tests gives a quantitative indication of the solids contained in the reactors. The solid classes measured include the concentrations of total suspended solid (TSS), volatile suspended solids (VSS) and inorganic suspended solids (ISS).

The concentrations of total suspended solids (TSS) and volatile suspended solids (VSS) were determined using Standards Methods (1985, 2540(D) and 2540(E), respectively. To measure TSS and VSS, A 50 mℓ sample was centrifuged for 10 minutes at 3500 rpm in a centrifuge. Following centrifugation, the supernatant in the tube was decanted and the solids accumulating at the bottom of the tube were transferred to an evaporating dish and dried in the oven for 24 hours. TSS concentration was then calculated as equivalent to the remaining mass of oven-dried solids. Following TSS measurement, the evaporating dish (containing its dried sample) was incinerated in a furnace at 550°C for about 20 minutes to determine the concentration of inorganic suspended solids (ISS). ISS was calculated using the mass of solids remaining after incineration. The concentration of VSS was calculated by subtracting ISS from TSS, i.e.

$$VSS = TSS - ISS$$

² The reagents were supplied by the Gallery Discrete Analyser manufacturer and the composition of these reagents is not disclosed

3.4.7 Alkalinity and VFA

The 5-pH point titration method was used to measure alkalinity and volatile fatty acids (VFA) (Moosbrugger *et al.*, 1993). In addition to total alkalinity, the method also allows the determination of subspecies alkalinities such as hydrogen alkalinity, ammonia alkalinity. The test used a filtered sample of 10-50 ml that was titrated to five predetermined pH points with a dilute hydrochloric acid (HCl) while gently stirring the sample. The predetermined pH points are the initial sample pH, 6.7, 5.9, 5.2 and 4.3. The cumulative HCl titrated to the sample, and the pH closest to each of the predetermined points are entered into the 5-pH point titration program. The program then calculates the H₂CO₃ alkalinity (mgCaCO₃) and VFA (acetate, A_T). In addition to HCl volumes and pH titration points, sample FSA and OP measurements (as determined in Section 3.4.5) needed to be entered into the 5-pH point titration program to determine the ammonia and phosphate subspecies alkalinities.

3.4.8 pH

The pH was determined using an Accsen pH metre and an Accsen pH probe. To minimise significant carbon dioxide loss, pH was measured as fast as possible after the sample was taken from the reactor.

3.4.9 Gas production and composition

The biogas produced by the reactors was captured in the water column. The biogas volume was then determined as equivalent to the volume water displaced in the column as discussed in Section 3.3.6. This means, the volume of biogas produced was measured indirectly by measuring the column water level. Therefore, the columns' water levels were taken regularly to give the cumulative biogas volume and methane potential curve of each reactor.

Biogas composition (CH₄ partial pressure) was measured with a Shimadzu gas chromatograph (GC) (Nexis GC-2030). The biogas sample was taken from the reactor headspace through the feed line using a syringe. To avoid gas loss from the syringe, the gas samples were taken just before testing took place. The Shimadzu GC used a flame ionisation detector (FID) to determine the fraction of methane in the biogas. The test was carried out by injecting a 50µl of biogas with

the column oven and FID temperatures set at 170°C and 250°C, respectively. Lastly, a standard curve was generated using 24.08% and 48.13% methane. Nitrogen gas(N₂) was used as a makeup gas at a flow rate of 24.0 mL/min.

3.5 Experimental results evaluation

3.5.1 Overview

The repeatability and accuracy of the experiment result were evaluated using two approaches. The first approach was the experimental error and uncertainty, which uses statistical analysis and the second approach was the mass balance method which is based on the mass conservation principle. The experimental and error and uncertainty and the mass balanced methods are explained in Sections 3.5.2 and 3.5.3.

3.5.2 Experimental error and uncertainty

To guarantee the repeatability of the experiment, the ABMP experiment was conducted in triplicates (i.e., by replicating each seeding condition three times), which allowed statistical analysis of the measured data.

The triplicates were fed with the same mixture, and the experiments were conducted in parallel and under similar conditions. However, replication does not guarantee accurate and reliable results because systemic and random errors are very common, especially in laboratory experiments, which leads to inaccurate data. Therefore, the repeatability and accuracy in this project were evaluated by calculating the mean and standard deviation.

The mean is an indicator of the central value for multiple replicates for a particular data point, while the standard deviation measures the deviation of the measured replicates around the central value (mean). In other words, the mean was used to represent the central point of all the replicates analysed for each seeding condition, while standard deviation was used to show the spread of the replicates' results relative to the central point (mean). The mean and standard deviation were calculated using Equations 3.2 and 3.3, respectively.

$$\langle x \rangle = \frac{1}{N} \sum_{i=1}^N x_i \quad 3.2$$

$$\sigma_x = \sqrt{\frac{1}{N-1} \sum_{i=1}^N (x_i - \langle x \rangle)^2} \quad 3.3$$

Where:

$\langle x \rangle$ - mean

N - Total number of replicates

x_i – Individual replicate value

σ_x - Standard deviation

For this project, instead of analysing results for every individual replicate, the mean value, which (central point of the combined replicates) was used. Therefore, in some cases, the experiment results are presented in terms of mean and standard deviation in the format of $x = \langle x \rangle \pm \sigma_x$. However, in some cases after careful analysis of the results, some replicates' results were not included in the mean calculation.

3.5.3 Mass Balances

Mass balances are governed by the fundamental principle of mass conservation, which states that the mass into the system is equal to the mass out of the system. Therefore, mass balances are a suitable method to check the reliability and accuracy of the experimental results. Mass balance checks were carried out on COD, TKN and TP over the ABMP experiment. However, obtaining 100% mass balances in laboratory experiments is challenging due to systematic and random errors, such as instrument calibration, poorly maintained equipment, and inaccurate readings. Therefore, it was adopted that COD balances within 100%±10% and TP and TKN balances with balances within 100%±20% indicates accurate and reliable results. However, in this study, COD balances within 100%±20% were also considered accurate after careful data evaluation. The general formula for calculating mass balance is given in Equation 3.4.

$$\text{Mass Balance} = \frac{\text{Mass flux}_{eff}}{\text{Mass flux}_{inf}} \times 100 \quad (\%) \quad 3.4$$

3.5.3.1 COD Mass Balance

The ABMP experiment reactors are simply AD reactors, whereby COD from the influent organic substrate is converted to biogas (comprised mainly of CH₄ and CO₂) and particulate AD biomass. Therefore, to carry out a COD balance, COD contained in the influent, effluent, and AD evolved gas were accounted for. The ABMP reactors were batch fed once; therefore, influent COD mass was equal to the COD measured on the starting day of the experiment multiplied by the total feed volume of the ABMP reactor. The effluent streams include samples drawn from reactors for analytical tests (as discussed in Section 3.3.5), biogas (i.e., the COD of all the CH₄ evolved during the experiment) and the COD mass remaining in the reactor at the end of the experiment. The distribution of COD during the ABMP experiment is depicted in Figure 3-6.

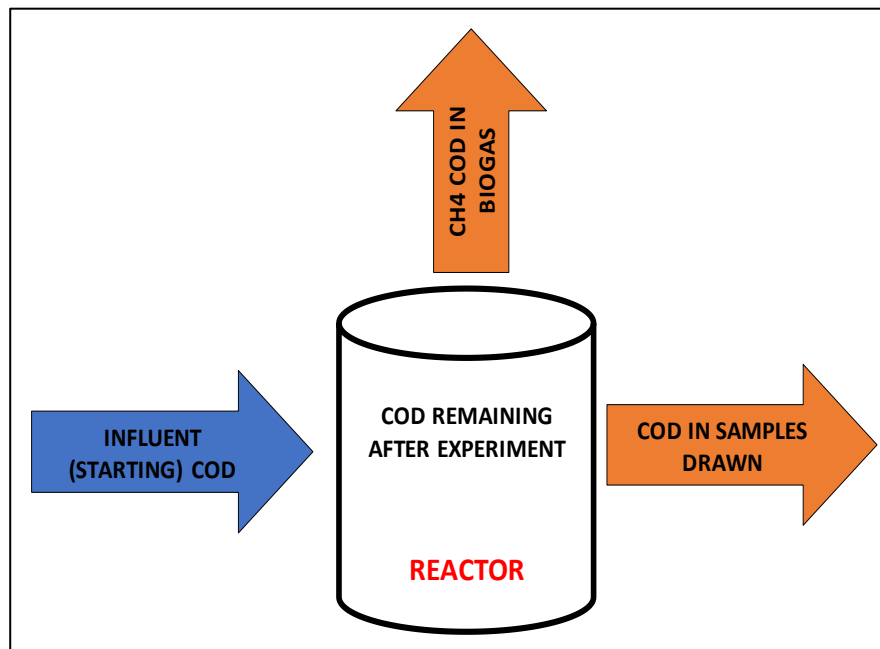


Figure 3-6. ABMP COD influent and effluent streams

The ABMP reactor COD balance is summarised by Equation 3.5.

$$MCOD_{Inf} = MCOD_{CH_4} + MCOD_{Rem} + MCOD_{Samp} \quad (\text{mgCOD}) \quad 3.5$$

The COD mass in the influent was calculated by multiplying the starting COD concentration by the liquid volume fed into the reactor. The COD mass drawn or sampled from the reactor was determined by multiplying each sample's liquid volume by its measured concentration. These individual COD masses drawn from the reactor were added together to form accumulated sampled COD mass.

The calculation of equivalent methane COD mass in biogas had a higher level of complexity. Biogas volume was measured using inverted columns, and the partial pressure of methane was determined using gas chromatography, as previously mentioned in Sections 3.3.6 and 3.4.9. Therefore, the daily methane gas production is the product of methane partial pressure and cumulative biogas volume. By use of universal gas law, it was possible to calculate methane molar equivalent. Methane COD equivalent is then equal to methane molar equivalent multiplied by 64 gCOD/mol. i.e.

$$n = \frac{PV}{RT} \quad (\text{mol}) \quad 3.6$$

$$MCOD_{CH_4} = 64000n \quad (\text{mgCOD}) \quad 3.7$$

Where; P = gas pressure (as described in Section 3.3.6)

R = universal gas law constant

T = atmospheric temperature

The COD mass balance and thus Equations 3.5 to 3.7 can then be combined into Equation 3.8.

$$\begin{aligned}
& COD_{Inf} \times Vol_{Inf} \\
&= 64000 \frac{PV}{RT} + COD_{rem} \times Vol_{rem} \\
&+ \sum_{i=day\ 1}^{Last\ day} (COD_{samp} \times Vol_{samp}) \quad (mgCOD) \quad 3.8
\end{aligned}$$

3.5.3.2 TKN and TP Mass balances

The conservation of TKN and TP masses were also checked using mass balance. During AD, the hydrolysis of complex organics results in FSA and OP released from organic N and organic P, respectively, into the aqueous solution. Some of the released FSA and OP are used up as nutrients for the AD biomass growth, while the remainder stays in the aqueous phase to form the AD effluent (i.e., all influent TKN & TP transformed components remain part of the TKN & TP in the effluent). This means the influent concentrations of TKN and TP and effluent concentrations of TKN and TP, respectively, are equal. This also translates to equal influent and effluent masses because unfiltered TKN and TP measurements include total flux of N and P, respectively, accounting for both inorganic and organic concentrations. The TKN and TP mass balances were calculated using Equation 3.4 above.

3.5.4 Percentage change

The percentage (%) change was used to describe the average change in concentration of different parameters (for each seeding condition). Equation 3.9 was used to calculate the % change.

$$\% \text{ change} = \frac{\text{Avg. initial conc.} - \text{Avg. final conc.}}{\text{Avg. initial conc.}} \times 100 \quad (\%) \quad 3.9$$

Positive per cent change is reported as an increase, while negative per cent change is reported as a decrease in concentration.

3.6 Influent fractionation

3.6.1 Overview

In wastewater treatment, influent substrates can be fractionated into the four main organic groups namely:

- i) Biodegradable soluble organics (BSO), which further fractionate into volatile fatty acids (VFA) and fermentable biodegradable soluble organics (FBSO);
- ii) Biodegradable particulate organics (BPO);
- iii) Unbiodegradable soluble organics (USO) and
- iv) Unbiodegradable particulate organics (UPO).

Based on each group's COD, C, H, O, N and P concentrations, each group is assigned a unique CHONP composition (more to this in Section 3.7.3). A CHONP composition for each of the organic groups is a required input for most wastewater models such as PWM_SA model. Figure 3-7 shows an example of COD fractionation into different groups.

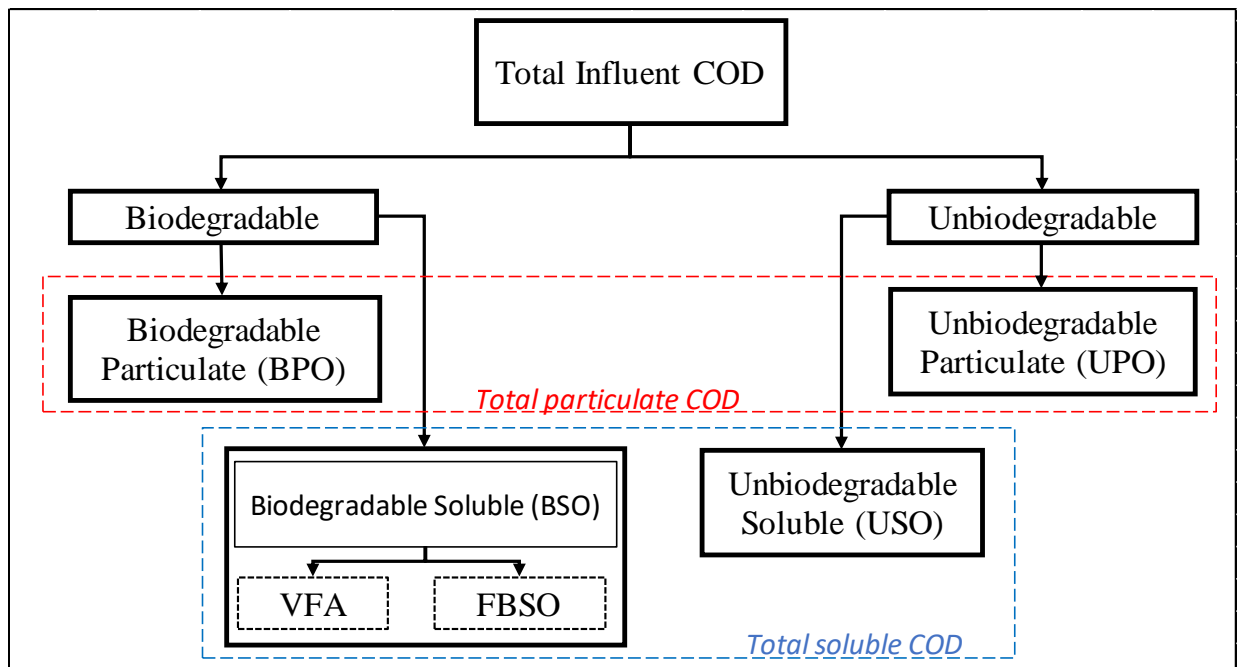


Figure 3-7: Example of COD fractionation

Substrate fractionation in this project was based on the observed changes in the ABMP control and test reactor. This is possible because, during AD, biodegradable organics are broken down, and as a result, organics and inorganics materials are released into the bulk liquid or as gas. Therefore, the changes observed in measured parameters between the start and end of the experiment was attributed to biodegradable organics.

3.6.2 Substrate concentration

Influent fractionation required the substrate concentration to be determined. Although only test reactors contained substrate, the determination of the substrate concentration required both control and test reactor results. During the experiment, residual biodegradable organics in the inoculum (both in control and test reactors) and substrate biodegradable organics (in the test reactors only) were broken down, resulting in a release of inorganics into the aqueous solution and biogas. In other words, the changes observed in the reactors during the experiment were due to the breakdown of biodegradable organics. Therefore, for each reactor, the concentrations of the biodegradable organics (various constituents) were determined by taking the difference of the experiment's initial concentrations and end concentrations. The determination of biodegradable organics' various concentrations can be simplified as follows:

- a) The carbon (C) content was based on weak acid/base chemistry whereby the release of C was calculated from the changes in (1) CH₄ and CO₂ concentrations, and (2) H₂CO₃ alkalinity.
- b) The nitrogen (N) content was calculated from the change in FSA concentration
- c) The phosphorus (P) content was calculated from the change in OP concentration
- d) The COD content was determined from the change in COD concentration
- e) The VSS content was determined from the change in VSS concentration
- f) The contents of hydrogen (H) and oxygen (O) is not measured directly, however their mass ratios can be calculated if the contents listed from a)-e) above are known

For both control and test reactors, these biodegradable concentrations results were required to quantify the biodegradable organics contained in the inoculum and substrates: The control reactors were used to establish the baseline that quantified the products released due to the breakdown of biodegradable organics present in the inoculum. Therefore, products released above this baseline inside the test reactors were due to the substrate present in the reactors. The concentration of the substrate in the test reactor is given by Equation 3.10.

$$\text{Sub. Concentration} = [(Test_{end} - Test_{start}) - (Control_{end} - Control_{start})] \quad 3.10$$

3.6.3 Influent fractionation

Equation 3.10 indicates that the substrate's biodegradable concentration is represented by the products released or taken up in the test reactor minus the influence of the inoculum in the test reactor. Using the concentration obtained as discussed in Section 3.6.3, the fractionation of the influent can be summarised below:

- i) Residual biodegradable materials present in the inoculum was quantified by the decrease in COD and VSS of the control reactor throughout the experiment.
- ii) The concentration of COD and VSS at the end of the experiment represented unbiodegradable material present in the control reactors. This is because it was ensured that the sludge age was long enough to ensure the degradation of all residual biodegradable organics.
- iii) The decrease of COD and VSS between the start and end of the experiment in the test reactors quantified biodegradable material present in the inoculum and the selected substrate.
- iv) Lastly, the COD and VSS concentration at the experiment's end in the test reactors quantified the unbiodegradable material present in both the inoculum and selected substrate.

Figure 3-8 below illustrates the theoretical fractionation process in the control and test reactors.

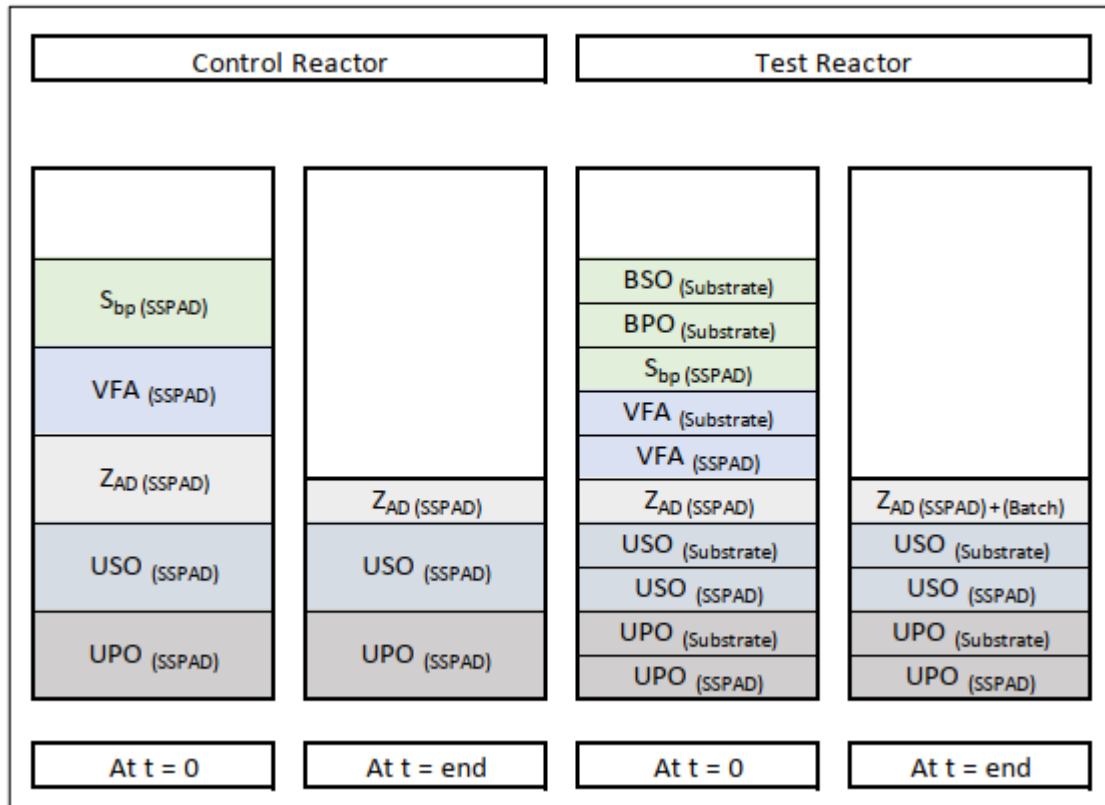


Figure 3-8: ABMP fractionation in control and test reactors (Gaszynski, 2021)

However, it should be noted that the inoculum in the test reactors was diluted 1.07 times relative to the control reactors in this project (see Section 3.3.4). Therefore, the influence of the inoculum in the test reactors was $1 \div 1.07$ (0.93) times the influence of the inoculum in the control reactors. This dilution factor in the test reactors was accounted for at all times.

3.7 Organic composition

3.7.1 Overview

The substrates' organic composition fractionates into unbiodegradable and biodegradable organics. The available data and model utilised in this study only allowed unbiodegradable organics to be characterised in terms of unbiodegradable fractions of the total organics, while biodegradable organics were identified in their chemical (CHONP) composition, using stoichiometry. Both unbiodegradable and biodegradable characterisation used relied on the changes observed in the ABMP experiments

In this project, the stoichiometric method was used for biodegradable organics composition identification, which was calculated from the change in elemental concentration during the experimental period. Therefore, composition determination required the ABMP initial and final concentrations measurements and relied on these results' accuracy and validity.

3.7.2 Unbiodegradable fractions

As mentioned in Section 3.6.3, it was assumed that the final organic concentration (measured on the last day of experiment, i.e., day 41) represent the unbiodegradable organic fraction of the feed. Therefore, the unbiodegradable fraction of the inoculum was calculated simply by dividing the final concentration by initial concentration. Likewise, the unbiodegradable fraction of the substrates in the test reactors were calculated as the fraction of final and initial concentration, taking into account the influence of the inoculum in the test reactors. Equations 3.11 and 3.12 were used to calculate unbiodegradable fractions for inoculum and substrates, respectively.

$$f'u (inoc.) = \frac{C_{end(ABMP,C)}}{C_{start(ABMP,C)}} \quad 3.11$$

$$f'u (sub.) = \frac{[C_{start,(ABMP,T)} - C_{end(ABMP,T)}] - [C_{start(ABMP,C)} - C_{end(ABMP,C)}]}{C_{start,(ABMP,T)} - C_{start(ABMP,C)}} \quad 3.12$$

Where;

$C_{start(ABMP,C)}$ - ABMP control reactor initial concentration

$C_{end(ABMP,C)}$ - ABMP control reactor end concentration

$C_{start,(ABMP,T)}$ - ABMP test reactor initial concentration

$C_{end(ABMP,T)}$ - ABMP test reactor end concentration

Only unbiodegradable fractions for COD (UPO; $f_{s'up}$ and USO; $f_{s'us}$) and VSS (i.e., f_{cv}) were evaluated in this study. Due to insufficient measurement data, the unbiodegradable carbon, organic nitrogen, and organic phosphorus fractions were not calculated. Furthermore, the

chemical composition of the unbiodegradable composition was outside the scope of the study as discussed in Section 1.4. Nevertheless, simulation of wastewater process in models such as the steady-state AD model of Ikumi *et al.*, (2015) and PWM_SA requires input of unbiodegradable composition. Therefore, during the experiment simulation, characterisation of unbiodegradable relied on literature data such as mass fractions and elemental composition. However, the use of this literature data may have an effect on the simulation results, particularly substrates containing food waste (tests B and C), because of limited literature data on food waste.

3.7.3 Biodegradable organic composition

In bioprocess stoichiometry, there are two unknowns involved, namely, (1) the organic present in the reactant (substrate) and (2) biomass (from growth stoichiometry). Because of mass-balanced stoichiometry, the concentration of the compounds, both in the aqueous and gas phase, depends on the two unknowns. Therefore, the composition of the two unknowns can be identified by tracking the changes in the aqueous and gas-phase concentrations (Brouckaert *et al.*, 2021).

In the ABMP experiment, the control reactor tracks the aqueous and gas phase concentrations to quantify the inoculum's biomass ($Z_{AD} + S_{bp}$) concentration. Likewise, the test reactor tracks the aqueous and gas-phase concentrations to quantify the concentration of biomass and organic substrate present in the reactor. Therefore, the influence of the organic substrate is the difference between the test and the control reactor. The two unknowns (biomass and organic substrate) can be determined from measured aqueous and gas phase start and end concentrations (COD, VSS, FSA, OP, H_2CO_3 alkalinity and biogas) of the control and test reactors.

3.7.4 Elemental composition

Organic elemental composition are vital inputs of wastewater models. These models accept an input of organic elemental composition in the generalised form of $C_xH_yO_zN_aP_bS_c$ (CHONPS). However, the S content was not considered for this project, resulting in a CHONP generic form. The subscripts x, y, z, a and b in CHONP are elemental mass ratios representing the mass of each element relative to the total mass of the organic compound (i.e., mass of element/mass of compound). Therefore x,y,z,a and b mass ratios are defined by f_C (gC/gVSS), f_H (gH/gVSS) f_O

(gO/gVSS), f_N (g OrgN/gVSS) and f_P (g OrgP/gVSS) respectively (Ekama, 2009). Because of elemental mass balance, the sum of these mass fractions is equal to one, i.e.,

$$f_C + f_H + f_O + f_N + f_P = 1 \quad 3.13$$

The f_C , f_N and f_P mass ratios can be determined directly from the analytical measurements taken during the experiment. However, f_O and f_H cannot be determined from commonly measured parameters but can be obtained using the COD/VSS (f_{CV}) mass fraction, which uses commonly measured parameters of COD and VSS together with f_C , f_N and f_P . In this project, the mass ratios were determined from the change in aqueous and gas concentrations between the start and end of the ABMP experiment, i.e.,

- (i) change in COD and VSS concentration (f_{CV});
- (ii) change in C concentration (C in H_2CO_3 alkalinity, C in gas (CO_2 and CH_4)) (f_C);
- (iii) change in N concentration (N in FSA) (f_N), and
- (iv) change in P concentration (P in OP) (f_P).

These changes that occurred during the ABMP experiment represent the influence of biodegradable organic material in the substrates (Ekama, 2009).

Using f_{CV} , f_C , f_N and f_P obtained above, f_H and f_O were calculated using the Equations 3.14 and 3.15 obtained from Ekama, (2009)

$$f_H = \frac{2}{18} \left(1 + f_{CV} - \frac{44}{12} f_C + \frac{10}{14} f_N - \frac{71}{31} f_P \right); \quad 3.14$$

and

$$f_O = \frac{16}{18} \left(1 - \frac{1}{8} f_{CV} - \frac{8}{12} f_C - \frac{17}{14} f_N - \frac{26}{31} f_P \right) \quad 3.15$$

Once the mass ratios of all elements (C, H, O, N and P) were obtained, the elemental composition of the organic substrate is given by Equation 3.16.

$$C_x H_y O_z N_a P_b \quad 3.16$$

Were, $x = \frac{fC}{12}$, $y = \frac{fH}{1}$, $z = \frac{fO}{16}$, $a = \frac{fN}{14}$, and $b = \frac{fP}{31}$

Lastly, the elemental composition was adjusted to that of 1 mol of carbon ($x = 1$) by multiplying through by $\frac{12}{fC}$, i.e.

$$C_1 H_{\frac{y}{x}} O_{\frac{z}{x}} N_{\frac{a}{x}} P_{\frac{b}{x}} \quad 3.17$$

3.8 Modelling ABMP experiment

The mass balanced steady-state AD model of Ikumi *et al.*, (2015), programmed into Microsoft (MS) Excel, was used to simulate ABMP batch reactors in this project. The model has recently been extended by Maake & Ikumi (2022) to allow the modelling of augmented batch experiments. Simulating the ABMP experiment required three main steps. (i) Firstly, the parent AD (PAD) was replicated as accurately as possible using the steady-state AD model to estimate the PAD effluent that was used to inoculate ABMP reactors. This required running a steady-state AD model by providing the input characteristic feed and operational parameters to the AD model such that the AD model could predict the effluent characteristics. (ii) Following the PAD modelling, the control reactor was modelled to identify the compositions of residual biodegradable and biomass present in the inoculum and eventually establish the baseline of the test reactors that contained the substrates. This involved running the model backwards, such that the input to the model was the AD effluent variables. Then, the solver function in MS Excel was used to calculate the required input characteristic parameters that would allow for the given (measured) ABMP effluent to equal the one predicted by the AD model. (iii) Lastly, the test reactors were modelled to determine the biodegradable organic's composition contained in the test reactors. This was carried out in the same way for (ii), but characteristics of the seed sludge (biomass and residual biodegradable organics) were also used as input to the model parameter estimating calculation.

The reason that the steady-state AD model could be used to run the ABMP experiment (which is more of a dynamic scenario) in this case was that the ABMP experiment was carried out for a very long solids retention time to the point at which reactions were deemed to be complete (i.e., all the biodegradable organics were utilised, there was no more biogas being generated and only unbiodegradable organics remained in the reactor). The endpoint of the ABMP experiment, when the reactors have been run for a long sludge retention time, is similar to conditions for a steady-state AD experiment where the solids retention time is long, and the effluent contains unbiodegradable organics. In addition, the steady-state AD that generated the seed sludge was operated at a solid retention time of approximately 50 days; hence with the iterative calculation of the seed sludge and feed characteristics, it was possible to reasonably predict the steady-state AD effluent characteristics in (i). This is supported by Ekama (2009), who stated that experiments in which many bioprocesses have reached completion could suitably be modelled with steady-state models. Therefore, the ABMP experiments in this study were deliberately operated at a long sludge age in this project to ensure that many bioprocesses have reached completion.

3.8.1 Overview

3.8.2 Model description

The mass balanced steady-state AD model Ikumi *et al.* (2015) is an extension of the steady-state AD model of Sötemann *et al.* (2005). The steady-state model of Sötemann *et al.* (2005) is made up of three steps that can be summarised as follows:

1. The kinetic hydrolysis part which determines the percentage of COD removal and methane gas generated for a selected sludge age,
2. The stoichiometric part that determines the gas composition in terms of partial pressure of CO₂, and
3. A carbonate system weak acid-base (A/B) chemistry part calculate the pH from the CO₂ partial pressure and the alkalinity generated during the digestion process.

The steady-state AD model of Sötemann *et al.* (2005) is calibrated for hydrolysis of PS only.

The steady-state AD model Ikumi *et al.* (2015) was developed by making the following additions to the steady-state AD model of Sötemann *et al.* (2005):

1. Phosphorus to the organics and biomass composition, polyphosphate (PP) in the phosphate accumulating organisms (PAO) and OP speciation in the aqueous phase.
2. Anaerobic digestion of WAS and WAS and PS blend, each with its separate CHONP composition.
3. Three-phase (liquid-gas-solid) in the weak/acid-base chemistry part which allows struvite precipitation to be modelled.

The abovementioned additions mean the mass balanced steady-state AD model of Ikumi *et al.* (2015) has the ability to: (1) predict the release of N and P from the substrate during anaerobic digestion and (2) track various compounds and elements such as COD, Carbon (C), hydrogen (H), oxygen (O), N and P besides identifying potential mineral precipitation issues. Lately, Maake & Ikumi (2022) modified the steady-state AD model of Ikumi *et al.* (2015) to simulate augmented batch AD reactors, such as the ABMP experiment used in this study.

3.8.3 Parent AD modelling

The parent anaerobic digester (PAD) model was used to identify the active biomass concentration (Z_{AD}) that was used to inoculate the ABMP reactors. The inoculum contained Z_{AD} and biodegradable organics (S_{bp}). The Z_{AD} affects the kinetic rates of the ABMP reactors, while the S_{bp} affects the biogas generation in the ABMP reactors. However, it was challenging to separate S_{bp} and Z_{AD} in the control reactors and S_{bp} , Z_{AD} and substrate BPO in the test reactors. Therefore, the steady-state equations of Sötemann *et al.* (2005) model were used to estimate biomass concentration. The following steps summarise the procedure:

- i) The hydrolysis rate of the organics can be determined based on the anaerobic digester at a steady state by carrying out the mass balance on Z_{AD} , i.e.:

$$r_h = \frac{Z_{AD}}{Y_{AD}} \left(\frac{1}{R} + b_{AD} \right) \quad \text{mgCOD}/(\text{g.d}) \quad 3.18$$

Where:

r_h = Hydrolysis rate (gCOD/ℓ.d)

Y_{AD} = Biomass yield (gCOD biomass/ gCOD organics)

R = Sludge age (d)

b_{AD} = Biomass death rate (ℓ/d)

- ii) Alternatively, the hydrolysis rate can be obtained can also be obtained based on steady-state and carrying out the mass balance on biodegradable organics. i.e.:

$$r_h = \frac{S_{bpi} - S_{bp}}{R} + b_{AD}Z_{AD} \quad \text{mgCOD}/(\ell.d) \quad 3.19$$

Where:

S_{bpi} = Influent BPO COD concentration

S_{bp} = residual BPO COD concentration

- iii) The Z_{AD} concentration in the anaerobic digester and that of the effluent can then be given by:

$$Z_{AD} = \frac{Y_{AD}(S_{bpi} - S_{bp})}{[1 + b_{AD}R(1 - Y_{AD})]} \quad \text{mgCOD}/\ell \quad 3.20$$

- iv) Finally, the methane COD concentration (assuming that it all remains dissolved in the solution) is given by:

$$S_m = (1 - Y_{AD})Rr_h \quad \text{mgCOD}/\ell \quad 3.21$$

- v) The COD concentration of the biomass in the reactor (and thus the effluent) was calculated based on daily methane production (S_m), which was determined by

assuming a mass balanced system. In a mass balance system, S_m is equal to the difference between unfiltered influent and effluent COD concentrations. Therefore, biomass concentration can be calculated as follows:

$$Z_{AD} = \frac{Y_{AD} S_m}{[1 + b_{AD} R(1 - Y_{AD}) + Y_{AD} R b_{AD}(1 - Y_{AD})]} \quad \text{mgCOD}/\ell \quad 3.22$$

As mentioned in Section 3.2.2, the inoculum used to inoculate the ABMP reactors was obtained from two AD systems which were operated at different but approximately similar long sludge ages (i.e., 49 and 52 days). Therefore, the biomass concentration from each reactor was modelled separately, and after that, they were combined into a single biomass concentration using Equation 3.23. Eventually, this combined Z_{AD} concentration was used as the biomass concentration, which was used throughout the entire ABMP modelling process.

$$\text{Combined } Z_{AD} = \frac{Z_{AD1} x V_1 + Z_{AD2} x V_2}{V_1 + V_2} \quad \text{mgCOD}/\ell \quad 3.23$$

3.8.4 ABMP reactors modelling

The ABMP reactors were operated for a long sludge age sludge (i.e., 76 days) to ensure that they reached a state at which bioprocesses were deemed to have been completed, making them suitable for modelling with steady-state models, as explained above. The mass-balanced steady-state AD model of Ikumi *et al.* (2015) was used as the AD model to replicate all ABMP reactors virtually. The initial concentrations of the following components were fixed to the experiment measured starting concentrations: unfiltered COD, FSA, TP, OP, VSS, ISS, pH and H_2CO_3 alkalinity. The experimentally observed end concentrations of the same components were also inputted to the model, as target end values to be used in the parameter estimation (PE) procedure. Moreover, the starting liquid volume of the ABMP reactors was fixed at 5ℓ.

In usual practice, the hydrolysis kinetic rate constants (k_M and K_S) are important inputs for AD steady-state modelling. However, in this project, the sludge age at which the ABMP data was collected (i.e., the endpoint of the experiment) was very long; hence, the bioprocesses were deemed complete at this point. Thus, hydrolysis kinetics did not need to be applied – as long as

the kinetics resulted in all the influent BPO having been used up (i.e., converted to methane). Despite the hydrolysis kinetics constants deemed unimportant for this project, the model still required their input. Therefore, in all cases, the kinetics rates of primary sludge obtained from Ikumi *et al.* (2014) (i.e., $k_M = 1.80$; $K_S = 7.96$) were used instead (these kinetics allowed for all BPO breakdown within the long 76d sludge age period).

The BPO and UPO compositions of the substrates and the seed sludge were obtained by carrying out the parameter estimation (PE) process as mentioned in Section 3.8.3. In this study, PE was facilitated by a solver function, which is a function coded in MS Excel. This solver allows the modeller to run iterative trial and error simulations to minimise the error between experimentally observed results and modelled results. Various error criteria can be used in parameter estimation, but the squared error criteria (Claeys, 2008) were used in this study.

3.8.4.1 Control reactor experiment

The ABMP control reactor was used to (1) determine the biodegradable organics contained in the inoculum and (2) establish the baseline for the test reactors, which were fed with different substrates. The inoculum's composition in the ABMP reactor can be fractionated into UPO, BPO (residual biodegradable organics) and biomass. The UPO COD concentration was determined through the parameter estimation (PE) process discussed below. However, it was challenging to separate the inoculum's biomass and residual biodegradable organics' COD concentration, and hence their composition. As a result, for the purpose of model simplicity, the composition of the inoculum's biomass and residual biodegradable have been lumped into one compound and hence referred to as the 'seed sludge' in this study. Therefore, this seed sludge was used as the baseline composition in the test reactors, as discussed in Section 3.8.4.2. Furthermore, because the concentrations of particulate organics (both biodegradable and unbiodegradable) are relatively much more significant than soluble organics, the soluble organics were lumped together with the particulates (i.e., BPO include BSO and UPO include BSO). Figure 3-9 shows the fractionation of organics during ABMP modelling.

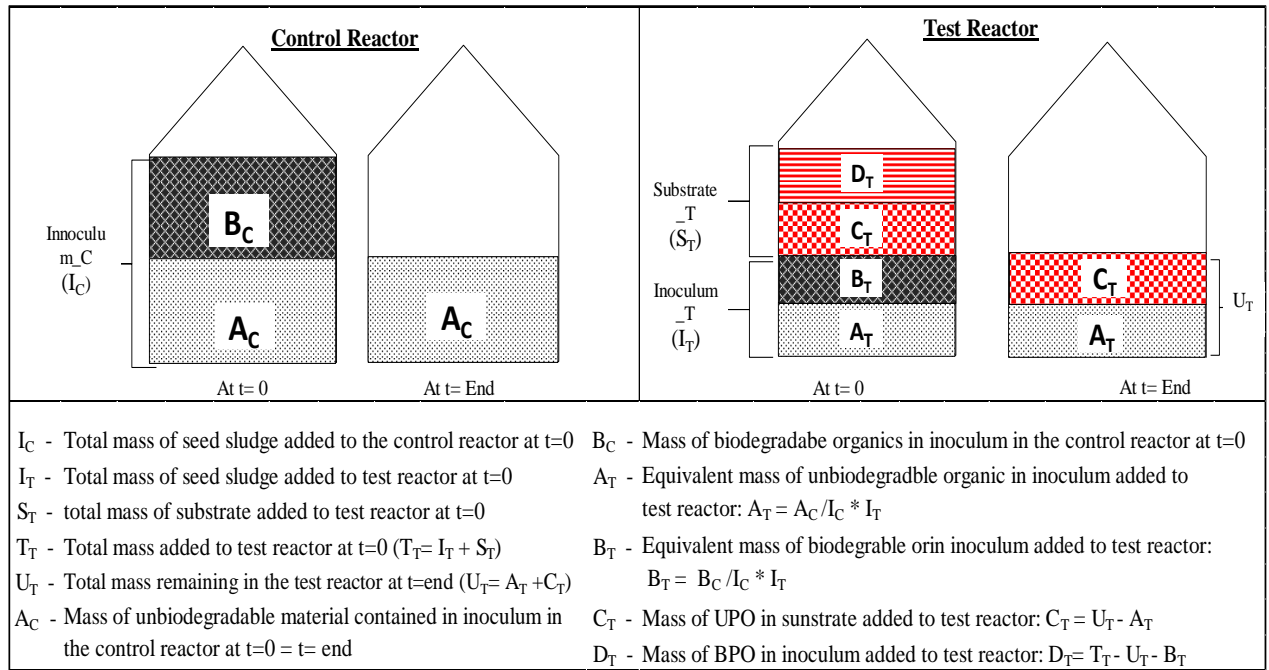


Figure 3-9: Organic component fractionation and lumping in ABMP modelling

A parameter estimation (PE) procedure was used to determine the composition of the seed sludge contained in the control reactor. The biomass concentration obtained in PAD modelling (Section 3.8.3) was a direct input (accounting for the inoculum dilution during seeding as discussed in Section 3.3.4). The model's initial concentrations of unfiltered COD, FSA, TP, OP, VSS, ISS, pH and H_2CO_3 alkalinity were set equal to the experiment's measured starting concentrations of the control reactor. The measured end concentrations were entered in the model as targets, which were then compared to the modelled end concentrations. The influence of the seed sludge present in the control reactor was then determined by the PE procedure, which was facilitated by a solver function in MS Excel, as described in Section 3.8.1.

The seed sludge mass fractions (f_{cv} , f_c , f_n and f_p) and $f_{s'up}$ were parameterised during the parameter estimation process. In addition, the measured end concentration of VSS, H_2CO_3 alkalinity, ISS, FSA, OP and pH were entered in the model as variables, from which objective values were selected. The objective values were selected carefully by iterative trial and error such that a suitable objective value is not an outlier and minimises the sum of squared errors. Therefore, the solver was used to adjust the parameters by running multiple iterative trial and error simulations until the slightest error between experimentally measured and model-predicted is obtained. In addition, during PE iterations, it was also ensured that the obtained parameters were comparable

with literature data where possible. Table 3-6 shows the ABMP control reactors parameters and their objective values.

Table 3-6: ABMP control reactor parameters and objective values

Parameter	Objective Value
$f_{s'up}$	Final measured VSS
BPO f_{CV}	Final measured VSS
BPO f_N	Final measured FSA
BPO f_P	Final measured OP
BPO f_C	Final measured pH and H_2CO_3

After finding the BPO f_{CV} , f_C , f_N and f_P mass ratios, the unknown mass fractions for f_H and f_O and the elemental CHONP composition were calculated using equations from Section 3.7.3.

The model was also used to evaluate the composition of UPO and endogenous residue (ER) in terms of its mass fractions (i.e., f_{CV} , f_C , f_N and f_P). The f_{CV} was obtained from the modelled UPO COD and OPO VSS. Because carbon was not reliably measured in this study, the UPO f_C mass ratio was obtained using the UPO TOC:COD ratio (UPO TOC:COD = 0.348 obtained from (Ekama & Brink, 2007)) and the modelled UPO COD and UPO VSS. Finally, the UPO f_N and f_P mass ratios were obtained by taking the fraction of measured unbiodegradable organic (UPO OrgN and UPO OrgP) and the modelled UPO VSS. The UPO OrgN and OrgP were assumed to be relatively much more significant than USO OrgN and OrgP (as is often the case), respectively, and thus UPO and USO OrgN and OrgP were lumped together. Table 3-7 below summarises the source of data used for UPO & ER composition.

Table 3-7: Source of data for UPO composition determination

Parameter	Source of data
UPO f_{cv}	Modelled UPO COD and VSSS
UPO f_c	UPO TOC: COD ratio from Ekama & Brink (2007) and modelled OPO COD and VSS
UPO f_n	Measured UPO OrgN and modelled UPO VSS
UPO f_p	Measured UPO OrgP and modelled UPO VSS

3.8.4.2 Test reactors experiments

The ABMP test reactors were used to identify the composition of the substrates that were contained in the test reactors, as discussed in Section 3.3.4. The test reactors contained the baseline seed sludge (as obtained from Section 3.8.4.1) and a substrate of interest, as depicted in Figure 3-8 above. The seed sludge used in the test reactor has the same composition as the one used in the control reactor but had a different concentration due to seed sludge's dilution in the test reactors, as discussed in Section 3.3.4. Therefore, the modelled seed sludge composition (as discussed in Section 3.8.4.1) was entered as a known parameter in the modelled test reactor experiment. The substrates organic material compositions were then used in the model's PE as unknown parameters. In addition, similar to control reactor modelling, UPO & USO and BPO and BPO & BSO were lumped into a single compound and simply referred to as UPO and BPO, respectively. Figure 3-9 illustrates how the seed sludge and substrate in the ABMP modelled experiment was fractionated.

A PE procedure was used to determine the BPO composition of the substrates, which were present in the test reactors. The model's initial concentrations of all constituents for each test experiment group were adjusted and fixed to the average measured concentrations (test reactors experiment measured concentrations results were discussed in Section 3.4). The measured end concentrations were entered as objective values. The influence of the substrates' biodegradable organics in the test reactor was determined through a PE process by running iterative trial and error simulation runs using MS Excel's in build solver function. During the PE process, $f_{s,up}$ and the BPO mass fractions (f_{cv} , f_c , f_n and f_p) were parameterised. The objective target value for each parameter was carefully selected after running multiple trial and error runs. An appropriate objective value for a specific parameter was assigned such that this objective value is not an outlier and minimizes the total resulting errors. Table 3-8 shows the ABMP test reactors

parameters and their selected objectives. The error criteria used in this project was the squared error (Claeys, 2008).

Table 3-8: ABMP test reactors parameters and objective values

Parameter	Objective Value		
	Test A	Test B	Test C
$f_{s'up}$	Final measured VSS	Final measured COD	Final measured COD
BPO f_{cv}	Final measured VSS	Final measured COD	Final measured COD
BPO f_n	Final measured FSA	Final measured FSA	Final measured FSA
BPO f_p	Final measured OP	Final measured OP	Final measured OP
BPO f_c	Final measured pH	Final measured pH	Final measured pH

After finding the BPO f_{cv} , f_c , f_n and f_p mass ratios, the unknown mass fractions for f_H and f_O and the elemental CHONP composition were calculated using equations from Section 3.7.4. In addition, these modelled parameters resulted in modelled end concentrations for COD, FSA, TP, OP, VSS, ISS, pH and H_2CO_3 alkalinity. Furthermore, the UPO composition was determined using the same procedure for the control reactor discussed in Section 3.8.4.1.

4. ABMP Experiment Results and Discussion

4.1 Introduction

This chapter presents the results of the augmented biomethane potential (ABMP) experiment. The ABMP experiment consisted of control and test reactors, as discussed in Section 3.3.3. However, control reactors and test reactors were analysed differently, and thus they have been presented in separate sections under this chapter.

4.2 ABMP Control reactor results

Accurate analysis of control reactors results is critical because they set the baseline that quantifies the substrate biodegradable organics present in the test reactors, as discussed in Section 3.6. The baseline is set by quantifying the changes observed in the control reactors to identify the inoculum's composition. The changes that occur in the control reactor are basically due to the residual BPO present in the inoculum. The evaluation of the experimental results from the control reactor includes: Firstly, checking for statistical significance and reasonable mass balances to generate confidence in the experimental data. Secondly, determination of the inoculum's residual biodegradable organics' composition.

Since there were slight changes observed in control reactors, the duration of the control reactor depended on the test reactors (the test reactors were deemed to contain higher mass of biodegradable organics, hence would require a longer retention time for completion of bioprocesses through complete breakdown of these biodegradable organics). The experiment lasted for 76 days (i.e., sludge age =76 days). Before day 76, no significant biogas was produced by either control or test reactor for more than ten consecutive days (i.e., from day 66 onwards). Lack of biogas production from reactors gave confidence that all biodegradable organics in both control and test reactors had been utilised.

4.2.1 Control reactor analytical results

The setup and operation of the ABMP control reactors is discussed in Section 3.3. Generally, biomethane potential (BMP) and ABMP experiments are conducted in triplicates for results reliability purposes (Holliger *et al.*, 2016; Gaszynski *et al.*, 2019).

The reactors were labelled C-1, C2, C-3 and C-4. The reactors were seeded with an inoculum obtained from the parent anaerobic digester (PAD), diluted with distilled water before seeding, as shown in Table 3-4 in Section 3.3.4. For each reactor, the concentration of different constituents was measured using experimental test methods described in Section 3.4. Finally, the mean ($\langle x \rangle$) and standard deviation (σ_x) of the four control reactors were computed. In this report, the mean of the experimentally measured data was used. In Table 4-1, the control reactors results are presented in a format of $x = \langle x \rangle \pm \sigma_x$, showing the mean experimental results and the spread of the measured data.

Table 4-1: Summary of ABMP control reactor results

	Unit	Start	End	Change (Δ)
Time	Days	0	76.00	76
Unfiltered COD	mgCOD/l	3076.8 \pm 43	2408.8 \pm 64	-668
Filtered COD	mgCOD/l	157.9 \pm 8	103.7 \pm 12	-54
Particulate COD	mgCOD/l	2918.9	2305.1	-614
VFA COD as Acetate	mgCOD/l	-85 \pm 67	-51 \pm 13	34.18
TKN	mgN/l	241.7 \pm 9	245.2 \pm 12	4
FSA	mgN/l	83 \pm 2	128 \pm 3	45
TP	mgP/l	58.4 \pm 1	62.8 \pm 3	4
OP	mgP/l	4.6 \pm 0	10.9 \pm 1	6
TSS	mgTSS/l	2734 \pm 59	2326 \pm 59	-408
VSS	mgVSS/l	2054 \pm 53	1628.5 \pm 63	-426
ISS	mgISS/l	680 \pm 7	633.3 \pm 60	-47
pH	pH	7.5 \pm 0.1	7.5 \pm 0.1	0.0
Carbonate alkalinity	mg/l as CaCO ₃	750 \pm 57	929 \pm 70	179
VFA Alkalinity	mg/l as CaCO ₄	-85 \pm 67	-51 \pm 13	28
Total alkalinity	mg/l as CaCO ₃	685 \pm 2	923 \pm 28	264
Cumulative CH ₄ gas	mgCOD	0	443 \pm NA	443
Cumulative C in gas	mgC	0	0.2 \pm NA	0.2

The results in Table 4-1 indicate that unfiltered COD concentration in the control reactor decreased by 668 mgCOD/l (22% of the average influent COD) between start and day end. The change in unfiltered COD concentration represents the amount of residual biodegradable organics contained in the inoculum. Filtered COD concentration only decreased by 54 mgCOD/l, indicating little soluble biodegradable COD in the inoculum. Low biodegradable organics concentration was desired in the inoculum to ensure minimal influence of the inoculum in the test reactors. A relatively low standard deviation in both unfiltered and filtered COD measurements was observed, showing a relatively low disparity in the measured data. The particulate COD concentration was calculated as the difference between mean unfiltered and mean filtered COD concentrations.

A 5-pH point titration method was used to measure alkalinities (total, carbonate and VFA) and VFA COD, as discussed in Section 3.4.7. However, statistical analysis illustrated a significant

disparity in VFA alkalinity and VFA results, and as a result, VFA measurements for the entire experiment were regarded as spurious and hence non-utilisable. Therefore, VFA concentrations used for further analysis were set equal to zero, a decision based on the following assumptions: (1) generally all VFA measurements were below zero, (2) there was no significant difference in start and end pH and, (3) a long sludge ensured that all intermediate VFA produced was utilised before end of experiment.

Unlike VFA measurements, other results from 5-pH point titration (i.e., total and carbonate alkalinities) showed consistency and low disparities; and thus, they were utilisable. Both total and carbonate alkalinities concentration increased. Furthermore, total and carbonate alkalinity concentrations were nearly equal, which indicates that carbonate alkalinity was the dominant alkalinity sub-species³ in the solution. The change in carbonate alkalinity indicates the presence of biodegradable carbon content in the inoculum.

There were slight changes observed in TKN and TP concentrations between the start and end of the experiment. During anaerobic digestion, the organic content of TKN and TP are broken down and subsequently released inorganic components of TP and TKN (FSA and TP respectively) into the bulk liquid. Therefore, no changes in TP and TKN concentrations were expected. Thus, the changes observed are deemed due to measurement errors. Furthermore, the intermediate results (see Appendix A), shows that the concentration of TKN and TP were generally constant. On the other hand, FSA and TP increased by 45 mgN/ℓ and 6mgP/ℓ, representing 54% and 130% in FSA and OP, respectively. The changes in FSA and OP were quite significantly higher than expected, considering the fact that the SSPAD was operated at a very long sludge age. These changes in FSA and OP quantifies the organic N and P broken down and released into the bulk liquid.

The concentration of all solids (TSS, VSS and ISS) decreased significantly as expected. VSS concentration decreased by 21% throughout the experiment. This decrease in VSS quantifies the biodegradable particulates contained in the inoculum, which was subsequently broken down

³ In addition to VFA and carbonate, other sub-species such as ammonia and phosphate alkalinities may also be present in the solution

during the experiment. The ratio of change in particulate COD concentration to the concentration of VSS utilised (UPO f_{cv} , mgCOD/mgVSS) was 1.44. This UPO f_{cv} value is comparable to the UPO f_{cv} value of 1.481, which is commonly used in wastewater activated sludge models (Marais & Ekama, 1976).

4.2.2 Gas measurement for control reactors

The biogas produced by the control reactors was captured in the inverted columns as discussed in Section 3.3.6. In order to determine the methane content of the biogas, a biogas sample was collected from the reactors' headspace and analysed for methane gas partial pressure. Using the cumulative biogas measurements and gas composition, the methane potential curve (CH_4 mass) was determined.

4.2.2.1 Gas measurement

The biogas produced by the ABMP control reactors was captured in the inverted volumetric glass cylinders (columns). The setup and description of gas measurement are discussed in Sections 3.3.3 and 3.3.6. Cumulative biogas volume produced was converted to methane COD mass by using the universal gas law (see Equations 3.6 and 3.7 in Section 3.5.3.1 for the procedure for calculating methane COD mass).

As discussed in Section 3.3.6, control reactors were made up of type I (6ℓ) and type-II (2.5ℓ) reactors seeded with the same concentration but different volumes (hence different masses) of the inoculum. Due to this, the cumulative masses of biogas and methane produced from these two types of reactors were different. Therefore, masses from type II reactors were converted to equivalent type I reactor mass. Type I control reactors were made a reference because they are similar to reactors used by the test reactors. Therefore, as a general rule in this study, cumulative gas mass from type II control reactors was always multiplied by 2.5 to obtain type I equivalent masses. The process is described in detail in Section 3.3.4. Figure 4-1 shows CH_4 generated (as mgCOD) over the experimental period by the control reactors. In Figure 4-1, the cumulative methane mass produced C-3 and C-4 (type II control reactors) has been adjusted to type I equivalent.

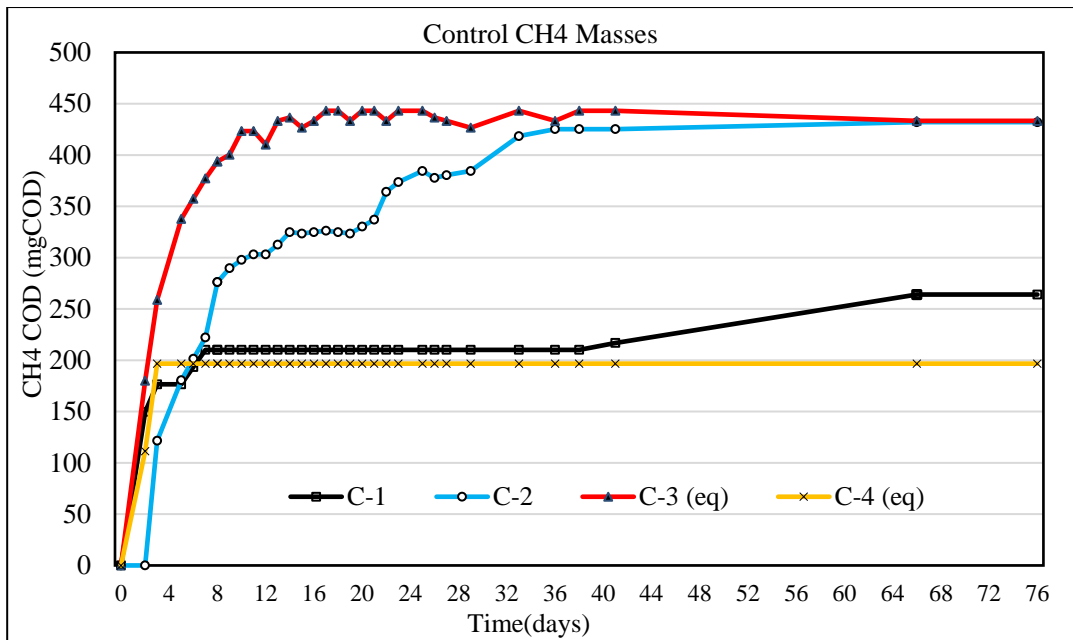


Figure 4-1. ABMP control reactors methane COD masses

There was quite a significant variance in cumulative methane COD mass. C-1 and C-4 flattened sooner than C-2 and C-3. However, it was observed that the aqueous COD concentration in all four reactors was generally changing at the same rate (see Appendix A). Therefore, it is unlikely that C-1 and C-4 flattened off sooner due to the absence of biodegradable COD. Therefore, it was concluded that the reason for the sudden end of gas production in C-1 and C-4 was a result of a gas leak. As a result, C-1 and C-4 were not considered when calculating average masses of methane COD or C contained in biogas.

4.2.2.2 Gas composition

Gas composition in terms of methane partial pressure was required to calculate methane COD produced by the control reactors. Gas composition was determined using a Gas Chromatography (GC) analyser. However, there was limited access to the GC equipment; thus, the methane partial pressure tests were not conducted regularly. Therefore, gas compositions were used with caution because they could not be tested for reliability. The average methane partial pressure for control reactor was measured as 51.5%.

4.2.3 Mass Balances

The mass balances of materials were used to evaluate the accuracy and validity of the control reactors. Mass balance follows the principle of mass conservation of materials, which states that the mass of materials entering the reactor should be equal to the mass of materials leaving the reactor. To determine the per cent mass balance, the materials were tracked from the influent to all the effluent streams. As discussed in Section 3.5.3, the influent in this study was made up of a single batch feed, while the effluent was made up of the following: (i) samples drawn from a reactor, (ii) biogas produced, and (iii) the liquid remaining in the reactor at the end of the experiment. In addition, experiments that yielded $100\pm 20\%$ mass balances were considered accurate and valid.

4.2.3.1 COD Balance

Equations 3.4 in Section 3.5.3.1 was used to calculate the fluxes of COD coming in and out of the batch reactors. Table 4-2 summarises the control reactors' COD balance. COD experiments are usually accepted to be accurate and valid if COD mass balance of $100\pm 10\%$ is achieved. However, in this study, experiments that achieved COD mass balances within $100\pm 20\%$ were accepted as valid after careful analysis (by increasing methane partial pressure to 100% to determine possible methane measurement error, as shown in Table 4-3) of the data.

Table 4-2. ABMP control reactor's observed COD balance

Reactor	Starting Mass	Mass Removed	Remaining Mass	CH ₄ Mass	Total effluent	Balance	Average balance
	mgCOD	mgCOD	mgCOD	mgCOD	mgCOD	mgCOD	mgCOD
C-1	15264	2295	9964	264.066	12523	82.0	83.3 ± 2.2
C-2	15456	2749	9612	432.084	12793	82.8	
C-3	6067	2319	2762	173.312	5255	86.6	
C-4	6259	2433	2612	78.676	5124	81.9	

None of the control reactors achieved a good COD balance as stipulated in Section 3.5.3. Therefore, to determine the likely cause of low COD balances, methane partial pressure was increased to 100% to determine the possible influence of methane partial pressure results,

because it unreliably measured (see Section 4.2.2.2). The results after increasing methane partial pressure are given in Table 4-3.

Table 4-3. Adjusted control reactors' COD balance (100% methane partial pressure)

Reactor	Starting Mass	Mass Removed	Remaining Mass	CH4 Mass	Total effluent	Balance	Average balance
	mgCOD	mgCOD	mgCOD	mgCOD	mgCOD	mgCOD	mgCOD
C-1	15264	2295	9964	861	13120	86.0	85.9 ± 2.6
C-2	15456	2749	9612	839	13201	85.4	
C-3	6067	2319	2762	337	5418	89.3	
C-4	6259	2433	2612	153	5198	83.0	

As shown in Table 4-3, increasing methane partial pressure to the maximum possible only increased the overall COD balance by less than 3%, and still remained below permissible COD balance stipulated in Section 3.5.3.1. This is an indication that unreliable gas composition data had slight influence on COD balance. Considering the fact that the aqueous COD measurements was statistically found to be accurate; it was therefore concluded that the poor COD balance resulted from an inaccurate gas (production) measurement. Gas measurement errors are believed to be common in BMP/ABMP experiments that uses cumulative gas measurement methods due to CO₂ that dissolve in water or other displacement fluids and possible gas leaks (Strömberg *et al.*, 2014; Gaszynski, 2021). Nevertheless, for this experiment, the control reactors' COD measurement (in exception of methane COD) was accepted to be accurate and valid.

4.2.3.2 TKN and TP Balance

The Equation 3.4 in Section 3.5.3.2 was used to calculate the mass balances shown in Table 4-4.

Table 4-4. Control reactors TKN and TP mass balance

Reactor	TKN mass balance				TP mass balance			
	TKN in	TKN Out	Balance	Average	TP in	TP out	Balance	Average
Unit	mgN		%		mgP		%	
C-1	1246	1183	94.9	100.4 ±4	290	300	103.3	103.1 ±8.5
C-2	1208	1218	100.9		299	298	99.6	
C-3	459	465	101.2		115	132	114.8	
C-4	493	515	104.5		120	114	94.7	

Seven out of eight (i.e., ~88%) of the TKN and TP balance for control reactors were within the acceptable limits of $100\pm 10\%$ as stipulated in Section 3.5.3.2, and thus the results were accepted to be accurate and valid.

4.2.4 Composition determination for inoculum in control reactor

Although there was no substrate present in the control reactor, the biodegradable composition of the residual biodegradable organics in the inoculum was evaluated as an ancillary aspect of the experimental investigation. The biodegradable composition was determined by a stoichiometric approach. The stoichiometric composition method involves quantifying COD, VSS, C, N, and P changes between the start and end of the experiment. Next, these changes were used to calculate the biodegradable organics' elemental mass ratios (f_{CV} , f_C , f_N , f_P , f_O and f_H). Finally, the mass ratios were then used to determine the biodegradable composition in a generic format of $C_xH_yO_zN_aP_b$ (CHONP elemental composition). The procedure for calculating mass ratios and the CHONP elemental composition by stoichiometry is detailed in Section 3.7.4.

Observed changes in COD, VSS, C, N, and P were previously shown in Table 4-1 and the mass ratios and elemental composition by stoichiometry results is shown in Table 4-5.

Table 4-5. ABMP control reactor changes and stoichiometric composition

Measured component	Unit	Change (Δ)
Total COD	mgCOD/l	-623.5
FSA	mgN/l	42.0
OP	mgP/l	5.9
VSS	mgVSS/l	-397.1
Carbonate Alk	mg/l as CaCO ₃	167.1
CH ₄ COD	mgCOD	413.5
C in gas	mgC	0.2
COD change		
Biodegradable COD	mgCOD/l	623.5
CH ₄ COD	mgCOD/l	82.7
Carbon Change		
C in gas	mgC/l	0.0
C in H ₂ CO ₃ alkalinity	mgC/l	40.1
Total C	mgC/l	40.1
VSS Change		
Biodegradable VSS	mgVSS/l	397.1
Mass ratio		
f_{CV}	gCOD/gVSS	1.570
f_C	gC/gVSS	0.101
f_N	gN/gVSS	0.106
f_P	gP/gVSS	0.015
f_H	gH/gVSS	0.249
f_O	gO/gVSS	0.529
Composition		
C	mol	1.000
H	mol	29.567
O	mol	3.929
N	mol	0.897
P	mol	0.057

The biodegradable composition of residual biodegradable organics contained in the inoculum can then be deduced from Table 4-5 as C₁H_{29.567}O_{3.929}N_{0.897}P_{0.057}. The carbon mass ratio was

significantly low compared to the wastewater sludges literature adopted f_c value of 0.515 (Marais & Ekama, 1976). This low C mass ratio also resulted in an unusual subscript of H in the elemental composition (CHONP). The low C mass ratio was possibly caused by an error in gas measurement, because significant C leaves the system as CO_2 . Similar findings were reported by Gaszynski, (2020), who obtained the inoculum's residual biodegradable's C mass fraction of 0.189 and a CHONP composition of $\text{C}_1\text{H}_{19.059}\text{O}_{1.681}\text{N}_{0.373}\text{P}_{0.010}$.

4.3 ABMP Test Reactor Results

The ABMP test reactors were used to identify the composition of biodegradable organics present in the chosen substrates. The chosen substrates were PS, food waste and a mixture of PS and food waste. Besides the substrates, the test reactors were also fed with the inoculum. The purpose of the test reactors in the experiment was to identify the CHONP elemental composition of the three substrates. This chapter presents the results, analysis and discussion of ABMP test reactors.

4.3.1 Test reactor analytical results

The substrates used in this experiment were PS (test A), food waste (test B) and a blend of PS and food waste (test C). The PS was obtained from Bellville Wastewater Treatment Works (BWWTW), while food waste was manually simulated to replicate a typical local food waste composition. A detailed description and preparation of the substrates was discussed in Section 3.3.2.. The inoculum used in the test reactors was similar to the inoculum used in control reactors. However, the inoculum in the test reactors was diluted 1.07 ($15 \div 14$) times relative to the inoculum in the control reactor (see Section 3.3.4). Therefore, the concentration of the reactants taken up and products released into the test reactors due to the inoculum was 0.93 ($14 \div 15$) times that of the control reactor.

The concentrations of various constituents were measured per experimental methods discussed in Section 3.4. The most critical measurement points were the starting day and end day, but some intermediate measurement points were measured for use in ancillary aspects of the project and to track consistency of the experiment. Both control and test reactors were carried out in parallel, and were operated for a period of 76 days. Before day 76, there was no significant biogas production observed for ten consecutive days (i.e., from day 66 onwards). Therefore, it was

assumed that all biodegradable organics were utilised by day 76. Finally, the mean ($\langle x \rangle$) and standard deviations (σ_x) of the test results of each set of test reactors were computed as part of statistical data analysis. In this report, the mean of the experimentally measured data was used for further data processing.

The starting and end results (i.e., results for day 0 and day 76) for ABMP test reactors' (tests A, B and C) results are given in Table 4-6. The results are presented in a format of $x = \langle x \rangle \pm \sigma_x$, showing the mean experimental results and the spread (standard of the measured data

Table 4-6: ABMP test reactors results

		Test A			Test B			Test C		
	Unit	Start	End	Change (Δ)	Start	End	Change (Δ)	Start	End	Change (Δ)
Time	Days	0	76	76	0	76	76	0	76	76
Unfiltered COD	mgCOD/l	4752 + 41	2693.1 \pm 47	-2059	4723.2 \pm 0	2520 \pm 34	-2203	4809.6 \pm 95	2907.8 \pm 77	-1902
Filtered COD	mgCOD/l	531.2 + 1	82.6 \pm 3	-334	641.3 \pm 5	77.8 \pm 1	-477	593.3 \pm 19	117.1 \pm 7	-395
Particulate COD	mgCOD/l	4220.8	2496.3	-1724.5	4081.9	2355.8	-1726.1	4216.3	2709.1	-1507.2
VFA COD as acetate	mgCOD/l	-19 \pm 34	-37 \pm 34	29	-3 \pm 17	-54 \pm 26	-51	-1 \pm 54	-17 \pm 3	-16
TKN	mgN/l	270.9 + 1	295.1 \pm 5	24	272.3 \pm 9	274.6 \pm 9	2	248.3 \pm 8	271.6 \pm 8	23
FSA	mgN/l	106 + 1	165 \pm 2	59	96 \pm 1	148 \pm 2	52	99 \pm 0	156 \pm 2	57
TP	mgP/l	65.2 \pm 1	76.7 \pm 7	8	54.4 \pm 3	61.9 \pm 5	6	66.4 \pm 0	63.7 \pm 11	1
OP	mgP/l	8.6 + 0	16.6 \pm 1	8	6.2 \pm 0	16 \pm 1	10	7.3 \pm 0	17.7 \pm 0	10
TSS	mgTSS/l	3910 \pm 31.2	2768 \pm 34	-1142	3458.7 \pm 52	2475.3 \pm 69	-983	3774.7 \pm 52	2634 \pm 69	-1141
VSS	mgVSS/l	3106 \pm 7	2045 \pm 24	-1140	2787.3 \pm 23	1894 \pm 55	-1203	3090 \pm 119.3	1927.3 \pm 60	-1280
ISS	mgISS/l	804 \pm 26	764 \pm 24	-81	671.3 \pm 34	649 \pm 7	-22	752 \pm 3	692 \pm 76	-60
pH	pH	7.3 \pm 0	7.1 \pm 0	0.0	7.2 \pm 0	7 \pm 0	0.1	7.3 \pm 0	6.9 \pm 0.1	-0.2
Carbonate alkalinity	mg/l as CaCO ₃	812 \pm 38	1189 \pm 85	377	660 \pm 63	1060 \pm 65	400	756 \pm 68	1058 \pm 36	302
VFA alkalinity	mg/l as CaCO ₄	-16 \pm 28	-29 \pm 16	-13	-2 \pm 13	-1 \pm 97	1	-1 \pm 44	-23 \pm 8	-22
Total alkalinity	mg/l as CaCO ₃	804 \pm 16	1198 \pm 62	-126	663 \pm 52	1082 \pm 62	419	761 \pm 29	1053 \pm 47	292
Cumulative CH ₄ gas	mgCOD	0	5595 \pm NA	5595	0	7087 \pm NA	7087	0	6814 \pm NA	6814
Cumulative C in gas	mgC	0	1765 \pm NA	1765	0	2193 \pm NA	2193	0	2295 \pm NA	2295

Note: Test A= Primary Sludge; Test B= Food waste; Test C= Primary sludge + Food waste

The results of the three tests from Table 4-6 shows significant changes (all decreases) were observed in both unfiltered and filtered COD concentrations between the start and end of the experiment. All changes observed were above the baseline set by the control reactors (higher observed changes in test reactors than the changes observed in the control reactors), indicating that there was indeed an influence of the substrates used in each test reactor. The change in COD concentrations in the test reactors quantifies the total biodegradable COD concentration in the reactor, which is a sum of the substrate and inoculum biodegradable CODs.

Unfiltered COD concentration changes were between 40 and 47 per cent, with the highest change observed in test B (food waste), followed by test A (PS) and lastly test C (PS and food waste blend). On the other hand, the change (decrease) in filtered COD followed a different order from unfiltered COD whereby the highest change was observed in test B and lowest in test A, with the changes observed between 63 and 74 per cent. The particulate COD concentration was calculated as the difference between mean unfiltered and mean filtered COD concentrations.

A 5-pH point titration method was used to measure alkalinities (total, carbonate and VFA) and VFA COD, as discussed in Section 3.4.7. However, statistical analysis illustrated a significant disparity in VFA alkalinity and VFA results for the entire experiment. As a result, VFA measurements for the entire experiment were regarded as spurious and hence non-utilisable. Therefore, VFA concentrations used for further analysis were set equal to zero, a decision based on the following assumptions: (1) generally all VFA measurements were below zero, (2) there was no significant difference in start and end pH and, (3) a long sludge ensured that all intermediate VFA produced was utilised before end of experiment.

Unlike VFA measurements, other results from 5-pH point titration (i.e., total and carbonate alkalinities) showed consistency and low disparities. Both total and carbonate alkalinities concentration increased. Furthermore, total and carbonate alkalinity concentrations were nearly equal, which indicates that carbonate alkalinity was the dominant alkalinity sub-species in the solution. The change in carbonate alkalinity indicates the presence of biodegradable carbon content in the inoculum.

The TKN and TP concentrations were expected to remain consistent throughout the experiment. As expected, there were generally insignificant changes observed in TKN and TP results.

However, there were a few cases where significant changes were observed, such as test A whereby, an increase of about 13% in TP concentration was observed. In this particular case, when intermediate measurements were observed, it was noted that the measurement on the first day was not consistent with the trend observed from the rest of the results (see Appendix A). This inconsistency suggests that there was an error in the first experiment TP results. Therefore, where there are significant TP or TKN changes, it is because of an error measurement in either the first or last day results.

The FSA and OP concentrations all increased significantly. For all tests, the observed increase in FSA concentrations was nearly the same in all three reactors in a range of 55% and 57%. This implies that both substrates have nearly similar biodegradable organic nitrogen content. However, unlike FSA, the increase in OP concentration differed significantly across the different tests. The highest OP increase was observed in test B (158%), followed by test C (143%) and lastly, test A in which OP increased by 93%.

The concentration of all solids (TSS, VSS and ISS) also decreased significantly. TSS concentrations of the three test reactors decreased between 28 and 30 per cent, while VSS concentrations decreases ranged between 37 and 43 per cent. The change in VSS quantifies the biodegradable particulates present in the reactor at the start of the experiment. To evaluate the relationship between COD and VSS changes, the change in particulate COD concentration was used. Therefore, the change in particulate COD to the concentration of VSS utilised, f_{cv} ratios (mgCOD/mgVSS) for tests A, B and C are 1.51, 1.43 and 1.18 respectively. The f_{cv} ratio for test C is significantly lower than the f_{cv} ratios for wastewater sludges found in literature, i.e., $f_{cv}=1.481$ adopted from Marais & Ekama, (1976).

The change in CH₄ COD and carbon masses were measured via biogas volume produced throughout the experiment and the biogas methane partial pressure. However, gas measurement was challenging due to possible CO₂ dissolving in the column water (as discussed in Section 2.7.3) and possible gas leakage (the gas measurement error in this project was discussed in Section 4.2.3.1). Therefore, to minimise the influence of these gas measurement errors, the replicate with the highest gas volume observed was regarded as the most accurate representation of gas produced. In other words, where results directly relied on gas measurement (i.e., the masses of CH₄ COD and C in gas), the highest gas reading was used instead of taking the average.

Furthermore, due to the high-level error of gas measurement, using gas measurement results for further processing was avoided where possible.

The gas results shows that the change in CH₄ COD mass was highest in test B, followed by test C, and lastly test A. The amount of CH₄ mass produced is directly proportional to aqueous COD lost (i.e., COD is transformed from aqueous phase to gas phase). On the other hand, test C recorded the highest carbon mass released as gas, followed by test B and lastly test A. The change in carbon in gas quantifies the fraction of biodegradable carbon in the reactor that was released as gas.

4.3.2 Gas measurement in test reactors

The biogas produced inside the batch test reactors was captured in the inverted columns. In order to determine the methane content of the biogas, a biogas sample was collected from the reactor's headspace for gas composition analysis. The setup and description of the gas measurement procedure is discussed in Section 3.3.6.

4.3.2.1 Gas measurement

The volume of gas produced by the batch reactors was converted to methane COD equivalence before analysis. During the conversion of gas volume to methane COD, the variance between atmospheric and column pressure was accounted for by using the universal gas law (Equation 3.6). Finally, the methane COD mass was calculated using Equation 3.7. Figure 4-2, Figure 4-3 and Figure 4-4 show the average cumulative methane COD mass for tests A, B and C reactors, respectively

.

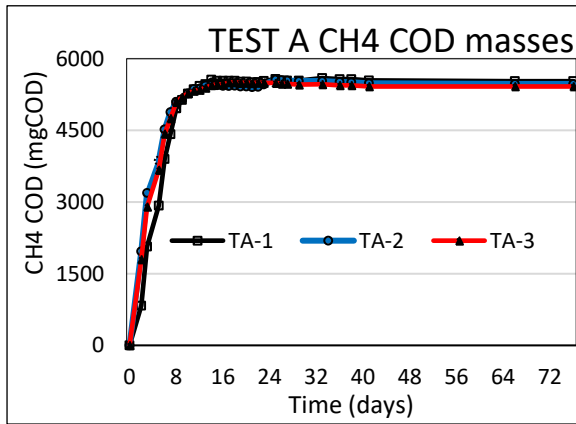


Figure 4-2. Test A batch reactor's methane COD mass

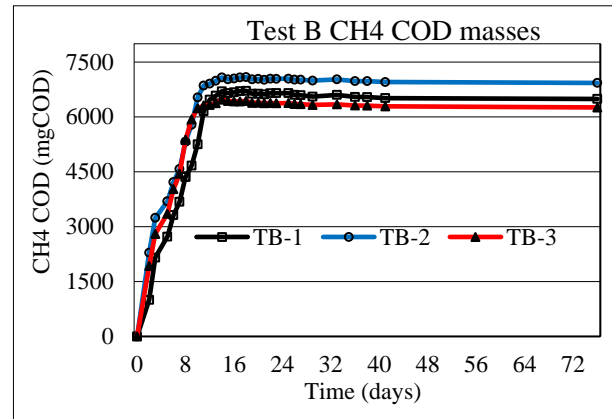


Figure 4-3. Test B batch reactor's methane COD mass

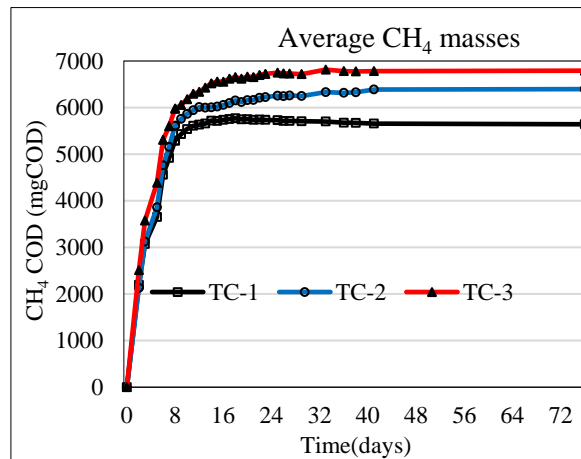


Figure 4-4. Test C batch reactor's methane COD mass

The results show a low variance in cumulative COD methane produced by test A and test B reactors. The low variance in cumulative biogas production between reactors containing the same substrate indicates that there was generally no difference in substrate behaviour in different reactors. In the case of test C, a low variance was observed until day 10, from which there was no significant methane production in reactor TC-1. It is suspected that there could have been a gas leak that caused sudden biogas production in reactor TC-1, because the aqueous COD results shows that TC-1 recorded a higher COD change than TC-2 and TC-3. Overall, there was low variance in cumulative curves across each test, particularly at the start of the experiment which indicates that the behaviours of different replicates were similar, and only started varying due to gas measurement errors.

4.3.2.2 Gas composition

Methane partial pressure was required to calculate methane COD produced by the test reactors, and was determined using a Gas Chromatography (GC) analyser as discussed in Section 3.4.9. However, there was limited access to GC equipment; thus, the methane partial pressure tests were not conducted regularly, resulting in fewer samples collected. Table 4-7 shows a summary of GC results.

Table 4-7. Test reactors' methane partial pressure

Test	Units	Reactor number			Average
		1	2	3	
Test A	%	-	-	59.1	59.1
Test B	%	64.5	56.4	62.4	61.1± 4.2
Test C	%	55.2	-	-	55.2

4.3.3 Mass balances

The mass balances of materials, which follows the principle of mass conservation, were used to evaluate the accuracy and validity of the test reactors. To determine the per cent mass balance, the materials in the test reactors were tracked from the influent to all the effluent streams. As discussed in Section 3.5.3, the influent in this study was made up of a single batch feed, while the effluent was made up of the following: (i) samples drawn from a reactor, (ii) biogas produced, and (iii) the liquid remaining in the reactor at the end of the experiment.

According to the principle of mass conservation of materials, the mass of materials entering the reactors should be equal to the mass of materials leaving the reactor. For the batch test reactors, materials were tracked from the influent to the effluent to determine the per cent mass balance. The influent is made up of a single batch feed, while the effluent is made up of the following (i) samples drawn from a reactor, (ii) biogas produced, and (iii) the liquid remaining in the reactor at the end of the experiment. COD, TKN and TP mass balances were carried out as discussed in Sections 4.3.3.1 and 4.3.3.2.

4.3.3.1 COD Balance

Equation 3.4 in Section 3.5.3.1 was used to calculate the fluxes of COD coming into and out of batch test reactors. In addition, the average methane partial pressures shown in Table 4-7 were used to calculate methane COD. Although in Section 3.5.3 a good COD mass balance was defined to be $100\pm 10\%$, COD mass balances over 80% were also considered acceptable after careful analysis (by increasing methane partial pressure to 100% to determine possible methane measurement error, as shown in Table 4-3). Table 4-8 shows the summary of COD mass balance for all test reactors.

Table 4-8. ABMP test reactor COD balance

Test	Reactor	Starting Mass	Mass Removed	Remaining Mass	CH ₄ Mass	Total effluent	Balance	Average	
		mgCOD	mgCOD	mgCOD	mgCOD	mgCOD	%	mgCOD	
Test A	TA-1	23616	2317	11451	5531	19298	81.7	84.4±3.7	
	TA-2	23904	SPOILED						
	TA-3	22656	1914	12376	5421	19711	87.0		
Test B	TB-1	23616	2015	10920	6493	19428	82.3	86.4±5.2	
	TB-2	23616	1733	11339	6930	20002	84.7		
	TB-3	22272	1844	12440	6258	20543	92.2		
Test C	TC-1	24384	2002	13305	5642	20949	85.9	85.4±3.9	
	TC-2	23712	2292	12404	6396	21092	89.0		
	TC-3	26688	1966	12914	6791	21671	81.2		

The average COD balance for tests A, B and C ranged between 84% and 86%. The achieved COD balance was below the required tolerance for a good COD balance, as stipulated in Section 3.5.3. It was concluded that low COD mass balances are a result of gas measurement error, as shown in Section 4.3.3.1. It is believed that it is challenging to obtain good COD mass balances BMP/ABMP experiments that uses volumetric biogas measurement as discussed in Sections 2.7.2 and 2.7.3.

4.3.3.2 TKN and TP mass balance

The TKN and TP mass balances of the test reactors were also carried out to evaluate the reliability of the experiment results. The aqueous concentrations of TKN and TP do not change during

anaerobic digestion. Therefore, as batch reactors, it was expected that the masses of their influent are equal to the effluent masses. Equation 3.4 in Section 3.5.3.2 was used to calculate the fluxes of TKN and TP entering and leaving batch reactors. The summary of TKN and TP results is given in Table 4-9.

Table 4-9. TKN and TP mass balances for test reactors

Reactor	TKN Balance				TP Balance					
	TKN in	TKN Out	Balance	Average	TP in	TP out	Balance	Average		
Unit	mgN		%		mgP		%			
TA-1	1897	1495	79	93.3 ±20.5	331	366	111	116.9 ±9		
TA-2	REACTOR SPOILED				REACTOR SPOILED					
TA-3	1351	1456	108		299	368	123			
TB-1	1376	1323	96	101 ±5.5	262	299	114	116 ±9.9		
TB-2	1309	1400	107		221	280	127			
TB-3	1400	1397	100		282	302	107			
TC-1	1253	1358	108	109.5 ±6.9	332	335	101	108.9 ±11.9		
TC-2	1197	1400	117		332	343	103			
TC-3	1274	1316	103		332	407	123			

Table 4-9 shows that there was generally a good TKN balance across all test reactors within a permissible 20% error balance.

4.3.4 Unbiodegradable organic composition

The unbiodegradable organic were characterised in terms of unbiodegradable fractions. As noted in Section 3.7.2 the unbiodegradable particulate and soluble organic concentrations of different parameters were measurable at the end of the ABMP experiment. In other words, the concentration of the substrate's unbiodegradable organic was calculated by subtracting the final concentration of the control reactor from the final concentration of the test reactor. Following this, the unbiodegradable fractions of the total organics (determined via COD and VSS measurements), were calculated (the complete procedure is discussed in Section 3.7.2.) Table 4-10 shows a summary of unbiodegradable fraction determination.

Table 4-10. Determination of substrates unbiodegradable fractions

ABMP test		CONTROL	TEST A		TEST B		TEST C	
Measured	Unit	Control	Test	Test-Control	Test	Test-Control	Test	Test-Control
Initial unfiltered COD	mgCOD/l	2872	4752	1880	4723	1852	4810	1938
Total VSS	mgVSS/l	2054	3106	1052	2787	733	3090	1036
Final unfiltered COD	mgCOD/l	2248	2693	445	2520	272	2908	660
Final soluble COD	mgCOD/l	97	197	100	164	67	199	102
USO COD	mgCOD/l	97	197	100	164	67	199	102
UPO COD	mgCOD/l	2151	2496	345	2356	204	2709	558
Final VSS	mgVSS/l	1520	1966	446	1584	64	1810	290
UPO VSS	mgVSS/l	1520	1966	446	1584	64	1810	290
Fractions								
UPO COD ($f_{s'up}$)	mgCOD/mgCOD	-	-	0.183	-	0.110	-	0.288
USO COD ($f_{s'us}$)	mgCOD/mgCOD	-	-	0.053	-	0.036	-	0.053
UPO COD/VSS (f_{cv})	mgCOD/mgVSS	-		0.773		3.190		1.923
Note: Test A= Primary Sludge; Test B= Food waste; Test C= Primary sludge + Food waste								

4.3.5 Biodegradable composition

Substrate biodegradable organic composition was a major objective for carrying out the ABMP experiment. The biodegradable composition was determined by a stoichiometric approach. The stoichiometric composition determination involves quantifying changes in COD, VSS, C, N and P between the start and end of the experiment. These changes were used to calculate the biodegradable organics' elemental mass ratios (f_{CV} , f_C , f_N , f_P , f_O and f_H). Finally, the mass ratios were then used to determine the elemental biodegradable composition in a generic format of $C_xH_yO_zN_A P_B$.

Determination of changes in COD, VSS, C, N and P required measurement of various components at the start and end of the experiment, which is shown in Table 4-11. However, the concentration given in Table 4-11 included the inoculum concentration, which does not form part of the substrate composition. As discussed earlier, the control reactor was used to set the baseline that quantified the substrate biodegradable organics in the test reactors. Therefore, the inoculum concentration inside the test reactor was accounted for by subtracting the measured change in control reactor concentration. As stated in Section 3.3.4, the concentration of the inoculum in test reactors was diluted 1.07 times (i.e., $15 \div 14$). Therefore, the concentration of the reactants taken up and products released into the test reactors due to the inoculum was 0.93 ($14/15$) times that of the control reactor. Thus, the observed changes in control reactor concentrations used in this section are slightly lower than those in Section 4.2.

The steps used for calculating the stoichiometric composition of the substrates is detailed in Section 2.7.3, and the results are shown in Table 4-11.

Table 4-11. Determination of substrate organic composition by stoichiometry

ABMP test		CTRL	TEST A		TEST B		TEST C	
Measured	Unit	Control	Test	Test-Control	Test	Test-Control	Test	Test-Control
		Change (Δ)	Change (Δ)	Change (Δ)	Change (Δ)	Change (Δ)	Change (Δ)	Change (Δ)
Total COD	mgCOD/l	-623.5	-2058.90	-1435.4	-2203.20	-1579.73	2907.80	-1278.3
FSA	mgN/l	42.0	59.00	17.0	52.00	10.00	156.00	15.0
OP	mgP/l	5.9	8.00	2.1	9.80	3.92	17.70	4.5
VSS	mgVSS/l	-397.1	-1140.00	-742.9	-1203.30	-806.17	1810.00	-882.9
Carbonate Alk	mg/l as CaCO ₃	167.1	377	209.9	400	232.93	1,058	134.9
CH ₄ COD	mgCOD	413.5	5595.00	5181.5	7087.00	6673.53	6814.00	6400.5
C in gas	mgC	0.2	1765.00	1764.8	2193.00	2192.81	2295.00	2294.8
COD change								
Biodegradable COD	mgCOD/l	-	-	1435.4	-	1579.7	-	1278.3
CH ₄ COD	mgCOD/l	-	-	1036.3	-	1334.7	-	1280.1
Carbon Change								
C in gas	mgC/l	-	-	353.0	-	438.6	-	459.0
C in H ₂ CO ₃ alkalinity	mgC/l	-	-	50.4	-	55.9	-	32.4
Total C	mgC/l	-	-	403.3	-	494.5	-	491.3
VSS Change								
Biodegradable VSS	mgVSS/l	-	-	742.9	-	806.2	-	882.9
Mass ratio								
f _{CV}	gCOD/gVSS	-	-	1.932	-	1.960	-	1.448
f _C	gC/gVSS	-	-	0.543	-	0.613	-	0.557
f _N	gN/gVSS	-	-	0.023	-	0.012	-	0.017
f _P	gP/gVSS	-	-	0.003	-	0.005	-	0.005
f _H	gH/gVSS	-	-	0.106	-	0.079	-	0.045
f _O	gO/gVSS	-	-	0.326	-	0.291	-	0.376
Composition								
C	mol	-	-	1.000	-	1.000	-	1.000
H	mol	-	-	2.336	-	1.540	-	0.977
O	mol	-	-	0.450	-	0.355	-	0.507
N	mol	-	-	0.036	-	0.017	-	0.026
P	mol	-	-	0.002	-	0.003	-	0.004

Note: Test A= Primary Sludge (PS); Test B= Food waste; Test C= Food waste + Primary Sludge

The biodegradable composition of the substrates in a generic format of $C_xH_yO_zN_aP_b$ can then be deduced from Table 4-11. For example, the composition for primary sludge (PS) (substrate in test A) is $C_1H_{2.336}O_{0.450}N_{0.036}P_{0.002}$, while for food waste (substrate in test B) is $C_1H_{1.540}O_{0.335}N_{0.017}P_{0.003}$, and mixing the two substrates on a ratio of 1:1 (test C) results in $C_1H_{0.997}O_{0.507}N_{0.026}P_{0.004}$. In Section 3.7.3, it was mentioned that carbon was determined from carbonate alkalinity and carbon in gas. However, the gas measurement was found to be inaccurate, which obviously affected the composition of C. Therefore, the mass ratio of C and the elemental compositions of the substrates tested in this study contains an error carried over from gas measurement.

5. ABMP Modelled Experiment

5.1 Introduction

The main focus of the modelling component in this project was to model the augmented biomethane potential (ABMP) experiment to identify the composition of the substrates used in the test reactors, namely, primary sludge (PS), food waste, and a blend of PS and food waste. In addition, modelling the parent anaerobic digester (PAD) was carried out as an ancillary aspect of this project. This chapter presents the modelled outcome of the PAD and ABMP experiments.

5.2 Modelled PAD experiment

The PAD was modelled using the steady-state model equations of Sötemann *et al.* (2005). This PAD modelling process allowed the concentration of the active biomass present in the PAD effluent to be reasonably estimated. The PAD effluent was used to inoculate the ABMP experiment reactors. Only the acidogens (Z_{AD}) biomass group was considered in this project. The active Z_{AD} concentration was obtained by characterising the PAD feed (PS) effluent and using the model equations and parameters to estimate the effluent Z_{AD} concentration. The model description and modelling procedure are detailed in Sections 3.8.2 and 3.8.3. In addition, the original mixed PAD effluent was diluted by half prior to ABMP reactor seeding, as discussed in Section 3.3.4. Table 5-1 presents the summary of the PAD model calculation output.

Table 5-1: PAD modelling output summary

Parameter	Unit	PAD 1	PAD 2
Volume	ℓ	17	26
Feed rate Q	ℓ/d	0.35	0.50
Sludge age	d	49	52
Influent dilution	-	1.17	1.25
Influent COD concentration (not-diluted)	mgCOD/ℓ	26,784	26784
Influent COD concentration (diluted)	mgCOD/ℓ	22958	21427
Effluent COD concentration	mgCOD/ℓ	11750	11597
Methane COD concentration	mgCOD/ℓ	11207	9830
Biomass yield Y_{AD} coefficient	mgCOD/ℓ	0.113	0.113
Biomass death rate b_{AD}	/d	0.041	0.041
Biomass (ZAD) COD concentration	mgCOD/ℓ	477	400
Mixed biomass (ZAD) COD concentration	mgCOD/ℓ	430	
Diluted effluent biomass COD concentration	mgCOD/ℓ	215	

5.3 Modelled ABMP control reactor experiment

The ABMP control reactor experiment was simulated using the mass balanced steady-state model of Ikumi *et al.* (2015) and was used to find inoculum's seed sludge's composition. The biomass concentration obtained in the modelled PAD experiment was entered as input. The diluted biomass concentration shown in Table 5-1 was further diluted 1.75 times during seeding, as mentioned in Section 3.3.4. The initial concentration of the modelled control reactor was set equal to the average measured control reactor concentrations. A detailed modelling process for the control reactor is discussed in Sections 3.8.4 and 3.8.4.1.

As discussed in Section 3.8.4.1, inoculum comprised UPO (UPO and USO lumped together) and seed sludge (residual biodegradable organics (BPO and BSO) and biomass lumped together). This seed sludge composition set the baseline in the test reactors, as discussed later in Section 5.4. After all the model required inputs were entered, a PE process was conducted by running iterative trial and error simulations searching for suitable parameters, which resulted in the lowest error between the measured and modelled results. The PE error in this study was evaluated using the squared error criteria. The overall PE error was obtained by calculating the mean error. However, each variable was weighed to ensure that the error calculation considers the differences

in concentration of different variables (objective values). For example, variables with higher concentrations were assigned a lower weighting factor and vice versa. And therefore, the overall error was calculated as a mean weighted squared error instead of a mean squared error. The parameters and their objective target values used for control reactors were previously shown Table 3-6. The weightings for the control reactor are shown in Table 5-2. The weighting values in Table 5-2 were selected after running multiple iterative trial and error simulations.

Table 5-2: Modelled ABMP control reactor variables and weights

Variable	Weight
Final VSS concentration	10
Final FSA concentration	2
Final OP concentration	1
Final pH	1

5.3.1 Modelled control reactor composition identification

Table 5-3 shows modelled parameters and composition of the seed sludge and UPO contained in the control reactor, which was achieved by the PE process. As mentioned in Section 3.8.4.1, the seed sludge comprises the inoculum's residual biodegradable organics and biomass lumped together to form one compound.

Table 5-3: ABMP control reactor modelled parameters and composition

Parameter	Seed sludge (BPO + biomass)	UPO
f_{cv}	1.481	1.457
f_C	0.338	0.507
f_H	0.140	0.065
f_O	0.385	0.319
f_N	0.111	0.078
f_P	0.027	0.031
$f_{s'up}$	-	0.723
Composition	$C_1H_{4.930}O_{0.854}N_{0.281}P_{0.031}$	$C_1H_{2.279}O_{0.709}N_{0.197}P_{0.036}$

5.3.2 Modelled control reactor results

Table 5-4 summarises results obtained for ending concentrations for various ABMP control reactors experiment constituents. The modelled results were compared to the experimentally measured end results.

Table 5-4: ABMP control reactor modelled results

Constituent	Unit	Start	End		Change	
		Measured	Measured	Modelled	Measured	Modelled
Total COD	mgCOD/ℓ	3076.8	2408.8	2474.5	-668.0	-602.3
Methane COD	mgCOD	0.0	443.0	3012.2	443.0	3012.2
VSS	mgVSS/ℓ	2054.0	1628.5	1628.5	-425.5	-425.5
ISS	mgISS/ℓ	680.0	647.5	680.0	-32.5	0.0
FSA	mgN/ℓ	83.0	128.0	128.0	45.0	45.0
OP	mgP/ℓ	4.6	10.9	10.9	6.3	6.3
H2CO3 Alkalinity	mg/ℓ as CaCO ₃	750.0	929.0	881.3	179.0	131.3
pH		7.50	7.50	7.50	0.00	0.00

The results show that, except for Total COD and methane COD, the model generally estimated the control reactor's end concentrations well, with differences between measured and modelled concentrations not more than 5%. The modelled end total COD Concentration was 10% higher than the measured end COD concentration. The mass of methane COD produced in the modelled experiment, which was based on 100% COD balance (because a mass balanced model was used), was 580% higher than the measured methane COD mass (approximately seven times more than measured methane). This discrepancy between the measured and modelled methane produced indicates a gas measurement error during the ABMP experiment.

5.4 Modelled ABMP test reactor experiment

The ABMP test reactors experiments were simulated using the mass balanced steady-state model of Ikumi *et al.* (2015). They were used mainly to identify the biodegradable composition of the substrates present in different test reactors. The UPO composition present in each test reactor experiment was also determined using the modelled test reactor but as an ancillary aspect of the project. The biomass concentration obtained from modelled PAD experiment (Section 5.2) and

the composition of seed sludge obtained from modelled control reactor (Section 5.3) were used as input for the test reactor experiment modelling. In addition, the starting concentrations of the modelled test reactors experiments were set equal to the average measured starting concentrations for each test experiment. A detailed modelling process for the control reactor is discussed in Sections 3.8.4 and 3.8.4.2. For the purposes of model simplicity, the substrates' particulate and soluble organics were lumped together (i.e., BPO & BSO lumped together, and UPO & USO lumped together) as discussed in Section 3.8.4.2. In other words, the BPO and UPO composition determined by modelled experiments include BSO and USO, respectively.

After all the model required inputs were entered, a PE process was conducted by running iterative trial and error simulations searching for suitable parameters, which resulted in the lowest error between the measured and modelled results. The PE and error evaluation for the test reactors followed the same procedure used in modelling the control reactor, discussed in Section 5.3. The parameter and their objective values for the test reactor were previously shown in Table 3-8. The weightings used for evaluating PE error for test reactors are shown in Table 5-5.

Table 5-5: Modelled ABMP test reactor experiment variables and weights

Test A		Test B		Test C	
Variable	Weight	Variable	Weight	Variable	Weight
Final VSS	10	Final COD	10	Final COD	10
Final FSA	3	Final FSA	3	Final FSA	3
Final OP	1	Final OP	1	Final OP	1
Final pH	1	Final pH	1	Final pH	1

5.4.1 Modelled test reactor composition identification

Table 5-6 shows the modelled parameters and composition of the substrates' BPO and UPO contained in the test reactors. The parameters and composition of the biomass present in the test reactors was determined by control reactor modelling in Section 5.3. Furthermore, as mentioned in Section 3.8.4.2, the BPO and UPO compositions in *Table 5-6* include BSO and USO

Table 5-6: ABMP test reactor modelled parameters and substrate composition

Test A (Primary sludge)			
Parameter	Biomass	BPO	UPO
f _{cv}	1.481	1.500	1.432
f _C	0.338	0.311	0.498
f _H	0.140	0.150	0.064
f _O	0.385	0.509	0.345
f _N	0.111	0.021	0.062
f _P	0.027	0.009	0.031
f _{s^{up}}	-	0.334	
Composition	C ₁ H _{4.93} O _{0.854} N _{0.281} P _{0.031}	C ₁ H _{5.751} O _{1.227} N _{0.056} P _{0.011}	C ₁ H _{1.537} O _{0.52} N _{0.106} P _{0.024}
Test B (food waste)			
Parameter	Biomass	BPO	UPO
f _{cv}	1.481	1.721	1.334
f _C	0.338	0.380	0.464
f _H	0.140	0.147	0.069
f _O	0.385	0.467	0.354
f _N	0.111	0.002	0.083
f _P	0.027	0.004	0.030
f _{s^{up}}	-	0.039	
Composition	C ₁ H _{4.93} O _{0.854} N _{0.281} P _{0.031}	C ₁ H _{4.598} O _{0.924} N _{0.004} P _{0.004}	C ₁ H _{1.772} O _{0.572} N _{0.153} P _{0.025}
Test C (primary sludge and food waste blend)			
Parameter	Biomass	BPO	UPO
f _{cv}	1.481	1.765	1.392
f _C	0.338	0.447	0.485
f _H	0.140	0.124	0.067
f _O	0.385	0.403	0.350
f _N	0.111	0.016	0.071
f _P	0.027	0.009	0.028
f _{s^{up}}	-	0.174	
Composition	C ₁ H _{4.93} O _{0.854} N _{0.281} P _{0.031}	C ₁ H _{3.301} O _{0.676} N _{0.032} P _{0.008}	C ₁ H _{1.648} O _{0.543} N _{0.125} P _{0.022}

5.4.2 Modelled test reactor results

Table 5-7 shows the summary of measured starting concentration and modelled end concentrations of different constituents of the ABMP test reactor experiments. The change in concentrations for the measured experiment was compared to the changes in concentration for the modelled experiment.

Table 5-7: ABMP test reactors modelled experiment results

Component	Unit	Start	End		Change	
		Measured	Measured	Modelled	Measured	Modelled
Test A						
Total COD	mgCOD/l	4752.0	2693.1	3184.4	-2058.9	-1567.6
Methane COD	mgCOD	0.0	5595.0	7839.3	5595.0	7839.3
VSS	mgVSS/l	3106.0	1966.0	2010.2	-1140.0	-1095.8
ISS	mgISS/l	804.0	698.0	804.0	-106.0	0.0
FSA	mgN/l	106.0	165.0	165.0	59.0	59.0
OP	mgP/l	8.6	16.6	16.6	8.0	8.0
H ₂ CO ₃ Alkalinity	mg/l as CaCO ₃	812.0	1189.0	1168.8	377.0	356.8
pH		7.30	7.30	7.30	0.00	0.00
Test B						
Total COD	mgCOD/l	4723.2	2520.0	2520.0	-2203.2	-2203.2
Methane COD	mgCOD	0.0	7087.0	11017.7	7087.0	11017.7
VSS	mgVSS/l	2787.3	1584.0	1648.6	-1203.3	-1138.7
ISS	mgISS/l	671.4	563.3	671.4	-108.1	0.0
FSA	mgN/l	96.0	148.0	148.0	52.0	52.0
OP	mgP/l	6.2	16.0	16.0	9.8	9.8
H ₂ CO ₃ Alkalinity	mg/l as CaCO ₃	660.0	1060.0	1145.3	400.0	485.3
pH		7.20	7.30	7.30	0.10	0.10
Test C						
Total COD	mgCOD/l	4809.6	2907.8	2907.8	-1901.8	-1901.8
Methane COD	mgCOD	0.0	6814.0	9510.5	6814.0	9510.5
VSS	mgVSS/l	3090.0	1810.0	1864.9	-1280.0	-1225.1
ISS	mgISS/l	684.7	668.7	684.7	-16.0	0.0
FSA	mgN/l	99.0	156.0	156.0	57.0	57.0
OP	mgP/l	7.3	17.7	17.7	10.4	10.4
H ₂ CO ₃ Alkalinity	mg/l as CaCO ₃	756.0	1058.0	912.0	302.0	156.0
pH		7.30	7.10	7.10	-0.20	-0.20

The concentrations of VSS, FSA, OP, and pH across the three test experiments were generally well estimated by the modelled experiment, yielding not more than a 5% difference between modelled and measured concentrations. The modelled Total COD concentration for test A was

moderately (18%) higher than the measured concentration, while for tests B and C, the difference between modelled and measured COD concentration was less than 5%. On the other hand, the modelled methane COD produced was significantly higher (between 40 and 55%) than the measured methane COD for all test experiments. This discrepancy between the measured and modelled methane produced indicates a gas measurement error during the ABMP experiment. The modelled H_2CO_3 alkalinity concentration in tests A and C were 2% and 14% lower than the measured concentration, respectively. In contrast, test B's modelled H_2CO_3 alkalinity concentration was 8% higher than the measured concentration.

6. Conclusion and Recommendations

6.1 Introduction

This study assessed the potential to revise urban wastewater systems to include solid waste separation and discharge food waste to sewer systems. The assessment involved (1) reviewing alternative sustainable solid waste separation and food waste transport systems, and (2) a combination of experimental investigation and model simulation to define existing (without food waste) and probable (with food waste) anaerobic digestion (AD) systems' influent characteristics. This research investigation addressed two major obstacles limiting full-scale wastewater and food waste co-digestion projects: food waste handling systems and characterization of food waste. The findings of this research are vital inputs in the system-wide assessment for the co-digestion of wastewater and food waste. Therefore, this chapter provides a summary of the conclusions drawn from the findings emerging from this study, followed by areas where further efforts motivated by research would be required.

6.2 Summary of conclusion

In this project, it was comprehensively reviewed three potential alternative sustainable systems for solid waste separation and transportation of food waste to anaerobic digestion (AD) systems in South Africa. The review was based on various full-scale case studies from four countries that have implemented sewage sludge and food waste co-digestion at WWTPs. The review revealed that manual food waste handling systems are commonly used in sewage sludge and food waste co-digestion projects. However, these manual food waste handling systems requires complex food waste transport and pre-treatment processes and produces bad odours. On the other hand, a novel food waste disposer (FWD) that disposes food waste directly into the sewer systems is scientifically proven suitable for resource recovery and food waste handling. Therefore, FWDs are largely being promoted to eliminate manual food waste handling and limit bad odours. However, the impact of FWD on the sewer systems and WWTPs and its potential energy and potable water usage has not been well established. Nevertheless, the choice of sustainable food waste handling systems needs to be case-specific because it should consider a wide range of local factors.

The Augmented biomethane potential (ABMP) experiment, comprised of a control reactor and three sets of test reactors fed with different substrates (i.e., primary sludge, food waste and a blend of primary sludge and food waste), was operated for 76 days to determine the characteristics of sewage sludge and food waste. The experimental results were evaluated using statistical analysis and mass balances. The statistical analysis found volatile fatty acid (VFA) measurements to be spurious and hence were not utilized. On the other hand, a poor COD balance was observed, caused by gas (methane COD) measurement error.

Using the ABMP experiment results, sewage sludge and food waste co-digestion was simulated using two model approaches: (i) the mass balanced bioprocess stoichiometry calculations and (ii) the parameter estimation (PE) process, which is embedded in a steady-state model. The results obtained through the PE process were deemed to be more accurate than the bioprocess stoichiometric calculations. This is because the PE procedure was able to identify and minimise errors between the measured and modelled results, whereas the bioprocess stoichiometry calculations relied on the measured results.

Using the modelled experiment results, which were deemed more accurate, the anaerobic digestion of food waste and anaerobic co-digestion of primary sludge and food waste generate 41% and 21% more methane COD gas than anaerobic digestion of primary sludge. Methane gas generated is equivalent to potential energy recoverable, and therefore this means that diverting food waste to WWTPs, can potentially enhance energy recovery.

6.3 Recommendations

A system-wide model for solid waste separation and food waste discharge to sewer systems was carried out within this project's scope. However, there is potential for further studies that can be addressed through extended investigation to either update the existing literature or provide new data for extending the model. Therefore, the following recommendations are made for further studies:

1. An investigation involving “real” food waste characterization, including food waste quantity and quality, need to be carried out in South Africa because the literature shows that food waste is poorly documented in South Africa.

2. A quantitative case study to investigate the feasibility of different food waste transport collection and transport system in South Africa. This is because the choice of a system for solid waste separation and food waste transport to a treatment facility is highly influenced by the setup of infrastructure such as sewer networks.
3. An investigation of the impact of food waste disposers (FWD) on (1) potable water and energy usage and (2) sewage network, i.e., corrosion, sedimentation and blockage need to be carried out.
4. A technical evaluation of a specific WWTP to determine the capacity of energy required to co-digest wastewater sludge and food waste and the potential energy that can be recovered need to be carried out.
5. Upgrading and calibration of existing models to include a food waste component and other potential organic waste groups.
6. Extensive testing followed by dynamic simulation of the experiments (i.e., using PWM_SA model) to accurately characterize food waste composition.
7. Evaluation the quality and quantity of processed sludge/by-products resulting from co-digestion of food waste with sewage sludge and determine their disposal or beneficial use options.
8. Evaluation of the financial and economic impacts of implementing wastewater sludge and food waste co-digestion technology.

7. References

- Angelidaki, I., Alves, M., Bolzonella, D., Borzacconi, L., Campos, J.L., Guwy, A.J., Kalyuzhnyi, S., Jenicek, P., *et al.* 2009. Defining the biomethane potential (BMP) of solid organic wastes and energy crops: A proposed protocol for batch assays. *Water Science and Technology*. DOI: <https://doi.org/10.2166/wst.2009.040>.
- Angula, S. & Ikumi, D. 2022. Potential co-disposal of food waste and wastewater in South Africa: A review.
- Arnell, M., Astals, S., Åmand, L., Batstone, D.J., Jensen, P.D. & Jeppsson, U. 2016. Modelling anaerobic co-digestion in Benchmark Simulation Model No. 2: Parameter estimation, substrate characterisation and plant-wide integration. *Water Research*. 98:138–146. DOI: <https://doi.org/10.1016/j.watres.2016.03.070>.
- Batstone, D.J., Keller, J., Angelidaki, I., Kalyuzhnyi, S., Pavlostathis, S., Rozzi, A., Sanders, W., Siegrist, H., *et al.* 2002. The IWA Anaerobic Digestion Model No 1. *Water Science & Technology*. 45(10):65–73.
- Bernstad, A., Malmquist, L., Truedsson, C. & la Cour Jansen, J. 2013. Need for improvements in physical pretreatment of source-separated household food waste. *Waste Management*. 33(3):746–754. DOI: <https://doi.org/10.1016/J.WASMAN.2012.06.012>.
- Bernstad Saraiva, A., Davidsson, A. & Bissmont, M. 2016. Lifecycle assessment of a system for food waste disposers to tank - A full-scale system evaluation. *Waste Management*. 54:169–177. DOI: <https://doi.org/10.1016/j.wasman.2016.04.036>.
- Bolzonella, D., Pavan, P., Battistoni, P. & Cecchi, F. 2003. The under sink garbage grinder: A friendly technology for the environment. *Environmental Technology*. 24(3):349–359. DOI: <https://doi.org/https://doi.org/10.1080/09593330309385567>.
- Botha, R.F. 2015. Characterization of organics for anaerobic digestion my modelling augmented biochemical methane potential test results. University of Cape Town.
- Brink, I. 2008. Measurement of Composition of Organic Constituents of Municipal Wastewater

for Plant-wide Modelling. University of Cape Town. DOI: <https://doi.org/10.1590/S0034-71402004000300002>.

Brouckaert, C.J., Ikumi, D.S. & Ekama, G.A. 2010. A 3 Phase Anaerobic Digestion Model. In *12th IWA AD conference*. Guadalajara, Mexico.

Brouckaert, C.J., Ekama, G.A., Brouckaert, B.M. & Ikumi, D.S. 2021. Integration of complete elemental mass-balanced stoichiometry and aqueous-phase chemistry for bioprocess modelling of liquid and solid waste treatment systems – part 2: Bioprocess stoichiometry. *Water SA*. 47(3):289–308. DOI: <https://doi.org/10.17159/wsa/2021.v47.i3.11858>.

Burton, S., Cohen, B., Harrison, S., Pather-Elias, S., Stafford, W., van Hille, R. & von Blottnitz, H. 2009. Energy from wastewater - a feasibility study. *Report to the Water Research Commission*. (July):1–11.

Cecchi, F. & Cavinato, C. 2019. Smart approaches to food waste final disposal. *International Journal of Environmental Research and Public Health*. 16(16). DOI: <https://doi.org/10.3390/ijerph16162860>.

Claeys, F. 2008. A generic software framework for modelling and virtual experimentation with complex biological systems. Ghent University.

De Clercq, D., Wen, Z., Gottfried, O., Schmidt, F. & Fei, F. 2017. A review of global strategies promoting the conversion of food waste to bioenergy via anaerobic digestion. *Renewable and Sustainable Energy Reviews*. 79:204–221. DOI: <https://doi.org/10.1016/j.rser.2017.05.047>.

Cronje, N., van der Merwe, I. & Muller, I.-M. 2018. Household food waste: A case study in Kimberly, South Africa. *Journal of Consumer Sciences*. 46(August):1–9.

Davidsson, Bernstad Saraiva, A., Magnusson, N. & Bissmont, M. 2017. Technical evaluation of a tank-connected food waste disposer system for biogas production and nutrient recovery. *Waste Management*. 65:153–158. DOI: <https://doi.org/10.1016/j.wasman.2017.03.052>.

Donnenfeld, Z., Crookes, C. & Hedden, S. 2018. A delicate balance: Water scarcity in South Africa. *Southern Africa Report*. 13(March):1–24. Available: <https://issafrica.org/research/southern-africa-report/a-delicate-balance-water-scarcity-in-south->

africa.

Edwards, J., Othman, M., Crossin, E. & Burn, S. 2017. Anaerobic co-digestion of municipal food waste and sewage sludge: A comparative life cycle assessment in the context of a waste service provision. *Bioresource Technology*. 223:237–249. DOI: <https://doi.org/10.1016/J.BIORTECH.2016.10.044>.

Ekama, G.A. 2009. Using bioprocess stoichiometry to build a plant-wide mass balance based steady-state WWTP model. *Water Research*. 43(8):2101–2120. DOI: <https://doi.org/10.1016/j.watres.2009.01.036>.

Ekama, G.A. 2017. Optimizing water and resource recovery facilities (WRRF) for energy generation without compromising effluent quality. *IWA Conference on Sustainable Wastewater Treatment and Resource Recovery: Research, Planning, Design and Operation*. 1–14.

Ekama, G.A. & Brink, I.C. 2007. Building a Steady State Plant Wide Wastewater Treatment Plant Model With Bio-Process Stoichiometry. *Water Institute of South Africa*. (July).

Ekama, G.A. & Wentzel, M.C. 2004. A predictive model for the reactor inorganic suspended solids concentration in activated sludge systems. *Water Research*. 38(19):4093–4106.

Ekama, G.A. & Wentzel, M.C. 2008. Organic Matter Removal. In *Biological Wastewater Treatment: Principles, Modelling and Design*. M. Henze *et al.*, Eds. London, UK: IWA Publishing. 53–86.

Ekama, G.A. & Wenzel, M.C. 2008. Organic Material removal. In *Biological Wastewater Treatment: Principle, Modelling and Design*. M. Henze *et al.*, Eds. London, UK: IWA Publishing. 53–86.

Ekama, G.A., Barnard, J.L., Günthert, F.W., Krebs, P., McCorquodale, J.A., Parker, D.S. & Wahlberg, E.J. 1997. Secondary Settling Tanks - Theory, Modelling, Design and Operation. *Scientific and Technical Report*.

Evans, T.D. 2012. Domestic Food Waste – the Carbon and Financial Costs of the Options. *Municipal Engineer*. 165(ME1):3–10.

- Ferry, A. & Giljova, S. 2015. *Biogas potential in selected waste water treatment plants*. Pretoria.
- Gaszynski, C. 2021. Identification of wastewater primary sludge composition using augmented batch tests and mathematical models. University of Cape Town.
- Gaszynski, C.E., Ikumi, D.S. & Ekama, G.A. 2019. Utilisation of augmented batch tests to determine sludge characteristics. In *IWA Watermatex*. 1–4.
- Ghoor, T. 2020. Developments in Anaerobic Digestion Modelling. University of Cape Town.
- Grau, P., Vanrolleghem, P.A. & Ayesa, E. 2007. BSM2 plant-wide model construction and comparative analysis with other methodologies for integrated modelling. In *The Seventh International IWA Symposium on Systems Analysis and Integrated Assessment in Water Management*. Washington DC, USA.
- Gray, D.M.D., Suto, P. & Peck, C. 2008. *Anaerobic digestion of food waste: Funding opportunity no. EPA-R9-WST-06-004*. Available: <https://archive.epa.gov/region9/organics/web/pdf/ebmudfinalreport.pdf>.
- Gujer, W. & Zehnder, A.J.B. 1983. Conversion processes in anaerobic digestion. In *Water Science and Technology*. V. 15. DOI: <https://doi.org/10.2166/wst.1983.0164>.
- Guyen, H. & Ozturk, I. 2018. Impact of Food Waste Addition To Municipal Wastewater on Environmental Infrastructure. In *6th Eur. Conf. Ren. Energy Sys*. Istanbul, Turkey. Available: https://www.researchgate.net/publication/326571680_Impact_of_food_waste_addition_to_municipal_wastewater_on_environmental_infrastructure.
- Hagey, P. 2011. Utility district ramps up food waste to energy program. *BioCycle*. 52(11):39–40.
- Hagos, K., Zong, J., Li, D., Liu, C. & Lu, X. 2017. Anaerobic co-digestion process for biogas production : Progress , challenges and perspectives. *Renewable and Sustainable Energy Reviews*. 76(March 2016):1485–1496. DOI: <https://doi.org/10.1016/j.rser.2016.11.184>.
- Harding, T.H. 2009. A steady state stoichiometry model describing the anaerobic digestion of biological excess phosphorus removal from waste activated sludge. University of Cape Town.

Henze, M., Gujer, W., Mino, T., Matuso, T., Wentzel, M.C. & Marais, G.V.R. 1995. Wastewater and Biomass Characterization for the Activated Sludge Model No. 2: Biological Phosphorus Removal. *Water science and technology: a journal of the International Association on Water Pollution Research*. 31(2):1–11.

Henze, M., Gujer, W., Mino, T. & van Loosdrecht, M.C.M. 2000. *Activated sludge models ASM1, ASM2, ASM2d and ASM3*. London, UK: IWA Publishing.

Holliger, C., Alves, M., Andrade, D., Angelidaki, I., Astals, S., Baier, U., Bougrier, C., Buffière, P., *et al.* 2016. Towards a standardization of biomethane potential tests. *Water Science and Technology*. DOI: <https://doi.org/10.2166/wst.2016.336>.

Hulsbeek, J.J.W., Kruit, J., Roeleveld, P.J. & Van Loosdrecht, M.C.M. 2002. A practical protocol for dynamic modelling of activated sludge systems. *Water Science and Technology*. 45(6):127–136. DOI: <https://doi.org/10.2166/wst.2002.0100>.

Iacovidou, E., Ohandja, D., Gronow, J., Iacovidou, E., Ohandja, D. & Gronow, J.A.N. 2012. The Household Use of Food Waste Disposal Units as a Waste Management Option: A Review. *Critical Reviews in Environmental Science and Technology*. 42:14(May):1485–1508. DOI: <https://doi.org/10.1080/10643389.2011.556897>.

Ikumi, D.S. 2011. The Development of a Three Phase Plant-Wide Mathematical Model for Sewage Treatment. University of Cape Town.

Ikumi, D.S., Harding, T.H. & Ekama, G.A. 2014. Biodegradability of wastewater and activated sludge organics in anaerobic digestion. *Water Research*. 56:267–279. DOI: <https://doi.org/10.1016/j.watres.2014.02.008>.

Ikumi, D.S., Harding, T.H., Vogts, M., Lakay, M.T., Mafungwa, H.Z., Brouckaert, C.J. & Ekama, G.A. 2015. *Mass Balances Modelling Over Wastewater Treatment Plants III*. Cape Town.

Iqbal, A., Ekama, G.A., Zan, F., Liu, X., Chui, H.K. & Chen, G.H. 2020. Potential for co-disposal and treatment of food waste with sewage: A plant-wide steady-state model evaluation. *Water Research*. 184:116175. DOI: <https://doi.org/10.1016/j.watres.2020.116175>.

Jones, R.M. & Takács, I. 2004. Importance of anaerobic digestion modelling on predicting the overall performance of wastewater treatment plants. In *The Anaerobic Digestion Tenth World Congress*. Montreal, Canada. 1371–1375.

Li, W.W., Yu, H.Q. & Rittmann, B.E. 2015. Chemistry: Reuse water pollutants. *Nature*. 528(7580). DOI: <https://doi.org/10.1038/528029a>.

Van Lier, J.B., Mahmoud, N. & Zeeman, G. 2008. Anaerobic wastewater treatments. In *Biological Wastewater Treatment: Principle, Modelling and Design*. M. Henze *et al.*, Eds. London, UK: IWA Publishing.

Maake, V. & Ikumi, D. 2022. Using Augmented Batch Tests to Quantify kinetics of Anaerobic breakdown of Waste Sludge Containing Enhanced Cultures of Polyphosphate Accumulating Organisms.

Macintosh, C., Astals, S., Sembera, C., Ertl, A., Drewes, J.E., Jensen, P.D. & Koch, K. 2019. Successful strategies for increasing energy self-sufficiency at Grüneck wastewater treatment plant in Germany by food waste co-digestion and improved aeration. *Applied Energy*. 242(November 2018):797–808. DOI: <https://doi.org/10.1016/j.apenergy.2019.03.126>.

Marais, G.V.R. & Ekama, G.A. 1976. The activated sludge process . Part 1 - Steady state behaviour. *Water SA*. 2(October 1976):163–200.

Mebranthu, M.K. 2007. Aerobic Digestion of Waste Activated Sludge from Biological Nutrient Removal Activated Sludge Systems. University of Cape Town.

Mehariya, S., Kumar, A., Karthikeyan, P., Punniyakotti, E., Wong, J.W.C.C., Patel, A.K., Obulisamy, P.K., Punniyakotti, E., *et al.* 2018. Co-digestion of food waste and sewage sludge for methane production: Current status and perspective. *Bioresource Technology*. 265:519–531. DOI: <https://doi.org/10.1016/j.biortech.2018.04.030>.

Mehariya, S., Kumar, A., Karthikeyan, P., Punniyakotti, E. & Wong, J.W.C. 2018. Co-digestion of food waste and sewage sludge for methane production: Current status and perspective. *Bioresource Technology*. 265:519–531. DOI: <https://doi.org/10.1016/j.biortech.2018.04.030>.

Menardo, S. & Balsari, P. 2012. An Analysis of the Energy Potential of Anaerobic Digestion of

Agricultural By-Products and Organic Waste. *Bioenergy Research*. 5(3):759–767. DOI: <https://doi.org/10.1007/s12155-012-9188-0>.

Moosbrugger, R.E., Wentzel, M.C., Ekama, G.A. & Marais, G. v R. 1993. A 5 pH Point Titration Method for Determining the Carbonate and SCFA Weak Acid/Bases in Anaerobic Systems. *Water Science & Technology*. 28(2):237–245.

Mosey, F.E. 1983. Mathematical modelling of the anaerobic digestion process: Regulatory mechanisms for the formation of short-chain volatile acids from glucose. In *Water Science and Technology*. V. 15. DOI: <https://doi.org/10.2166/wst.1983.0168>.

Musvoto, E. & Ikumi, D. 2016. *Energy Use Reduction in Biological Nutrient Removal Wastewater Treatment Plants: A South African Case Study*. Gezina.

Nahman, A. & de Lange, W. 2013. Costs of food waste along the value chain: Evidence from South Africa. *Waste Management*. 33(11):2493–2500. DOI: <https://doi.org/10.1016/j.wasman.2013.07.012>.

Nahman, A., de Lange, W., Oelofse, S. & Godfrey, L. 2012. The costs of household food waste in South Africa. *Waste Management*. 32(11):2147–2153. DOI: <https://doi.org/10.1016/j.wasman.2012.04.012>.

Nghiem, L.D., Koch, K., Bolzonella, D. & Drewes, J.E. 2017. Full scale co-digestion of wastewater sludge and food waste: Bottlenecks and possibilities. *Renewable and Sustainable Energy Reviews*. 72:354–362. DOI: <https://doi.org/10.1016/j.rser.2017.01.062>.

Oelofse, S.H.H. & Nahman, A. 2013. Estimating the magnitude of food waste generated in South Africa. *Waste Management and Research*. 31(1):80–86. DOI: <https://doi.org/10.1177/0734242X12457117>.

Owen, W.F., Stuckey, D.C., Healy, J.B., Young, L.Y. & McCarty, P.L. 1979. Bioassay for monitoring biochemical methane potential and anaerobic toxicity. *Water Research*. 13(6):485–492. DOI: [https://doi.org/10.1016/0043-1354\(79\)90043-5](https://doi.org/10.1016/0043-1354(79)90043-5).

Parajuli, P. 2011. Biogas measurement techniques and the associated errors. University of Jyväskylä.

Petterson, D. 2019. The future of sustainable sludge management. *Water&sanitaion Africaanitaion Africa*. 14(2):34–46.

Raposo, F., Fernández-Cegrí, V., de la Rubia, M.A., Borja, R., Béline, F., Cavinato, C., Demirer, G., Fernández, B., *et al.* 2011. Biochemical methane potential (BMP) of solid organic substrates: Evaluation of anaerobic biodegradability using data from an international interlaboratory study. *Journal of Chemical Technology and Biotechnology*. 86(8). DOI: <https://doi.org/10.1002/jctb.2622>.

Ristow, N.E., Sötemann, S.W., Loewenthal, R.E., Wentzel, M.C. & Ekama, G.A. 2005. *Hydrolysis of Primary Sewage Sludge under Methanogenic, Acidogenic and Sulfate-reducing Conditions*.

Seco, A., Ruano, M. V., Ruiz-Martinez, A., Robles, A., Barat, R., Serralta, J. & Ferrer, J. 2020. Plant-wide modelling in wastewater treatment: showcasing experiences using the Biological Nutrient Removal Model. *Water Science and Technology*. 1–15. DOI: <https://doi.org/10.2166/wst.2020.056>.

Sembera, C., Macintosh, C., Astals, S. & Koch, K. 2019. Benefits and drawbacks of food and dairy waste co-digestion at a high organic loading rate: A Moosburg WWTP case study. *Waste Management*. 95:217–226. DOI: <https://doi.org/10.1016/j.wasman.2019.06.008>.

Shen, Y., Linville, J.L., Urgan-Demirtas, M., Mintz, M.M. & Snyder, S.W. 2015. An overview of biogas production and utilization at full-scale wastewater treatment plants (WWTPs) in the United States: Challenges and opportunities towards energy-neutral WWTPs. *Renewable and Sustainable Energy Reviews*. 50:346–362. DOI: <https://doi.org/10.1016/j.rser.2015.04.129>.

Sikosana, M., Randall, D.G., J, P.D., M, O., Ruuso, V. & von Blottnitz, H. 2016. *Nutrient and Energy Recovery from Sewage: Towards an Integrated Approach*.

Sikosana, M.K.L.N., Randall, D.G. & Blottnitz, H. Von. 2017. A technological and economic exploration of phosphate recovery from centralised sewage treatment in a transitioning economy context Municipal wastewater Return to Sludge recycle. *Water SA*. 43(2):343–353.

Sötemann, S.W., van Rensburg, P., Ristow, N.E., Wentzel, M.C., Loewenthal, R.E. & Ekama,

- G.A. 2005. Integrated chemical / physical and biological processes modelling Part 2 - Anaerobic digestion of sewage sludges. *Water Science and Technology*. 31(4):545–568. DOI: <https://doi.org/10.2166/wst.2006.553>.
- Sötemann, S.W., Ristow, N.E., Wentzel, M.C. & Ekama, G.A. 2005. A steady state model for anaerobic digestion of sewage sludges. *Water SA*. 31(4):511–528. DOI: <https://doi.org/10.4314/wsa.v31i4.5143>.
- Stillwell, A.S., Hoppock, D.C. & Webber, M.E. 2010. Energy recovery from wastewater treatment plants in the United States: A case study of the energy-water nexus. *sustainability*. 2(4):945–962. DOI: <https://doi.org/10.3390/su2040945>.
- Strömberg, S., Nistor, M. & Liu, J. 2014. Towards eliminating systematic errors caused by the experimental conditions in Biochemical Methane Potential (BMP) tests. *Waste Management*. 34(11):1939–1948. DOI: <https://doi.org/10.1016/J.WASMAN.2014.07.018>.
- Swartz, C.D., Van Der Merwe-Botha, M. & Freese, S.D. 2013. *Energy Efficiency in the South African Water Industry: a Compendium of Best practices and Case Studies*. Available: www.wrc.org.za.
- Takács, I. & Ekama, G.A. 2008. Final Settling. In *Biological Wastewater Treatment: Principle, Modelling and Design*. M. Henze *et al.*, Eds. London, UK: IWA Publishing.
- Thomas, P. 2011. The effects of food waste disposers on the wastewater system : a practical study. *Water and Environment Journal*. 25(August 2008):250–256. DOI: <https://doi.org/10.1111/j.1747-6593.2010.00217.x>.
- Tredoux, G., King, P. & Cave, L. 1999. Managing urban wastewater for maximising water resource utilisation. *Water Science & Technology*. 39(10–11):353–356.
- Vanrolleghem, P.A. 2002. Principles of respirometry in activated sludge wastewater treatment. In *Proceedings International Workshop on Recent Development in Respirometry for Wastewater Treatment Plant Monitoring and Control*. Taiwan: Taipei.
- Volcke, E.I.P., van Loosdrecht, M.C.M. & Vanrolleghem, P.A. 2006. Continuity based model interfacing for plant-wide simulation: A general approach. *Water Research*. 40:2817–2828.

Wentzel, M.C. & Ekama, G.A. 2003. Characterization of Municipal Wastewater. In *Handbook of Water and Wastewater Microbiology*. London: Academic.

Wentzel, M.C., Ekama, G.A., Dold, P.L. & Marais, G.V.R. 1990. Biological Excess Phosphorus Removal - Steady State Process Design. *Water SA*. 16(1):29–48.

Wentzel, M.C., Ekama, G.A. & Loewenthal, R.E. 2003. Fundamentals of biological behaviour and wastewater strength tests. In *The handbook of water and wastewater microbiology*. 1st ed. London: Academic. 145–173.

Wentzel, M.C., Comeau, Y., Ekama, G.A., van Loosdrecht, M.C.M. & Brdjanovic, D. 2008. Phosphorus Removal. In *Biological Wastewater Treatment: Principle, Modelling and Design*. M. Henze *et al.*, Eds. London, UK: IWA Publishing.

Wu, W.Y.X. 2015. Development of a Plant-wide Steady-state Wastewater Treatment Plant Design and Analysis Program. University of Cape Town.

Xie, S., Hai, F.I., Zhan, X., Guo, W., Ngo, H.H., Price, W.E. & Nghiem, L.D. 2016. Anaerobic co-digestion: A critical review of mathematical modelling for performance optimization. *Bioresource Technology*. 222:498–512. DOI: <https://doi.org/10.1016/J.BIORTECH.2016.10.015>.

Zan, F., Dai, J., Hong, Y., Wong, M., Jiang, F. & Chen, G. 2018. The characteristics of household food waste in Hong Kong and their implications for sewage quality and energy recovery. *Waste Management*. 74:63–73. DOI: <https://doi.org/10.1016/j.wasman.2017.11.051>.

Zan, F., Iqbal, A., Guo, G., Liu, X., Dai, J., Ekama, G.A. & Chen, G. 2020. Integrated food waste management with wastewater treatment in Hong Kong: Transformation, energy balance and economic analysis. *Water Research*. (xxxx). DOI: <https://doi.org/10.1016/j.watres.2020.116155>.

Zhen, H., Ekman, D.R., Collette, T.W., Glassmeyer, S.T., Mills, M.A., Furlong, E.T., Kolpin, D.W. & Teng, Q. 2018. Assessing the impact of wastewater treatment plant effluent on downstream drinking water-source quality using a zebrafish (*Danio Rerio*) liver cell-based metabolomics approach. *Water Research*. 145:198–209. DOI:

<https://doi.org/10.1016/j.watres.2018.08.028>.

Appendix A : ABMP Experiment test data

Table 7-1: ABMP data-1*

Test	Unfiltered COD (mgCOD/l)						Filtered COD (mgCOD/l)						TKN (mgN/l)					TP (mgP/l)				
	24-Jun	28-Jun	07-Jul	04-Aug	23-Aug	08-Sep	24-Jun	28-Jun	07-Jul	04-Aug	23-Aug	08-Sep	24-Jun	28-Jun	07-Jul	04-Aug	08-Sep	24-Jun	28-Jun	07-Jul	04-Aug	08-Sep
Days elapsed	0	4	13	41	60	76	0	4	13	41	60	76	0	4	13	41	76	0	4	13	41	76
C-1	3,053	3,696	1,640	2,227	2,284	2,435	154	156	171	111	108	NA	249	NA	258	NA	237	58	54	56	60	60
C-2	3,091	3,840	2,863	2,275	2,359	2,416	161	157	152	106	100	180	242	NA	225	256	244	60	51	61	66	60
C-3	3,034	3,744	2,829	2,381	2,585	2,425	150	167	156	90	104	NA	230	252	225	246	232	57	53	56	61	66
C-4	3,130	3,648	3,430	2,285	2,500	2,359	167	159	159	73	121	156	246	242	231	233	258	60	58	60	64	57
Mean	3,077	3,732	2,846	2,292	2,322	2,409	158	160	156	82	104	156	242	247	258	251	243	58	53	58	63	61
St. deviation	43	82	24	64	136	34	8	5	4	12	9	NA	9	7	19	12	11	1	3	2	3	4
TA-1	4,723	5,760	3,016	2,659	2,698	2,726	530	472	202	84	109	196	379	296	245	276	299	66	65	65	67	73
TA-2	4,781	5,376	2,970	NA	NA	NA	532	374	188	NA	NA	NA	272	352	248	NA	NA	64	74	76	NA	NA
TA-3	4,531	5,232	3,470	2,707	2,659	2,660	532	392	177	81	98	198	270	329	242	280	291	60	71	75	77	74
Mean	4,752	5,304	2,993	2,683	2,678	2,693	531	383	189	83	104	197	271	326	245	278	295	65	72	76	77	73
St. deviation	41	102	33	34	27	47	1	12	12	3	8	1	1	28	7	3	5	1	4	6	7	0
TB-1	4,723	5,712	2,909	2,352	2,506	2,496	645	480	190	77	106	169	275	315	249	258	265	52	53	58	60	60
TB-2	4,723	4,512	2,816	2,362	2,525	2,544	703	513	165	79	125	159	262	289	230	279	280	44	58	57	64	56
TB-3	4,454	5,664	2,923	2,400	2,832	2,792	637	480	219	119	96	197	280	121	244	274	279	56	67	59	70	60
Mean	4,723	5,688	2,883	2,371	2,515	2,520	641	491	191	78	109	164	272	315	241	270	275	54	62	58	62	60
St. deviation	0	34	58	25	14	34	5	19	27	1	15	7	9	19	10	11	9	3	7	1	5	2
TC-1	4,877	5,472	3,427	2,506	2,986	2,995	580	457	215	117	121	223	251	125	257	264	272	75	63	66	56	67
TC-2	4,742	5,040	3,992	2,755	2,947	2,848	586	349	227	117	111	175	239	305	256	287	280	66	59	65	71	69
TC-3	5,338	5,328	3,810	2,966	2,986	2,880	614	465	232	106	125	NA	255	291	284	274	263	66	75	60	95	81
Mean	4,810	5,400	3,427	2,506	2,973	2,908	593	461	225	117	123	199	248	298	266	275	272	66	66	64	64	68
St. deviation	95	102	NA	NA	22	77	19	5	9	7	3	34	8	10	16	12	8	0	3	3	11	8

* In some cases, after careful analysis of the results, some replicates' results were not included in the mean and standard deviation calculation.

Table 7-2: ABMP data-2*

Test	TSS (mgTSS/l)						VSS (mgVSS/l)						ISS (mgISS/l)					
Date	24-Jun	28-Jun	07-Jul	04-Aug	23-Aug	08-Sep	24-Jun	28-Jun	07-Jul	04-Aug	23-Aug	08-Sep	24-Jun	28-Jun	07-Jul	04-Aug	23-Aug	08-Sep
Days elapsed	0	4	13	41	60	76	0	4	13	41	60	76	0	4	13	41	60	76
C-1	2,724	2,494	2,552	2,366	2,396	2,350	2,040	1,814	1,858	1,792	1,728	1,684	684	680	694	574	668	666
C-2	2,712	2,648	2,578	2,354	2,182	2,222	2,040	1,948	1,884	1,722	1,574	1,604	672	700	694	632	608	618
C-3	2,818	2,612	2,542	2,258	2,284	2,186	2,130	1,906	1,859	1,780	1,644	1,550	688	706	683	478	640	636
C-4	2,682	2,692	2,496	2,568	2,390	2,346	2,006	2,008	1,834	1,874	1,728	1,676	676	684	662	694	662	670
Mean	2,734	2,651	2,542	2,326	2,313	2,276	2,054	1,919	1,859	1,792	1,669	1,629	680	693	683	633	645	648
St. deviation	59	40	34	59	101	84	53	82	20	63	74	64	7	12	15	60	27	25
TA-1	3,928	3,254	2,966	2,792	2,734	2,664	3,104	2,516	2,178	2,062	1,954	1,912	824	738	788	730	780	752
TA-2	3,928	2,496	2,230	NA	NA	0	3,114	2,496	2,230	NA	NA	NA	814	810	740	NA	NA	NA
TA-3	3,874	3,346	2,968	2,744	2,952	2,832	3,100	2,492	2,204	2,028	2,096	2,020	774	854	764	716	856	812
Mean	3,910	3,300	2,967	2,768	2,734	2,664	3,106	2,501	2,204	2,045	2,025	1,966	804	801	764	723	818	782
St. deviation	31	65	1	34	NA	NA	7	13	26	24	100	76	26	59	24	10	54	42
TB-1	3,478	2,688	2,498	2,400	2,406	2,114	2,808	2,004	1,908	1,954	1,670	1,578	670	684	590	446	736	536
TB-2	3,498	2,912	2,596	2,490	2,490	2,160	2,792	2,234	1,958	1,846	1,696	1,604	706	678	638	644	818	556
TB-3	3,400	3,034	2,546	2,536	2,408	2,168	2,762	2,296	1,946	1,882	1,738	1,570	638	738	600	654	670	598
Mean	3,459	2,973	2,547	2,475	2,435	2,147	2,787	2,265	1,937	1,894	1,701	1,584	671	700	609	649	741	546
St. deviation	52	86	49	69	48	29	23	44	26	55	34	18	34	33	25	7	74	32
TC-1	3,720	2,968	2,738	2,526	2,682	2,488	2,966	2,276	2,064	1,888	1,948	1,804	754	692	674	638	734	684
TC-2	3,850	3,030	2,638	2,282	2,690	2,518	3,100	2,320	1,992	1,898	1,968	1,878	750	710	646	384	722	640
TC-3	3,754	3,214	2,708	2,742	2,592	2,430	3,204	2,466	2,044	1,996	1,958	1,748	550	748	664	746	634	682
Mean	3,775	2,999	2,695	2,634	2,655	2,479	3,090	2,298	2,033	1,927	1,958	1,810	752	717	661	692	697	669
St. deviation	67	44	51	153	54	45	119	31	37	60	10	52	3	29	14	76	55	25

* In some cases, after careful analysis of the results, some replicates' results were not included in the mean and standard deviation calculation.

Table 7-3. ABMP data – 3*

Test	FSA (mgN/l)						OP (mgP/l)						pH					
	24-Jun	28-Jun	07-Jul	04-Aug	23-Aug	08-Sep	24-Jun	28-Jun	07-Jul	04-Aug	23-Aug	08-Sep	24-Jun	28-Jun	07-Jul	04-Aug	23-Aug	08-Sep
Days elapsed	0	4	13	41	60	76	0	4	13	41	60	76	0	4	13	41	60	76
C-1	85	96	105	119	127	133	4	6	9	17	11	12	7.4	7.5	7.3	7.1	7.1	7.2
C-2	83	99	105	118	126	127	5	7	9	11	11	11	7.6	7.5	7.4	7.3	7.2	7.4
C-3	80	91	104	117	123	124	5	8	9	15	11	10	7.7	7.4	7.4	7.4	7.4	7.6
C-4	84	100	102	112	108	86	4	7	9	11	10	10	7.5	7.6	7.4	7.5	7.3	7.5
Mean	83	98	104	116	125	128	5	7	9	11	11	11	7.5	7.5	7.4	7.4	7.3	7.5
St. deviation	2	2	1	3	2	4	0	0	0	1	0	1	0.1	0.0	0.0	0.1	0.2	0.2
TA-1	106	97	123	153	159	165	9	9	16	18	16	17	7.3	6.9	7.0	7.1	7.1	7.3
TA-2	105	98	125	NA	NA	NA	9	10	16	NA	NA	NA	7.3	6.9	6.9	0.0	0.0	0.0
TA-3	107	100	120	149	155	162	10	11	16	16	17	18	7.3	6.9	7.0	7.1	7.2	7.3
Mean	106	98	123	151	159	165	9	10	16	16	16	17	7.3	6.9	7.0	7.1	7.1	7.3
St. deviation	1	2	3	3	3	2	0	0	0	0	0	1	0.0	0.0	0.0	0.0	7.0	7.2
TB-1	95	79	119	137	149	149	6	8	14	18	15	16	7.2	6.6	7.0	7.0	7.0	7.2
TB-2	97	101	120	141	147	148	6	10	14	21	15	16	7.2	6.7	6.9	7.0	7.0	7.1
TB-3	96	88	120	145	155	152	6	9	14	15	16	17	7.2	6.6	6.9	7.0	7.1	7.3
Mean	96	83	120	141	148	148	6	9	14	15	15	16	7.2	6.6	6.9	7.0	7.0	7.3
St. deviation	1	6	1	4	4	2	0	1	0	0	0	1	0.0	0.1	0.0	0.0	7.1	7.2
TC-1	99	98	123	149	157	156	7	9	15	21	17	17	7.3	6.8	7.0	7.0	7.1	7.2
TC-2	99	96	120	142	151	154	7	9	15	15	17	18	7.3	6.8	6.9	6.9	7.0	7.0
TC-3	99	103	120	142	156	157	7	11	15	20	16	18	7.3	6.8	6.9	6.9	6.9	7.1
Mean	99	100	120	142	155	156	7	9	15	17	17	18	7.3	6.8	6.9	6.9	7.0	7.1
St. deviation	0	4	2	4	3	2	0	0	0	3	0	0	0.0	0.0	0.1	0.1	0.0	0.0

* In some cases, after careful analysis of the results, some replicates' results were not included in the mean and standard deviation calculation.

Table 7-4. ABMP data – 4*

Test	Carbonate alk (mg CaCO ₃ /l)				Total alk (mg CaCO ₃ /l)				Total alk (mg CaCO ₃ /l)				VFA COD (mgCOD/l as acetate)			
	24-Jun	28-Jun	04-Aug	08-Sep	24-Jun	28-Jun	04-Aug	08-Sep	24-Jun	28-Jun	04-Aug	08-Sep	24-Jun	28-Jun	04-Aug	08-Sep
Days elapsed	0	4	41	76	0	4	41	76	0	4	41	76	0	4	41	76
C-1	-7	-118	-27	NA	686	706	911	NA	684	592	922	NA	-8	-143	-32	NA
C-2	-79	-24	-47	-47	762	681	908	990	686	666	886	970	-96	-28	-56	-56
C-3	-139	-25	-46	-46	822	579	970	853	686	567	954	831	-169	-30	-55	-55
C-4	-57	NA	-51	-51	731	NA	946	946	683	NA	929	929	-68	NA	-61	-61
Mean	-71	-24	-42	-48	750	693	934	929	685	608	923	949	-85	-67	-51	-57
St. deviation	55	54	11	3	57	18	30	70	2	52	28	29	67	66	13	3
TA-1	15	49	-51	-18	769	754	925	1,129	793	817	945	1,154	18	59	-61	-22
TA-2	-22	-11	NA	NA	839	911	NA	NA	822	947	NA	NA	-26	-13	NA	NA
TA-3	-40	-6	-11	-41	827	910	1,175	1,249	795	920	1,199	1,241	-49	-7	-13	-49
Mean	-16	-8	-31	-29	812	911	1,050	1,189	804	934	1,072	1,198	-19	13	-37	-35
St. deviation	28	33	29	16	38	0	177	85	16	69	180	62	34	40	34	19
TB-1	5	-25	-69	111	551	673	1,041	950	561	653	1,014	1,091	7	-31	-83	133
TB-2	6	37	-39	-57	615	639	1,118	1,015	626	683	1,119	976	7	45	-47	-69
TB-3	-18	-221	-26	-55	704	1,041	939	1,106	700	830	959	1,073	-23	-266	-32	-66
Mean	-2	-70	-45	1,067	660	656	1,080	1,060	663	668	1,067	1,082	-3	7	-54	-1
St. deviation	13	135	22	97	63	24	55	65	52	21	74	62	17	162	26	116
TC-1	39	66	-16	-30	683	729	1,041	1,050	728	801	1,075	1,037	729	1,041	1,050	-36
TC-2	7	-20	-14		767	785	1,096	1,119	779	773	1,116	1,130	785	1,096	1,119	-17
TC-3	-48	24	-11		818	794	1,125	1,067	775	831	1,151	1,068	794	1,125	1,067	-29
Mean	-1	23	-14	1,114	756	769	1,087	1,058	761	802	1,114	1,053	769	1,087	1,058	-27
St. deviation	44	43	2	8	68	35	43	36	29	29	38	47	54	52	3	10

* In some cases, after careful analysis of the results, some replicates' results were not included in the mean and standard deviation calculation.

Appendix B: ABMP modelled experiment summary

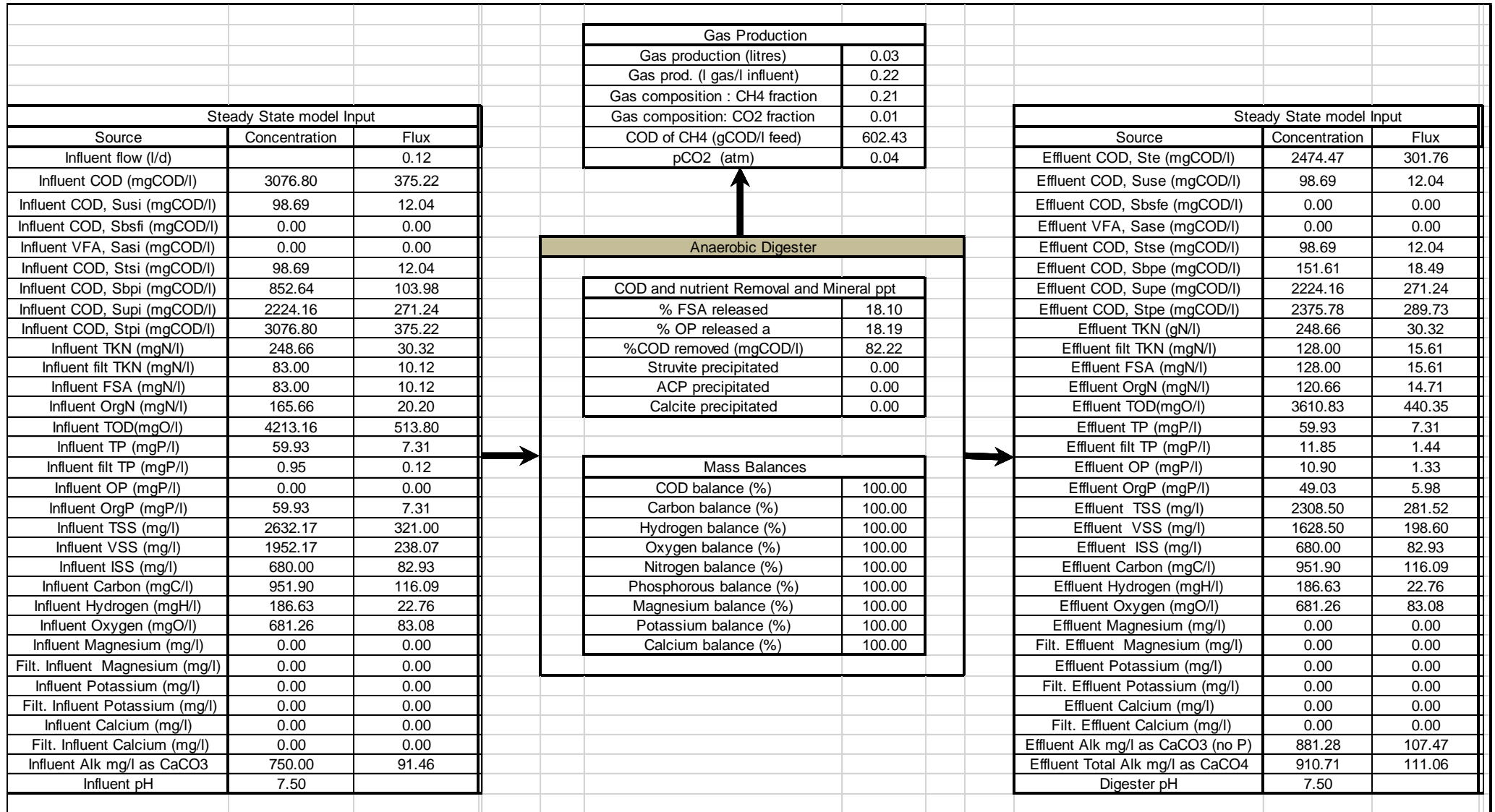


Figure 7-1: ABMP Control reactor experiment simulation summary

Steady State model Input			Gas Production		Steady State model Input		
Source	Concentration	Flux			Source	Concentration	Flux
Influent flow (l/d)		0.12			Effluent COD, Ste (mgCOD/l)	3184.40	388.34
Influent COD (mgCOD/l)	4752.00	579.51			Effluent COD, Suse (mgCOD/l)	299.20	36.49
Influent COD, Susi (mgCOD/l)	299.20	36.49			Effluent COD, Sbsfe (mgCOD/l)	0.00	0.00
Influent COD, Sbsfi (mgCOD/l)	0.00	0.00			Effluent VFA, Sase (mgCOD/l)	0.00	0.00
Influent VFA, Sasi (mgCOD/l)	0.00	0.00			Effluent COD, Stse (mgCOD/l)	299.20	36.49
Influent COD, Stsi (mgCOD/l)	299.20	36.49			Effluent COD, Sbppe (mgCOD/l)	180.23	21.98
Influent COD, Sbppe (mgCOD/l)	1642.10	200.26			Effluent COD, Supe (mgCOD/l)	2704.96	329.87
Influent COD, Supi (mgCOD/l)	2704.96	329.87			Effluent COD, Stpe (mgCOD/l)	2885.20	351.85
Influent COD, Stpi (mgCOD/l)	4347.06	530.13			Effluent TKN (gN/l)	286.87	34.98
Influent TKN (mgN/l)	286.87	34.98			Effluent filt TKN (mgN/l)	165.00	20.12
Influent filt TKN (mgN/l)	106.00	12.93			Effluent FSA (mgN/l)	165.00	20.12
Influent FSA (mgN/l)	106.00	12.93			Effluent OrgN (mgN/l)	121.87	14.86
Influent OrgN (mgN/l)	180.87	22.06			Effluent TOD(mgO/l)	4495.37	548.22
Influent TOD(mgO/l)	6062.97	739.39			Effluent TP (mgP/l)	78.70	9.60
Influent TP (mgP/l)	78.70	9.60			Effluent filt TP (mgP/l)	19.45	2.37
Influent filt TP (mgP/l)	2.87	0.35			Effluent OP (mgP/l)	16.58	2.02
Influent OP (mgP/l)	0.00	0.00			Effluent OrgP (mgP/l)	62.12	7.58
Influent OrgP (mgP/l)	78.70	9.60			Effluent TSS (mg/l)	2814.19	343.19
Influent TSS (mg/l)	3793.13	462.58			Effluent VSS (mg/l)	2010.19	245.15
Influent VSS (mg/l)	2989.13	364.53			Effluent ISS (mg/l)	804.00	98.05
Influent ISS (mg/l)	804.00	98.05			Effluent Carbon (mgC/l)	1399.17	170.63
Influent Carbon (mgC/l)	1399.17	170.63			Effluent Hydrogen (mgH/l)	326.37	39.80
Influent Hydrogen (mgH/l)	326.37	39.80			Effluent Oxygen (mgO/l)	1245.02	151.83
Influent Oxygen (mgO/l)	1245.02	151.83			Effluent Magnesium (mg/l)	0.00	0.00
Influent Magnesium (mg/l)	0.00	0.00			Filt. Effluent Magnesium (mg/l)	0.00	0.00
Filt. Influent Magnesium (mg/l)	0.00	0.00			Effluent Potassium (mg/l)	0.00	0.00
Influent Potassium (mg/l)	0.00	0.00			Filt. Effluent Potassium (mg/l)	0.00	0.00
Filt. Influent Potassium (mg/l)	0.00	0.00			Effluent Calcium (mg/l)	0.00	0.00
Influent Calcium (mg/l)	0.00	0.00			Filt. Effluent Calcium (mg/l)	0.00	0.00
Filt. Influent Calcium (mg/l)	0.00	0.00			Effluent Alk mg/l as CaCO3 (no P)	1168.83	142.54
Influent Alk mg/l as CaCO3	1000.00	121.95			Effluent Total Alk mg/l as CaCO4	1210.72	147.65
Influent pH	7.30				Digester pH	7.30	

COD and nutrient Removal and Mineral ppt	
% FSA released	20.57
% OP released a	21.06
%COD removed (mgCOD/l)	89.02
Struvite precipitated	0.00
ACP precipitated	0.00
Calcite precipitated	0.00

Mass Balances	
COD balance (%)	100.01
Carbon balance (%)	100.00
Hydrogen balance (%)	100.00
Oxygen balance (%)	100.00
Nitrogen balance (%)	100.00
Phosphorous balance (%)	100.00
Magnesium balance (%)	100.00
Potassium balance (%)	100.00
Calcium balance (%)	100.00

Gas Production	
Gas production (litres)	0.07
Gas prod. (l gas/l influent)	0.60
Gas composition : CH4 fraction	0.55
Gas composition: CO2 fraction	0.05
COD of CH4 (gCOD/l feed)	1567.85
pCO2 (atm)	0.09

Figure 7-2: ABMP test A reactor experiment simulation summary

Steady State model Input			Gas Production		Steady State model Input		
Source	Concentration	Flux			Source	Concentration	Flux
Influent flow (l/d)		0.12	Gas production (litres)	0.11	Effluent COD, Ste (mgCOD/l)	2520.00	307.32
Influent COD (mgCOD/l)	4723.20	576.00	Gas prod. (l gas/l influent)	0.93	Effluent COD, Suse (mgCOD/l)	299.20	36.49
Influent COD, Susi (mgCOD/l)	299.20	36.49	Gas composition : CH4 fraction	0.79	Effluent COD, Sbsfe (mgCOD/l)	0.00	0.00
Influent COD, Sbsfi (mgCOD/l)	0.00	0.00	Gas composition: CO2 fraction	0.14	Effluent VFA, Sase (mgCOD/l)	0.00	0.00
Influent VFA, Sasi (mgCOD/l)	0.00	0.00	COD of CH4 (gCOD/l feed)	2203.55	Effluent COD, Stse (mgCOD/l)	299.20	36.49
Influent COD, Stsi (mgCOD/l)	299.20	36.49	pCO2 (atm)	0.15	Effluent COD, Sbpe (mgCOD/l)	210.44	25.66
Influent COD, Sbpri (mgCOD/l)	2307.90	281.45			Effluent COD, Supe (mgCOD/l)	2010.36	245.17
Influent COD, Supri (mgCOD/l)	2010.36	245.17			Effluent COD, Stpe (mgCOD/l)	2220.80	270.83
Influent COD, Stpri (mgCOD/l)	4318.26	526.62			Effluent TKN (gN/l)	279.73	34.11
Influent TKN (mgN/l)	279.73	34.11			Effluent filt TKN (mgN/l)	148.00	18.05
Influent filt TKN (mgN/l)	96.00	11.71			Effluent FSA (mgN/l)	148.00	18.05
Influent FSA (mgN/l)	96.00	11.71			Effluent OrgN (mgN/l)	131.73	16.07
Influent OrgN (mgN/l)	183.73	22.41			Effluent TOD(mgO/l)	3798.38	463.22
Influent TOD(mgO/l)	6001.58	731.90			Effluent TP (mgP/l)	66.37	8.09
Influent TP (mgP/l)	66.07	8.06			Effluent filt TP (mgP/l)	18.87	2.30
Influent filt TP (mgP/l)	2.87	0.35			Effluent OP (mgP/l)	16.00	1.95
Influent OP (mgP/l)	0.00	0.00			Effluent OrgP (mgP/l)	50.37	6.14
Influent OrgP (mgP/l)	66.07	8.06			Effluent TSS (mg/l)	2319.98	282.92
Influent TSS (mg/l)	3596.98	438.66			Effluent VSS (mg/l)	1648.58	201.05
Influent VSS (mg/l)	2925.58	356.78			Effluent ISS (mg/l)	671.40	81.88
Influent ISS (mg/l)	671.40	81.88			Effluent Carbon (mgC/l)	1317.95	160.73
Influent Carbon (mgC/l)	1317.95	160.73			Effluent Hydrogen (mgH/l)	349.78	42.66
Influent Hydrogen (mgH/l)	349.78	42.66			Effluent Oxygen (mgO/l)	1246.18	151.97
Influent Oxygen (mgO/l)	1246.18	151.97			Effluent Magnesium (mg/l)	0.00	0.00
Influent Magnesium (mg/l)	0.00	0.00			Filt. Effluent Magnesium (mg/l)	0.00	0.00
Filt. Influent Magnesium (mg/l)	0.00	0.00			Effluent Potassium (mg/l)	0.00	0.00
Influent Potassium (mg/l)	0.00	0.00			Filt. Effluent Potassium (mg/l)	0.00	0.00
Filt. Influent Potassium (mg/l)	0.00	0.00			Effluent Calcium (mg/l)	0.00	0.00
Influent Calcium (mg/l)	0.00	0.00			Filt. Effluent Calcium (mg/l)	0.00	0.00
Filt. Influent Calcium (mg/l)	0.00	0.00			Effluent Alk mg/l as CaCO3 (no P)	1145.29	139.67
Influent Alk mg/l as CaCO3	1000.00	121.95			Effluent Total Alk mg/l as CaCO4	1185.72	144.60
Influent pH	7.20				Digester pH	7.30	

Figure 7-3: ABMP test B reactor experiment simulation summary

Steady State model Input			Gas Production		Steady State model Input		
Source	Concentration	Flux			Source	Concentration	Flux
Influent flow (l/d)		0.12	Gas production (litres)	0.11	Effluent COD, Ste (mgCOD/l)	2907.80	354.61
Influent COD (mgCOD/l)	4809.60	586.54	Gas prod. (l gas/l influent)	0.87	Effluent COD, Suse (mgCOD/l)	299.20	36.49
Influent COD, Susi (mgCOD/l)	299.20	36.49	Gas composition : CH4 fraction	0.69	Effluent COD, Sbsfe (mgCOD/l)	0.00	0.00
Influent COD, Sbsfi (mgCOD/l)	0.00	0.00	Gas composition: CO2 fraction	0.18	Effluent VFA, Sase (mgCOD/l)	0.00	0.00
Influent VFA, Sasi (mgCOD/l)	0.00	0.00	COD of CH4 (gCOD/l feed)	1902.10	Effluent COD, Stse (mgCOD/l)	299.20	36.49
Influent COD, Stsi (mgCOD/l)	299.20	36.49	pCO2 (atm)	0.20	Effluent COD, Sbppe (mgCOD/l)	196.11	23.92
Influent COD, Sbppe (mgCOD/l)	1992.17	242.95			Effluent COD, Suppe (mgCOD/l)	2412.49	294.21
Influent COD, Suppe (mgCOD/l)	2412.49	294.21			Effluent COD, Stpe (mgCOD/l)	2608.60	318.12
Influent COD, Stpe (mgCOD/l)	4404.66	537.15			Effluent TKN (gN/l)	284.98	34.75
Influent TKN (mgN/l)	284.98	34.75			Effluent filt TKN (mgN/l)	155.96	19.02
Influent filt TKN (mgN/l)	99.00	12.07			Effluent FSA (mgN/l)	155.96	19.02
Influent FSA (mgN/l)	99.00	12.07			Effluent OrgN (mgN/l)	129.03	15.73
Influent OrgN (mgN/l)	185.98	22.68			Effluent TOD(mgO/l)	4210.17	513.44
Influent TOD(mgO/l)	6111.97	745.36			Effluent TP (mgP/l)	70.44	8.59
Influent TP (mgP/l)	69.89	8.52			Effluent filt TP (mgP/l)	20.54	2.50
Influent filt TP (mgP/l)	2.87	0.35			Effluent OP (mgP/l)	17.67	2.15
Influent OP (mgP/l)	0.00	0.00			Effluent OrgP (mgP/l)	52.77	6.44
Influent OrgP (mgP/l)	69.89	8.52			Effluent TSS (mg/l)	2549.61	310.93
Influent TSS (mg/l)	3620.77	441.56			Effluent VSS (mg/l)	1864.91	227.43
Influent VSS (mg/l)	2936.07	358.06			Effluent ISS (mg/l)	684.70	83.50
Influent ISS (mg/l)	684.70	83.50			Effluent Carbon (mgC/l)	1429.73	174.36
Influent Carbon (mgC/l)	1429.73	174.36			Effluent Hydrogen (mgH/l)	315.07	38.42
Influent Hydrogen (mgH/l)	315.07	38.42			Effluent Oxygen (mgO/l)	1174.38	143.22
Influent Oxygen (mgO/l)	1174.38	143.22			Effluent Magnesium (mg/l)	0.00	0.00
Influent Magnesium (mg/l)	0.00	0.00			Filt. Effluent Magnesium (mg/l)	0.00	0.00
Filt. Influent Magnesium (mg/l)	0.00	0.00			Effluent Potassium (mg/l)	0.00	0.00
Influent Potassium (mg/l)	0.00	0.00			Filt. Effluent Potassium (mg/l)	0.00	0.00
Filt. Influent Potassium (mg/l)	0.00	0.00			Effluent Calcium (mg/l)	0.00	0.00
Influent Calcium (mg/l)	0.00	0.00			Filt. Effluent Calcium (mg/l)	0.00	0.00
Filt. Influent Calcium (mg/l)	0.00	0.00			Effluent Alk mg/l as CaCO3 (no P)	912.04	111.22
Influent Alk mg/l as CaCO3	750.00	91.46			Effluent Total Alk mg/l as CaCO4	953.42	116.27
Influent pH	7.30				Digester pH	7.10	

Figure 7-4: ABMP test C reactor experiment simulation summary